FORECASTING REGIME SHIFTS IN COMPLEX DYNAMICAL SYSTEMS

A Candidacy Proposal

Submitted to the Graduate School
of the University of Notre Dame
in Partial Fulfillment of the Requirements
for the Degree of

Doctor of Philosophy

by

Tua A. Tamba

M.D. Lemmon, Director

Graduate Program in Department of Electrical Engineering
Notre Dame, Indiana

May 2014

FORECASTING REGIME SHIFTS IN COMPLEX DYNAMICAL SYSTEMS

Abstract

by

Tua A. Tamba

Regime shifts refer to sudden changes in the structure and function of a system due to forces from external disturbances. Such shifts occur because the system has *alternative stable states* and external disturbances force the system's operating point to shifts from one stable state to another. Examples of regime shifts includes the collapse of coastal fisheries as a result of human-induced nutrient enrichment and the voltage collapse in power network due to variations in storm frequency or user demand. Due to these undesired consequences of regime shifts, there is a great challenge in finding methods to forecast their occurence. Our works address this challenge using sums of squares (SOS) optimization techniques. We first identify two scenarios in which regime shifts may occur and then formulate some real-valued quantities that can be used as indicators of how close the system is to each type of regime shifts. The first scenario of regime shifts will be called *bifurcation-induced regime shifts* which occurs because the system undergoes a bifurcation due to variation on the parameters that exceeds a critical treshold. We use a quantity known as "minimum distance-to-bifurcation" as a measure of how close the system is to this type of regime shifts and formulate an SOS optimization problem to compute the global minimum of this quantity. We show that by using techniques from algebraic geometry and SOS relaxation method, the computation of this quantity in a class of nonnegative system with *kinetic realization* can be simplified. The second scenario

of regime shifts will be called *noise-induced regime shifts* which occurs because the underlying system has multiple stable equilibria and external stochastic disturbances drive the system's state from the region of attraction (ROA) of one stable equilibrium to the ROAs of alternative stable equilibria. We use probabilistic quantities called *mean first passage times* and *finite time stochastic reachability* to characterize the *expected time* and the *likelihood* for this type of regime shifts to occur. We formulate an SOS optimization problem for searching a positive semidefinite function, called *Barrier certificate*, that generates a *supermartingale* and provides an upper bound for each of these quantities.

CONTENTS

FIGURES

TABLES

CHAPTER 1

Introduction

1.1 Motivation

Regime shifts [99, 36, 57] refer to sudden changes in the structure or function of a system due to the presence of forces from external disturbances. An important concept in the study of regime shifts is the idea that systems may have *alternative stable states* [79, 98, 74] such that the presence of external disturbances forces these systems' operating point to shift from one stable states to another. In general, there are two mechanisms in which regime shifts occur [97]. First, regime shifts may occur because the system undergoes a bifurcation due to variation on system's parameters that exceeds a critical threshold [15, 99, 13]. We call this mechanism *bifurcation-induced regime shifts*. Second, regime shifts may occur because the system has multiple stable equilibria and external stochastic disturbances drive the system state from the region of attraction (ROA) of one stable equilibrium to the ROA of an alternative stable equilibrium [11, 19, 30]. This mechanism will be called *noise-induced regime shifts*. In either scenario, regime shifts can be catastrophic for users who have grown accustomed to the quality of services provided by the system prior to the shift. Examples of regime shifts includes the bloom of algae in shallow lakes as a result of human-induced nutrient enrichment [14, 96], the collapse of fisheries and coral reefs do to extreme natural events and human exploitation [99], the regime changes and crash of stock market prices [2], and the cascades of voltage collapse in electric power grids [26, 25]. Each of these shifts has the potential to disrupt the services that

these systems provide to the society. Forecasting impeding regime shifts in these systems is therefore crucial for the purpose of managing their security and sustainability [15, 1, 36].

This proposal presents computational methods to forecast the onset of regime shifts. The main idea in our methods is the formulation of some real-valued quantities which can be used as indicators of how close a system is to regime shifts. In bifurcation-induced regime shifts, this quantity is known as *minimum distance-to-bifurcation* $\gamma \in \mathbb{R}_{\geq 0}$ which measures the distance between a nominal parameter and the value of the parameter at which a bifurcation occurs [26]. In noise-induced regime shifts, these quantities are the *mean first passage time* (MFPT) and the *finite time stochastic reachability* [41, 72]. The MFPT is a random variable $\tau \in \mathbb{R}_{\geq 0}$ which measures the *average time* required for regime shifts to occur whereas the finite time stochastic reachability is a probability measures $\theta \in [0, 1]$ which indicates the *likelihood* for regime shifts to occur within a finite time period. The key technical approach in our method is on the use of sum of squares (SOS) relaxation techniques [88] to recast the computation of each of these quantities as an SOS optimization problem [89, 87]. The main advantage of this relaxation is that the formulated SOS optimization problem can be solved using the available SOS programming softwares [90, 75, 55].

1.2 Backgrounds and Prior Works

To better illustrate the two mechanisms in which regime shifts occur, let us consider the following scaled lake eutrophication model from [15, 99].

$$\dot{x} = a - bx + \frac{x^2}{1 + x^2}. \tag{1.1}$$

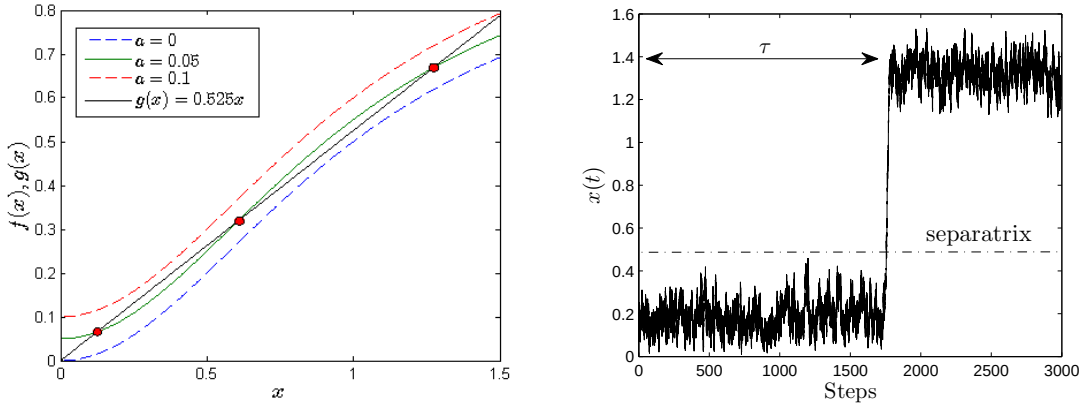

(a) Bifurcation-induced regime shifts.

(b) Noise-induced regime shifts.

Figure 1.1. Two scenarios of regime shifts.

In equation (1.1), the state variable x denotes the Phosphorus (P) concentration in lake water column whereas parameters $a \geq 0$ and $b \geq 0$ denote the rates of inflow and outflow of P into and out of the lake, respectively. The last term in the model denotes the the rate of P increase due to recycling from lake sediment.

1.2.1 Bifurcation-induced regime shifts

To investigate for possible bifurcations in system (1.1), one needs to analyze the characteristic of its equilibria. The equilibria of (1.1) can be computed by setting its right hand side terms to zero and are given by those values of x such that

$$\underbrace{a + \frac{x^2}{1+x^2}}_{f(x)} = \underbrace{bx}_{g(x)}.$$

Functions $f(x)$ and $g(x)$ in the above equality denote the rate of increase and decrease of x, respectively, and so the equilibria are given by the values of x at the intersections of these functions' curves. The plots of these curves for fixed b and various a are depicted in figure 1.1a and it show that the number of intersections between the

curves (i.e. equilibria) change as the value of parameter a is varied. In particular, for small inflow rate ($a \approx 0$), there is a single *oligotrophic* equilibrium which is characterized by pristine water lake with high oxygen level that supports species biodiversity. For larger inflow rate ($0.25 < a < 0.1$), this equilibrium bifurcates into two stable equilibria: an oligotrophic one and an *eutrophic* one (lake water characterized by algal bloom with low oxygen level that does not support species biodiversity). Finally, for even larger inflow rate ($a \geq 0.1$), these two stable equilibria coalesce to an eutrophic equilibrium through a saddle node bifurcation. These series of bifurcations therefore induce a transition from a lake with clear water to a lake with turbid water.

The preceeding example illustrates how variation on parameters which exceeds a critical value may induce bifurcations of the system's equilibria. In particular, these bifurcations are followed by the flip or regime shifts of the system's operating point from one stable state to another [99]. It is therefore clear that the problem of forecasting the onset of bifurcation-induced regime shifts is equivalent with the problem of searching for the value of a critical parameter at which a bifurcation occurs. This observation has motivated a large number of researchers to use numerical bifurcation analysis as an approach to predict the onset of regime shifts [96, 98, 13, 57]. The main issue in this approach is that the currently available numerical bifurcation software is limited to analysis of at most 3 parameters simultaneously. Moreover, searching for all possible bifurcations that may occur in a system is generally difficult especially when the dimension of the parameter space is high [73].

Another approach for predicting bifurcation-induced regime shifts is based on searching for the *closest* parameter value at which a bifurcation occurs. In particular, for dynamical systems

$$\dot{x}(t) = f(x(t), k), \quad x(0) = x_0, \tag{1.2}$$

whose vector fields are parameterized by real-valued parameter k, one may define a

quantity

$$\gamma = \inf_{k} |k^* - k^0|, \tag{1.3}$$

which measures the distance between a nominal parameter k_0 and the closest critical paramater k^* at which a bifurcation occurs. The quantity γ is often called the *minimum distance-to-bifurcation* [26, 25] and is an indicator of how close a system is to a bifurcation. Prior works have proposed several methods for computing γ in the context of robust stability analysis [69, 80, 84, 115] and voltage collapse problem in power systems [25, 26]. In general, these methods use numerical optimization techniques to search for the minimum γ subject to the constraints that the critical parameter k^* satisfy the bifurcation conditions [48, 73, see also table 4.1]. These methods, however, are computationally demanding since the search for the minimum γ requires the computation of system's equilibria x^* at every iteration.

Approach and Contribution: Our proposed method uses SOS optimization [87, 88] to compute an upper bound of γ for a class of nonnegative dynamical systems that have *kinetic realization*. The dynamical system in (1.2) is said to have a kinetic realization if there exists a matrix N and a vector of monomials $v(x, k)$ with variables x and parameters k such that $f(x, k) = Nv(x, k)$. As shown in [43, 44] (see also chapter 3), the special structure of these systems allows one to compute an analytical parameterization of their equilibria in term of the system parameters. This parameterization method was first proposed in the context of chemical reaction network [42, 43] and is based on techniques from algebraic geometry [44, 20, 4]. As will be discussed in chapter 4, the ability to compute this parameterization can help simplifies the computation of γ.

Our first contribution is on identifying larger class of systems (other than chemical reaction network models) for which the equilibrium parameterization method proposed in [43, 44] can be applied. We call these systems *nonnegative systems with*

kinetic realization and show through example how the equilibrium parameterization method from [43, 44] can be applied to them. Our second contribution is on the use of such parameterization to formulate an SOS optimization for computing an upper bound for γ. We show that the use of such equilibrium parameterization helps simplify the computation of γ in that the constraints of optimization can be expressed only in term of system's parameter rather than the system's parameter and equilibria.

1.2.2 Noise-induced regime shifts

Consider again the lake model (1.1) and let us now choose parameters $a = 0.06$ and $b = 0.525$ for which this system has two stable equilibria (oligotrophic and eutrophic) separated by one unstable equilibrium. The ROA of each equilibrium is the area below or above the dashed separatrix line depicted in figure 1.1b. In this case, any trajectory that starts from the region below (above) the separatrix line will remains within that region and eventually goes to the oligotrophic (eutrophic) equilibrium. Now assume that the system is driven by additive Wiener process $\{w(t)\}$ of constant variance σ so that its model is given by the stochastic differential equation (SDE)

$$\begin{aligned} dx(t) &= f(x)dt + g(x)dw(t), \\ &= \left(a - bx + \frac{x^2}{1+x^2}\right)dt + \sigma dw(t), \end{aligned}$$

where $f(x)$ and $g(x)$ are the *drift* and *diffusion*, respectively. One realization of this SDE for $\sigma = 0.05$ is depicted in figure 1.1b and it shows that the sample path that starts inside the region below the separatrix (oligotrophic state) eventually shifts to the region above the separatrix (oligotrophic state). This example illustrates the noise-induced regime shifts mechanism where the presence of noise in systems with multiple equilibria may forces the system's sample path to shift from the ROA of one equilibrium to the ROA of another equilibrium.

The above example suggests that the task of forecasting the onset of noise-induced regime shifts can be formulated either as an MFPT problem or as a stochastic reachability problem formally defined as follows.

- *MFPT problem:* Let $\{x(t)\}$ be a stochastic process whose state $x(t)$ at time $t \geq 0$ taking values on a bounded open subsets $\mathcal{X} \subseteq \mathbb{R}^n$ of the Euclidean space with smooth boundary $\partial\mathcal{X}$. Let $\mathcal{X}_0 \subset \mathcal{X}$ be an initial set such that $x(0) = x_0 \in \mathcal{X}_0$. The time at which the sample path of $\{x(t)\}$ hits the set $\partial\mathcal{X}$ is a random variable τ called the first passsage time and is defined as

$$\tau \equiv \inf_t \{t \geq 0 \,|\, x(t) \in \partial\mathcal{X}\}. \tag{1.4}$$

  The MFPT problem therefore concerns with the computation of the expected value $\mathbb{E}\{\tau\}$ of τ.

- *Stochastic reachability problem:* Let $\{x(t)\}$ be a stochastic process whose state $x(t)$ at time $t \geq 0$ taking values on a bounded open subsets $\mathcal{X} \subseteq \mathbb{R}^n$ of the Euclidean space. Let $\mathcal{X}_0 \subset \mathcal{X}$ be an initial set such that $x(0) = x_0 \in \mathcal{X}_0$ and let $\mathcal{X}_u \subset \mathcal{X}$ denotes an arbitrary set such that $\mathcal{X}_u \cap \mathcal{X}_0 = \emptyset$. The stochastic reachability problem concerns with the computation of the probability that, starting from the initial set $\mathcal{X}_0$, the sample paths of the process will reach the set $\mathcal{X}_u$ in a finite time $t \in [0, T]$. More formally, this problem seeks to compute a constant $\beta \in [0, 1]$ such that

$$\mathbb{P}\{x(t) \in \mathcal{X}_u, \text{ for some } 0 \leq t \leq T \,|\, x(0) \in \mathcal{X}_0\} \leq \beta. \tag{1.5}$$

There are two standard approaches commonly used to compute (1.4)-(1.5). The first approach computes (1.4)-(1.5) based on the solution of the Chapman-Kolmogorov or Fokker-Planck equations which encode the evolution of the process' probability density function [40, 93]. This approach is suitable for low dimensional systems [45, 86, 59] but is difficult to use for systems with dimensionality greater than one as it involves solving a set of partial differential equations with appropriate boundary conditions. The second approach is based on the Monte Carlo simulation method [70] and is one of the most frequently used methods in the research of noise-induced regime shifts forecasting [11, 97, 15, 14, 8, 100, 21]. This method, however, is computationally expensive as it requires exhaustive simulations of the process's sample

paths to infer conclusions about the statistics of the process such as those in (1.4)-(1.5).

Approach and Contribution: Our method for solving problems (1.4)-(1.5) is based on the Lyapunov-like method commonly used in stochastic stability analysis [72]. This method essentially search for a "stochastic" Lyapunov function, called *barrier certificates*, from which upper bounds for (1.4)-(1.5) can be deduced. The main advantage of this method is that it do not depend on the solution of the Fokker-Planck equation and do not require exhaustive simulations of the process' sample paths. Moreover, the search of the barrier certificates can be posed as an SOS optimization problem which can be solved efficiently using the available SOS programming softwares [90, 75, 55]. This method has been used recently to solve the reachability problem (1.5) for systems driven by Wiener processes [91] and has been applied to study regime shifts in cellular biology [32].

The main contribution of our work is the extension of the method in [91, 72] to compute upper bounds for (1.4)-(1.5) in systems modeled as jump diffusion processes. Our reason to use jump diffusion model (rather than pure diffusion) is motivated by the observations that many noise-induced regime shifts are triggered by the jumps or discontinous changes on the system's states as a result of extreme or abnormal events [12, 23, 30, 2]. These events are no longer suitable to be modeled by Wiener process but are better characterized as stochastic renewal process in the framework of jump diffusion processes. As in [91, 72], our method is also based on searching for appropriate barrier certificates which provide upper bounds for (1.4)-(1.5). By constructing a polynomial representation of the jump diffusion processes' infinitesimal generator, we show that the computation of these upper bounds can be formulated as SOS optimization problems.

1.3 Outline of proposal

The remainder of this proposal is structured as follows. Chapter 2 presents some mathematical backgrounds on algebraic geometry and SOS optimization. The concepts from algebraic geometry will be used in the discussion of equilibrium parameterization in chapter 3 as well as the method to forecast the bifurcation-induced regime shifts in chapter 4. On the other hand, the concept of SOS optimization will be used in chapters 4 and 5. In chapter 3, we describe the concept of kinetic realization in chemical reaction network modeling and discuss the method proposed in [43, 44] for computing an equilibrium parameterization of this realization. We show that such kinetic realization exist in a large class of systems (other than chemical reaction networks) and so the equilibrium parameterization method introduced in [43, 44] can also be applied to these systems. Chapter 4 presents our method to forecast the onset of bifurcation-induced regime shifts in a class of nonnegative systems with kinetic realization. We formulate the prediction for this type of regime shifts as a distance-to-bifurcation problem [26] and show that the solution to this problem for nonnegative systems with kinetic realization can be simplified using the the equilibrium parameterization techniques described in chapter 3. We present some examples to illustrate the effectiveness of the proposed method to predict regime shifts in different applications. Chapter 5 presents our proposed method to forecast the onset of noise-induced regime shifts in systems modeled by jump diffusion processes. Our approach to forecast this type of regime shifts is by formulating the prediction either as an MFPT problem or as a stochastic reachability problem. The main result in this chapter is the construction of a polynomial representation of the jump diffusion processes' infinitesimal generator thereby allows the use of SOS optimization methods to compute upper bounds for (1.4)-(1.5). The last chapter in this proposal describes an experimental test bed from ecology at which the effectiveness of the proposed methods for regime shifts forecasting will be evaluated. The proposed experimen-

tal design is motivated by recent studies on bifurcation phenomena in live microbial predator-prey system [38, 116].

Some parts of this proposal have been or will be published as the following papers.

1. T.A. Tamba and M.D. Lemmon, "Stochastic reachability of jump diffusion processes using sum of squares optimization," *in preparation for journal submission.*
2. T.A. Tamba and M.D. Lemmon, "The distance-to-bifurcation problem in nonnegative dynamical systems with kinetic realizations," *Proc. IEEE Conference on Control and Automation*, Taichung, Taiwan, June 2014.
3. T.A. Tamba and M.D. Lemmon, "Forecasting the resilience of networked dynamical systems under environmental perturbation," *Work in Progress session of the 3rd ACM Conference on High Confidence Networked System (HiCoNS)*, pp. 61-62, Berlin, Germany, April 2014.
4. T.A. Tamba and M.D. Lemmon, "Using first passage times to manage ecosystem regime shifts," *Proc. 52nd IEEE Conference on Decisions and Control*, pp. 2697-2702, Trieste, Italy, 2013.

A summary of research tasks that are expected to be completed at the end of the PhD project includes:

- development of software toolkit that implements regime shifts forecasting methods desribed in this proposal,
- performance comparison between the proposed method and the currently established methods for regime shifts prediction,
- evaluation of the proposed method for predicting ecological regime shifts in an experimental test bed of microbial predator and prey systems.

CHAPTER 2

ALGEBRAIC GEOMETRY AND SUM OF SQUARES (SOS) OPTIMIZATION

This chapter presents basic notations and mathematical backgrounds that will be used throughout the proposal. The materials covered in this chapter includes the basic concepts and methods from algebraic geometry and SOS optimization. The materials on algebraic geometry will be central for the discussion in chapters 3 and 4 whereas the materials on SOS optimization technique will be used in chapters 4 and 5. Several examples are provided throughout the text to illustrate the presented concepts. Most of the presented materials are drawn from existing literatures [20, 5, 88, 87] and so we urge interested readers to refer to these references for extended expositions and detailed proofs.

Notational convention: Let $\mathbb{R}$, $\mathbb{C}$, $\mathbb{Q}$ and $\mathbb{Z}$ denote the set of real, complex, rational and integer numbers, respectively. The set of *nonnegative* real, rational, and integer numbers are denoted as $\mathbb{R}_{\geq 0}, \mathbb{Q}_{\geq 0}$ and $\mathbb{Z}_{\geq 0}$, respectively, whereas the set of *positive* real, rational, and integer numbers are denoted as $\mathbb{R}_+, \mathbb{Q}_+$ and $\mathbb{Z}_+$, respectively. We denote the n-dimensional Euclidean vector space as $\mathbb{R}^n$. Given a vector $x \in \mathbb{R}^n$, we let x_i denote the ith component of x.

An n-dimensional *multi-index* $\alpha \in \mathbb{Z}^n_{\geq 0}$ is an n-tuple $\alpha \equiv (\alpha_1, \alpha_2, \cdots, \alpha_n)$ of nonnegative integers with absolute value $|\alpha| = \sum_{i=1}^n \alpha_i$. For two multi-indices $\alpha, \beta \in \mathbb{Z}^n_{\geq 0}$, we say that $\alpha \geq \beta$ if and only if $\alpha_i \geq \beta_i$ for $i = 1, 2, \ldots, n$. The sum/difference of two multi-indices is the component wise sum/difference of the indices.

Given a vector $x \in \mathbb{R}^n$ and a multi-index $\alpha \in \mathbb{Z}^n_{\geq 0}$, a *monomial* in x with total

degree $|\alpha|$ is a product of the form $x^\alpha \equiv x_1^{\alpha_1} x_2^{\alpha_2} \cdots x_n^{\alpha_n}$. We use *monomial ordering* to arrange a pair of monomials unambiguously in an ascending (or descending) order. Let $\alpha, \beta \in \mathbb{Z}_{\geq 0}^n$ be multi-indices of vector $x \in \mathbb{R}^n$. Let $\succ$ denotes a total ordering on $\mathbb{Z}_{\geq 0}^n$ such that for $\alpha, \beta \in \mathbb{Z}_{\geq 0}^n$ at least one of the following conditions is true: $\alpha > \beta$, $\alpha < \beta$, $\alpha = \beta$. A monomial ordering on $\mathbb{Z}_{\geq 0}^n$ is a *total ordering* if (i) given multi-indices $\gamma, \alpha, \beta \in \mathbb{Z}_{\geq 0}^n$ with $\alpha > \beta$, then $\alpha + \gamma > \beta + \gamma$, (ii) $\succ$ is a *well-ordering* such that every nonempty subset of $\mathbb{Z}_{\geq 0}^n$ has a smallest element. One of the most frequently used monomial ordering is the *lexicographic* (lex) order denoted as $\succ_{lex}$. We say that α and β is in lex order, $\alpha \succ_{lex} \beta$, if the left-most nonzero entry of the vector difference $\alpha - \beta$ is positive. Thus, $x^\alpha \succ_{lex} x^\beta$ holds if $\alpha \succ_{lex} \beta$. Another commonly used monomial ordering is the *graded reverse lexicographic* (grlex) order denoted as $\succ_{grlex}$. We say that α and β is in grlex order, $\alpha \succ_{grlex} \beta$, if $|\alpha| > |\beta|$ or $|\alpha| = |\beta|$ and the right-most nonzero entry of the vector difference $\alpha - \beta$ is negative.

The set of $n \times n$ real symmetric matrix is denoted as $\mathcal{S}^n$. A matrix $Q \in \mathcal{S}^n$ is *positive semidefinite* (psd) if $x^T Q x \geq 0$ for all $x \in \mathbb{R}^n$ and is *positive definite* if $x^T Q x > 0$ for all nonzero $x \in \mathbb{R}^n$. The set of $n \times n$ psd matrix is denoted as $\mathcal{S}_{\geq 0}^n$ and the set of $n \times n$ positive definite matrix is denoted as $\mathcal{S}_+^n$. We use the symbol "$\succeq$" to denote the *partial ordering* induced by $\mathcal{S}_{\geq 0}^n$ such that if $Q, R \in \mathcal{S}_{\geq 0}^n$, then $Q \succeq R$ if and only if $Q - R$ is psd.

2.1 Algebraic Geometry

At the basic level, algebraic geometry concerns with the study of the solutions (or zeros) of system of polynomial equations by focusing on the close relationship between the *geometric properties* of these solutions and the *algebraic structures* associated with them [20]. Some of the fundamental concepts in algebraic geometry includes *ideal*, *variety*, and *basis*. This section presents a review of these concepts and discusses the method of Gröbner basis for solving system of polynomial equations.

2.1.1 Ideals, varieties, and Gröbner basis

A fundamental concept in algebra is *field*. Intuitively, a field consists of a set $\mathbb{K}$ and binary operations addition ($+$) and multiplication ($\cdot$) such that if $a, b \in \mathbb{K}$ then their binary operations satisfy the associative, commutative, distributive, identitites, additive inverse, and multiplicative properties [78]. Examples of field includes the sets of real ($\mathbb{R}$), complex ($\mathbb{C}$) and rational ($\mathbb{Q}$) numbers. The set of integer numbers ($\mathbb{Z}$) is *not* a field since the only elements of $\mathbb{Z}$ that have multiplicative inverses are 1 and -1 (e.g. the multiplicative inverse of 2 is $1/2$ but $1/2 \notin \mathbb{Z}$).

Let $\mathbb{K}$ be any field. A dth order *polynomial* in the unknown $x \in \mathbb{R}^n$ with coefficients $k \in \mathbb{K}$ is a finite linear combination of monomials of the form

$$f(x,k) = \sum_{|\alpha| \leq d} k_\alpha x^\alpha, \text{ with } k_\alpha \in \mathbb{K}.$$

The set of all such polynomials form a *polynomial ring* and is denoted as $\mathbb{K}[x]$. We use the symbol $\mathbb{K}(k)[x]$ to denotes polynomial ring with unknown coefficients k in field $\mathbb{K}$ (see chapters 3-4). Unless stated otherwise, we often use the term "polynomials over $\mathbb{K}$" to denote the set of polynomials $f_i(x,k) \in \mathbb{K}[x]$ for $i = 1, \ldots, m$. We mostly consider polynomials over $\mathbb{R}$.

Given polynomial equation $f_i(x,k) = 0,\ (i = 1, \ldots, n)$, we define its *solution* as the set $\{x \in \mathbb{K}^n : f_i(x,k) = 0\}$ of common zeros in $\mathbb{K}^n$ of the polynomials.

Let $\alpha \in \mathbb{Z}^n_{\geq 0}$ be a multi-index and assume a fixed monomial ordering. Given a nonzero polynomial $f(x,k) \in \mathbb{K}[x]$, we define

- The *multidegree* of f as: $\texttt{multideg}(f) = \max(\alpha \in \mathbb{Z}_{\geq 0}), k_\alpha \neq 0$.
- The *leading monomial* of f as $\texttt{LM}(f) = x^{\texttt{multideg}(f)}$.
- The *leading coefficient* of f as: $\texttt{LC}(f) = k_{\texttt{multideg}(f)}$.
- The *leading term* of f as: $\texttt{LT}(f) = \texttt{LC}(f).\texttt{LM}(f)$.

Example 1. *Consider polynomial* $f(x,k) = 2x_1^2x_2^8 - 3x_1^5x_2x_3^4 + x_1x_2x_3^3 - x_1x_2^4$ *in* $\mathbb{R}[x]$ *where* $x = (x_1, x_2, x_3)$ *and* $k \in \mathbb{R}$. *By choosing the lex order for its monomials, we can rewrite polynomial* $f(x)$ *with monomials in a decreasing order of the form* $f(x) = -3x_1^5x_2x_3^4 + 2x_1^2x_2^8 - x_1x_2^4 + x_1x_2x_3^3$. *We then have* $\texttt{multideg}(f) = (5,1,4)$, $\texttt{LM}(f) = x_1^5x_2x_3^4$, $\texttt{LC}(f) = -3$, $\texttt{LT}(f) = -3x_1^5x_2x_3^4$.

The following definition defines an *ideal* in polynomial ring $\mathbb{R}[x]$.

Definition 1 ([20])**.** *The set* $I \subseteq \mathbb{R}[x]$ *is an* ideal *if it satisfies: (i)* $0 \in I$, *(ii)* $\forall a, b \in I \Rightarrow a + b \in I$, *and (iii)* $\forall a \in I, b \in \mathbb{R}[x] \Rightarrow a \cdot b \in I$.

Let $f_1, \ldots, f_m$ be polynomials in $\mathbb{R}[x]$ and set

$$I = \{\Sigma_{i=1}^m h_i f_i, \text{ with } h_i \in \mathbb{R}[x]\} = \langle f_1, \ldots, f_m \rangle \subseteq \mathbb{R}[x].$$

One can show that I is an ideal *generated* by $f_1, \ldots, f_m$. For ideal $I = \langle f_1, \ldots, f_m \rangle$, the set of polynomials $f_1, \ldots, f_m$ is called the *generator* of I. A set of all generators of I is called the *basis* of I. One advantage inusing the concept of ideal is that it allows for the use of different choices of generators. This is due to the fundamental result of the Hilbert's Basis Theorem [20] which states that every ideal $I \subseteq \mathbb{K}[x]$ is finitely generated (hence it has a finite basis) and therefore can always be expressed as $I = \langle f_1, \ldots, f_m \rangle$. According to the definiton of an ideal, this theorem implies that all polynomials of the form $\Sigma_{i=1}^m h_i f_i$ with $h_i \in \mathbb{K}[x]$ are also ideals generated by f_i's. Working with ideal therefore removes the dependency on particular generator and allows one to choose any generator that is more suitable for a given problem.

Now let $I = \langle f_1, \ldots, f_m \rangle \subseteq \mathbb{R}[x]$ be an ideal. For all $1 \leq i \leq m$, the set

$$\mathbb{V}(I) = \mathbb{V}(f_1, \ldots, f_m) = \{x \in \mathbb{C}^n : \ f_i(x) = 0\},$$

is called an *algebraic variety* (or simply variety) of I generated by f_i's. One may

observe that a variety $\mathbb{V}(I)$ is the set of common zeros in $\mathbb{C}^n$ (or complex solutions) of polynomial equations defined by ideal I. Given a variety $\mathcal{V} = \mathbb{V}(f_1, \ldots, f_m)$ at which polynomials $f_1, \ldots, f_m$ vanish, then by the definition of ideal, any polynomials of the form $\Sigma_{i=1}^{m} g_i f_i$ with $g_i \in \mathbb{R}[x]$ are also vanish on $\mathcal{V}$. More specifically, if ideals $I_1 = \langle f_1, \ldots, f_m \rangle$ and $I_2 = \langle g_1, \ldots, g_k \rangle$ are the same (i.e. they are generated from the same basis), then I_1 and I_2 define the same variety, i.e. $\mathbb{V}(I_1) = \mathbb{V}(I_2)$. This illustrates that the variety of an ideal is not affected by the choice of the basis [20].

From the preceeding discussions, one may see that solving a system of polynomial equations of the form $f_i(x, k) = 0,\ (i = 1, \ldots, n)$ is essentially equivalent with computing the variety $\mathbb{V}(I)$ of ideal $I = \langle f_i \rangle$. In other words, the solutions of polynomial equations $f_i = 0$ are the variety of the basis polynomials that generate ideal $I = \langle f_i \rangle$. This implies that even if the original polynomial equations are too complicated to be solved, the task of finding its solutions may often be simplified if the basis of the ideal generated by these polynomials can be computed. This fact is one of the basic approaches used in algebraic geometry for solving system of polynomial equations. In particular, this approach can always be used since the Hilbert Basis Theorem guarantees the existence of a finite basis of any ideal. A basis set that is useful for this approach is the Gröbner basis which can be computed using the freely available computer algebra softwares [22, 46]. Before we dwell on to the concept of Gröbner basis, we will first discuss a fundamental method for checking the existence or emptiness of algebraic varieties of an ideal.

2.1.2 Existence of algebraic varieties

One method for checking the existence (or emptiness) of algebraic variety of polynomials over $\mathbb{C}$ is using the result from the Hilbert's *nullstellensatz* stated below.

Theorem 2.1.1 (Nullstellensatz [20])**.** *Let $I \subseteq \mathbb{C}[x]$ be an ideal generated by a finite family of polynomials $(f_i)_{i=1,\ldots,m}$ in $\mathbb{C}[x]$. The following statements are equivalent:*

1. *The set*
$$\{x \in \mathbb{C}^n \mid f_i(x,k) = 0, \quad i = 1,\ldots,m\} \tag{2.1}$$
is empty.

2. *The polynomial* 1 *belongs to the ideal* I*, i.e.,* $1 \in I$*.*

3. *The ideal is equal to the whole polynomial ring:* $I = \mathbb{C}(k)[x]$*.*

4. *There exist polynomials* $g_i(x,k) \in \mathbb{C}[x]$ *such that:*
$$f_1(x,k)g_1(x,k) + \cdots + f_m(x,k)g_m(x,k) = 1. \tag{2.2}$$

The nullstellensatz essentially states that if for ideal $I = \langle f_i(x,k)\rangle$ there exist polynomials $g_i(x,k)$'s such that (2.2) is satisfied, then the complex solutions of polynomial equations $f_i(x,k) = 0$ does *not* exists (i.e. the set (2.1) is empty). The existence of polynomials $g_i(x,k)$'s therefore *certifies* the infeasibility of the complex solutions. The following example illustrates an application of the nullstellensatz.

Example 2. *Let* $I = \langle f_1, f_2\rangle \subseteq \mathbb{C}[x]$ *with* $x = (x_1, x_2)$, $f_1(x) = x_1^2$, $f_2(x) = 1 - x_1x_2$. *Note that* $\mathbb{V}(f_1, f_2) = \emptyset$ *since there exist no* $x \in \mathbb{C}^2$ *that satisfies* $f_1(x) = f_2(x) = 0$. *By the nullstellensatz, there exist* $g_1(x), g_2(x) \in \mathbb{C}^2[x]$ *such that* $f_1g_1 + f_2g_2 = 1$. *It can be verified that one of such* $g_i(x)$*'s are* $g_1(x) = 1 - x_1x_2 + x_2^2$ *and* $g_2(x) = 1 + x_1x_2 - x_1^2$.

A generalization of the nullstellensatz for proving the existence of solutions over the reals $\mathbb{R}$ is given by the *positivstellensatz* (p-satz) [103]. In particular, the p-satz gives a sufficient condition for the infeasibility of *real* solutions to a system of polynomial equalities and inequalities. In order to state the main result from the psatz theorem, let's first recall the definitions of *monoid* and *cone* [20, 78].

Consider polynomials $f_i(x,k) \in \mathbb{R}[x]$ for $i = 1,\ldots,m$. The *multiplicative monoid* $\mathcal{M}(f_i)$ generated by f_i is the set of finite products of the elements of f_i (including the identity and the empty product). A *cone* $\mathcal{C}$ of $\mathbb{R}[x]$ is a subset of $\mathbb{R}[x]$ such that (i) $a, b \in \mathcal{C} \Rightarrow a + b \in \mathcal{C}$, (ii) $a, b \in \mathcal{C} \Rightarrow a \cdot b \in \mathcal{C}$, and (iii) $a \in \mathbb{R}[x] \Rightarrow a^2 \in \mathcal{C}$. Given a set $S \subseteq \mathbb{R}[x]$, let $\mathcal{C}(S)$ be the smallest cone of $\mathbb{R}[x]$ that contains S. One may verify

that $\mathcal{C}(\emptyset)$ is the smallest cone in $\mathbb{R}[x]$ which can be expressed as a sum of squares. The cone associated to a finite set $S = \{a_1, \ldots, a_m\} \subseteq \mathbb{R}[x]$ can be expressed as

$$\mathcal{C}(S) = \{f + \Sigma_{i=1}^{r} g_i b_i \mid f, g_1, \ldots, g_r \in \mathcal{C}(\emptyset), \text{ and } b_1, \ldots, b_r \in \mathcal{M}(a_i)\}.$$

The following theorem is due to Stengle [103].

Theorem 2.1.2 (Positivstellensatz, [103]). *Let $\{f_i\}_{i=(1,\ldots,s)}$, $\{g_j\}_{j=(1,\ldots,t)}$ and $\{h_\ell\}_{\ell=(1,\ldots,u)}$ be finite families of polynomials in $\mathbb{R}[x]$. Denote by $\mathcal{C}$ the cone generated by $\{f_i\}_{i=(1,\ldots,s)}$, $\mathcal{M}$ the multiplicative monoid generated by $\{g_j\}_{j=(1,\ldots,t)}$, and I the ideal generated by $\{h_\ell\}_{\ell=(1,\ldots,u)}$. Then, the following properties are equivalent.*

- *The set*
$$\{x \in \mathbb{R}^n \mid f_i(x,k) \geq 0,\ g_j(x,k) \neq 0,\ h_\ell(x,k) = 0\} \tag{2.3}$$
is empty for $i = (1,\ldots,s)$, $j = (1,\ldots,t)$ and $\ell = (1,\ldots,u)$.
- *There exist $f \in \mathcal{C}$, $g \in \mathcal{M}$, and $h \in I$ such that $f + g^2 + h = 0$.*

The p-satz theorem essentially gives a sufficient condition for the non-existence of solutions to a system of polynomial equalities/inequalities. Such non-existence (or emptiness) of solutions is certified by the existence of *positivstellensatz refutation* in term of polynomials f, g and h. The following example illustrates one example use of the p-satz.

Example 3. *Consider the ideal $I = \langle x^2 + x + 1\rangle \subset \mathbb{R}[x]$. Clearly $\mathbb{V}(I)$ always exists in $\mathbb{C}$ and is given by $(-1 \pm \sqrt{-3})/2$. The p-satz can be used to verify that $\mathbb{V}(I)$ in $\mathbb{R}$ indeed does not exist. By letting*

$$f = \left(\sqrt{4/3}(x + 1/2)\right)^2, \quad g = 1, \quad h = -\frac{4}{3}(x^2 + x + 1),$$

the condition $f + g^2 + h = 0$ in p-satz theorem is satisfied, proving the emptiness of $\mathbb{V}(I)$ in $\mathbb{R}$.

2.1.3 The method of Gröbner basis

In this section, we present a technique for solving system of polynomial equations using the method of Gröbner basis. In particular, the discussion will be presented in the context of the Buchberger algorithm [9] which is one of the early algorithms used to compute the Gröbner basis.

2.1.3.1 The Buchberger algorithm

For a given ideal $I \subseteq \mathbb{K}[x]$ with a finite set of generators, the Buchberger algorithm takes these generators as an input and return a Gröbner basis G of I as an output in a finite steps. At the heart of the Buchberger algorithm is the *division algorithm* which generalizes the concept of Euclidean division algorithm for canceling out a polynomial's high-order leading monomial to obtain another polynomial with lower order leading monomial. To present the basic idea in the Buchberger algorithm, we will first discuss the concepts of the division algorithm and the $S-$polynomial.

Consider a polynomial $f(x)$ and let $S = \{s_1(x), s_2(x), \ldots, s_q(x)\}$ be a list of polynomial divisors. For a fixed monomial ordering $\succ$, a division algorithm is one that finds polynomials $\lambda_i(x)$ and a remainder term $\overline{f(x)}^S$ which satisfy

$$f(x) = \sum_{i=1}^{q} \lambda_i(x) s_i(x) + \overline{f(x)}^S, \tag{2.4}$$

and such that

- $\mathtt{LT}(\overline{f(x)}^S)$ is not divisible by any $\mathtt{LT}(s_i(x))$,
- $\mathtt{LT}(\overline{f(x)}^S) < \mathtt{LT}(f(x))$,
- $\mathtt{LT}(\lambda_i(x)s_i(x)) < \mathtt{LT}(f(x))$.

Let α and β be multi-indices. The *least common multiple* (LCM) of monomials x^α and

x^β is defined as

$$\texttt{LCM}(x^\alpha, x^\beta) = x_1^{\max(\alpha_1,\beta_1)} x_2^{\max(\alpha_2,\beta_2)} \dots x_n^{\max(\alpha_n,\beta_n)}.$$

The $S-$polynomial of a pair of polynomials f_1 and f_2 is defined as

$$S(f_1, f_2) = \frac{x^\gamma}{\texttt{LT}(f_1)} f_1 - \frac{x^\gamma}{\texttt{LT}(f_2)} f_2, \tag{2.5}$$

where $x^\gamma = \texttt{LCM}(\texttt{LM}(f_1), \texttt{LM}(f_2))$. Based on the definitions of division algorithm and $S-$polynomial, a Gröbner basis of an ideal I is formally defined as follows [9].

Theorem 2.1.3. *Let $I \subseteq \mathbb{K}[x]$ be an ideal with basis $G = \{g_1, \dots, g_q\}$. Then G is a Gröbner basis for I if and only if the remainder on division of every $S-$polynomial $S(g_i, g_j),\ (i \neq j)$ by G is zero.*

The definition of Gröbner basis in theorem 2.1.3 leads to the Buchberger algorithm [9] for finding a Gröbner basis of an ideal with finite generators. This algorithm essentially computes the $S-$polynomials of each generator pair and check whether the reminders upon division of the generator by each of the $S-$polynomial are zero. If there exist non-zero remainders, the original set of generator is extended by adding those non-zero remainders and then the iteration is repeated over the extended generator. A Gröbner basis is given by those extended generators whose $S-$polynomials divide the elements of the extended generator with zero remainder. As shown in [9], the Buchberger algorithm always terminates in a finite steps and so a Gröbner basis of an ideal can always be computed. In the following example, we illustrate the basic idea of Buchberger algorithm for computing the algebraic variety of an ideal.

Example 4. *Consider an ideal $I = \langle f_1, f_2 \rangle$ generated by two polynomials $f_1 = 2x_1^2 - 4x_1 + x_2^2 - 4x_2 + 3$ and $f_2 = x_1^2 - 2x + 3x_2^2 - 12x_2 + 9$. We will apply the Buchberger algorithm to compute a Gröbner basis of I. To begin, we use the generator of I as*

the initial Gröbner basis $G_0 = \{f_1, f_2\}$ *and consider the lex order* $x \succ_{lex} y$ *for the monomials of* I. *One may verify that ideal* I *is characterized by* $\gamma = (2, 0), \texttt{LM}(f_1) = 2x^2$ *and* $\texttt{LM}(f_2) = x^2$. *The* $S-$*polynomial of* f_1, f_2 *is then given by*

$$S(f_1, f_2) = \frac{x_1^2}{2x_1^2} f_1 - \frac{x_1^2}{x_1^2} f_2 = -\frac{5}{2}x_2^2 + 10x_2 - \frac{15}{2}.$$

Upon division of $S(f_1, f_2)$ *by* G_0,*it can be verified that the reminder* r_{12} *is simply* $S(f_1, f_2) \neq 0$. *We now define* $f_3 = S(f_1, f_2)$ *and then extend the Gröbner basis* G_0 *to* $G_1 = \{f_1, f_2, f_3\}$. *We repeat the computation of* $S-$*polynomial for the pair* (f_1, f_3) *and* (f_1, f_3). *Note that we don't need to recompute* $S(f_1, f_2)$ *as it does not change.*

$$S(f_1, f_3) = 4x_1^2x_2 - 3x_1^2 - 2x_1x_2^2 + \frac{1}{2}x_2^4 - 2x_2^3 + \frac{3}{2}x_2^2,$$
$$S(f_2, f_3) = 4x_1^2x_2 - 3x_1^2 - 2x_1x_2^2 + 3x_2^4 - 12x_2^3 + 9x_2^2.$$

Dividing these $S-$*polynomials by* G_1 *gives*

$$S(f_1, f_3)/G_1 = (2x_2 - 3/2)f_1 + (4x_1 - x_2^2 + 4x_2 - 3)f_3/5,$$
$$S(f_2, f_3)/G_1 = (2x_2 - 3/2)f_1 + (4x_1 - 6x_2^2 + 4x_2 - 3)f_3/5,$$

from which we have $r_{13} = r_{23} = 0$. *Thus, a Gröbner basis of* I *is* $\mathbb{G} = \{f_1, f_2, f_3\}$.

The Buchberger algorithm has been implemented in many computer algebra softwares such as Singular [22] and Macaulay2 [46]. One issue with the implementation of the Buchberger algorithm is that it has doubly exponential worst case complexity in the number of unknown variables. As shown in [31], when polynomial $f(x)$ in n unknown variables has a total degree not exceeding d, then the degree of polynomials in its Gröbner basis G is bounded by $2(d^2/2 + d)^{2^{n-1}}$. This bound is doubly exponential with respect to n but only polynomial with respect to d. The computation of Gröbner basis for high dimensional systems will therefore requires a large amount

of computer memory. Nevertheless, the use of Buchberger algorithm for computing Gröbner bases in many applications have shown that such worst case bound is not frequently encountered .

We point out that the Gröbner basis of an ideal is not unique. For instance, another Gröbner basis for ideal in example 4 is

$$\mathbb{G} = \{x_2^2 - 4x_2 + 3,\ x_1^2 - 2x_1 + 3x_2^2 - 12x_2 + 9\}$$

which is obtained from SINGULAR computer algebra [22] using the code snippet in listing 2.1. In this listing, the command `ring` declares a polynomial ring '`R`' with unknown variables '`x1,x2`' and real coefficients '`0`'. The monomial ordering in `R` is set to be the lex ordering '`lp`'. The command `poly` defines polynomial functions '`f1,f2`' whereas the command `ideal` defines the ideal `I`. Finally, a Gröbner basis '`G`' of ideal '`I`' is computed using the command `groebner(I)`.

Listing 2.1: Computing Gröbner basis of example 4 using SINGULAR.

```
> ring R = 0,(x1,x2),lp;
> poly f1 = 2*x1^2 - 4*x1 + x2^2 - 4*x2 + 3;
> poly f2 = x1^2 - 2*x1 + 3*x2^2 - 12*x2 + 9;
> ideal I = (f1,f2);
> ideal G = groebner(I);
> G;
G[1]=x2^2-4*x2+3
G[2]=x1^2-2*x1+3*x2^2-12*x2+9
```

2.1.3.2 Elimination and Extension Theorems

It is now intuitive to see how the Gröbner basis can be helpful to solve a system of polynomial equations. As shown in example 4, one element of the Gröbner basis is

given by $f_3 = -5x_2^2/2 + 10x_2 - 15/2$, in which variable x_1 has been *eliminated*. Since f_3 is a univariate polynomial, it can be solved easily using the root-finding methods. If the solution x_2 is *extended* through substitution to f_1 or f_2, one can then recover the whole solutions to $f_i = 0,\ i = (1, 2)$. This example therefpre illustrates that the method of Gröbner basis involves two main steps namely the *elimination* and the *extension* steps.

For given Gröbner basis of an ideal, the elimination step computes the rth *elimination ideal* of I defined as follows.

Definition 2. *Given $I = \langle f_1, \ldots, f_q \rangle \subseteq \mathbb{R}[x_1, \ldots, x_n]$, the rth elimination ideal I_r is the ideal of $\mathbb{R}[x_{r+1}, \ldots, x_n]$ defined by*

$$I_r = I \cap \mathbb{R}[x_{r+1}, \ldots, x_n].$$

One may see that the elimination ideal is obtained by eliminating subsets of unknown variables in the original ideal. For a given Gröbner basis of ideal I with lex monomial order, the Elimination Theorem can be used to compute a Gröbner basis for the rth elimination ideal of I.

Theorem 2.1.4 (Elimination Theorem [20])**.** *Let $I \subseteq \mathbb{R}[x_1, \ldots, x_n]$ be an ideal and let $\mathbb{G}$ be a Gröbner basis of I with respect to lexicographic order $x_1 \succ_{lex} x_2 \succ_{lex} \cdots \succ_{lex} x_n$. Then, for every $0 \leq r \leq n$, the set*

$$\mathbb{G}_r = \mathbb{G} \cap \mathbb{R}[x_{r+1}, \ldots, x_n]$$

is a Gröbner basis of the rth elimination ideal I_r of I.

The variety $\mathbb{V}(I_r)$ of the rth elimination ideal I_r can be obtained by solving the zeros of its Gröebner basis, $\mathbb{G}_r$. The variety $\mathbb{V}(I_r)$, however, is only a subvariety of the original ideal I (i.e. $\mathbb{V}(I_r) \subset \mathbb{V}(I)$) because it is only defined over variables that are

not eliminated from I. Thus it only serves as partial solution and should be extended to the total solutions of the original ideal I. Such extension, however, is not always guaranteed to be feasible. The Extension Theorem gives the conditions when such extension is feasible.

Theorem 2.1.5 (Extension Theorem [20]). *Let $I = \langle f_1, \ldots, f_m \rangle \subset \mathbb{R}[x]$ and let I_1 be the first elimination ideal of I. For each $1 \leq i \leq m$, write f_i in the form*

$$f_i = g_i(x_2, \ldots, x_n)x_1^{N_i} + \text{ terms in which } x_1 \text{ has degree} < N_i, \tag{2.6}$$

where $N_i > 0$ and $g_i \in \mathbb{R}[x]$ is nonzero. Assume we have a partial solution $(x_2^*, \ldots, x_n^*) \in \mathbb{V}(I_1)$. If $(x_2^*, \ldots, x_n^*) \notin \mathbb{V}(g_1, \ldots, g_m)$, then there exists $x_1^* \in \mathbb{C}$ such that $(x_1^*, \ldots, x_n^*) \in \mathbb{V}(I)$.

From the above discussion, one may see that the goal of the elimination step is to iteratively reduces the original problem into problems with smaller number of variables for which partial solutions can be computed. The extension step then back substitutes these partial solutions to the original ideal to obtain the total solution. The importance of Gröbner basis in these scheme is that it allows for a systematic execution of the elimination step. The following example illustrates the concept of Elimination and Extension Theorems for ideal in example 4.

Example 5. *Consider the ideal and Gröbner basis in example 4. We will use this example to show how the Gröbner basis, combined with elimination and extension steps, helps the computation of an algebraic variety of ideal $I = \langle f_1, f_2 \rangle \subseteq \mathbb{R}[x_1, x_2]$. Firs, we let $I_2 = \langle I \cap \mathbb{R}[x_2] \rangle$ which gives $I_2 = 0$. This means that any value of $x_2 = c_2$ is a partial solution and $c_2 \in \mathbb{R}$. We now evaluate whether this partial solution extends to the total solution $x_1 = c_1, x_2 = c_2$. Applying the Extension Theorem to the case of $\mathbb{R}[x_2] \subset \mathbb{R}[x_1, x_2]$, one can verify that the partial solution $x_2 = c_2$ extends to $x_1 = c_1, x_2 = c_2$ provided that the coefficient of the highest power of x_1 in the*

Gröbner basis f_1 or f_2 is not zero at $x_2 = c_2$. The coefficients of the highest power of x_1 in f_1 and f_2 are given by 1 and 2, respectively, which are not zero regardless of the value of x_2. This implies that the solution $x_2 = c_2$ always extends to the total solution $x_1 = c_1, x_2 = c_2$. Now using the Elimination Theorem, the Gröbner basis for I_2 is given by

$$\mathbb{G}(I_2) = \mathbb{G} \cap \mathbb{R}[x_2] = -\frac{5}{2}x_2^2 + 10x_2 - \frac{15}{2}.$$

Since the variety of an ideal is equivalent to the variety of its basis, then the partial solution x_2 is given by the zeros of $\mathbb{G}(I_2)$ which are $x_2^* = 1$ or $x_2^* = 3$. We have shown previously that this partial solution extends to the total solution and so we can directly substitutes it to either f_1 or f_2 and then solve for their corresponding zeros. Upon the substitution, one may verify that the algebraic variety of $I = \langle f_1, f_2 \rangle$ is given by

$$\mathbb{V}(I) = \{(x_1^*, x_2^*) \, : \, (0,1), \, (0,3), \, (2,1), \, (2,3)\},$$

which are the four intersection points between ellipses f_1 and f_2 shown in figure 2.1.

2.1.4 Toric ideal

This section introduces a class of ideal called *toric ideal* that will be central in the discussion of chapter 3.

Let $\mathcal{A} = (\alpha_1, \alpha_2, \ldots, \alpha_n) \in \mathbb{Z}^{m \times n}$ be a matrix whose ith column is denoted by the vector α_j for $j = 1, 2, \ldots, n$. For $x \in \mathbb{R}^n$, let $\psi_j(x) = \prod_{i=1}^m x_i^{\alpha_{ij}}$, $(j = 1, \ldots, n)$ be a mapping $\psi \, : \, \mathbb{C}^m \to \mathbb{C}^n$. Suppose we are interested to find the solution of a sparse polynomial equations of the form

$$c\psi(x) = 0. \tag{2.7}$$

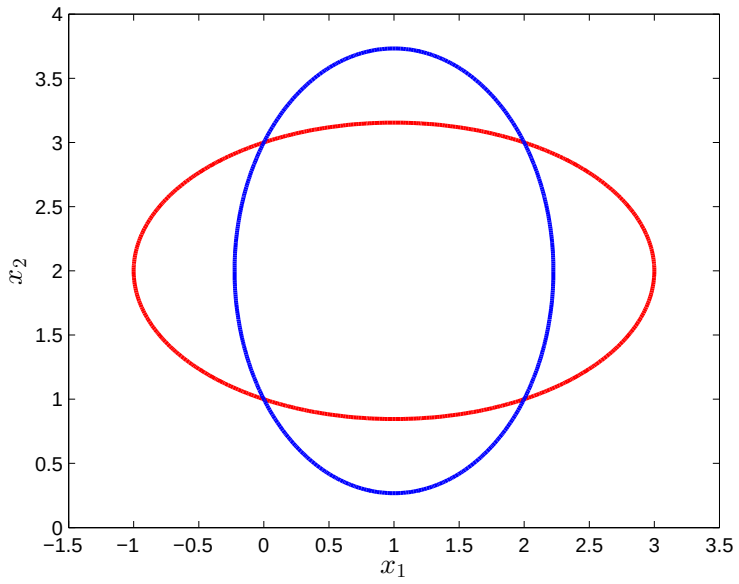

Figure 2.1. Algebraic variety of $I = \langle f_1, f_2 \rangle$ in example 5.

Our objective is to find some other polynomials $f_1, \ldots, f_k \in \mathbb{C}[z_1, \ldots, z_n]$ that generate linear equations of the form

$$cz = 0, \quad f_1(z) = 0, f_2(z) = 0, \ldots, f_k(z) = 0. \tag{2.8}$$

Notice that if z in (2.8) is in the image of ψ in (2.7), then the solutions of z in (2.8) will lead to the solutions of (2.7). If this condition is satisfied, then the following relationships between equations (2.8) and (2.7) can be obtained.

$$\begin{aligned} f_i(z) = 0 \text{ for all } z \in im(\psi) \quad &\Leftrightarrow \quad f_i(\psi(x)) = 0 \text{ for all } x \in \mathbb{C}^m. \\ f_i(\psi(x)) = 0 \text{ for all } x \in \mathbb{C}^n \quad &\Leftrightarrow \quad f_i(x^{\alpha_1}, \ldots, x^{\alpha_n}) \text{ for all } x \in \mathbb{C}^m. \end{aligned}$$

What is important to observe is that polynomial systems in (2.7) generate an ideal in $\mathbb{C}[z_1, \ldots, z_n]$.

Lemma 2.1.6. *Let* $\mathcal{A} = (\alpha_1, \ldots, \alpha_n) \in \mathbb{Z}^{m\times n}$. *The set of polynomials*

$$I_{\mathcal{A}} = \{f \in \mathbb{C}[z_1, \ldots, z_n] \mid f(x^{\alpha_1}, \ldots, x^{\alpha_n}) = 0, \ \textit{for all } x \in \mathbb{C}^m\} \tag{2.9}$$

is an ideal in $\mathbb{C}[z_1, \ldots, z_n]$.

Proof. The proof is based on the definition of ideal. First note that $0 \in I_{\mathcal{A}}$. Now for $f, g \in I_{\mathcal{A}}$ we have $f(x^{\alpha_1}, \ldots, x^{\alpha_n}) + g(x^{\alpha_1}, \ldots, x^{\alpha_n}) = 0 + 0 = 0$ which implies $f + g \in I_{\mathcal{A}}$. Finally, if $f \in I_{\mathcal{A}}$ and $g \in \mathbb{C}[z]$ then $f(x^{\alpha_1}, \ldots, x^{\alpha_n}) \cdot g(x^{\alpha_1}, \ldots, x^{\alpha_n}) = 0 \cdot g(x^{\alpha_1}, \ldots, x^{\alpha_n}) = 0$ and so $f \cdot g \in I_{\mathcal{A}}$. Thus $I_{\mathcal{A}}$ satisfies all the properties of an ideal and the statement is proved. □

Ideal $I_{\mathcal{A}}$ with properties stated in the above lemma is called *toric ideal* and its variety is called *toric variety* [4, 106]. Toric ideal arise in many applications such as integer programming [107] and chemical reaction network models [43]. One important property of toric ideal is that there exist efficient algorithms to compute its Gröbner basis with less computation complexity than the standard Buchberger algorithm [106]. One of such algorithms will be discussed in more details in chapter 3.

Example 6. *This example illustrates the concept of toric ideal described above. Suppose we are interested in solving the following polynomial equation defined on* $\mathbb{C}[x]$.

$$x - 2x^2 + x^3 = 0. \tag{2.10}$$

Our goal is to solve this equation implicitly. Let $\Psi(x) = [\psi_1(x), \psi_2(x), \psi_3(x)]^T$ *with* $\psi_1(x) = x, \psi_2(x) = x^2, \psi_3(x) = x^3$ *and let* $c = [1, -2, 1]$ *such that equation (2.10) can be rewritten as* $c\Psi(x) = 0$. *Now let's introduce the variables* $z_1 = x^2$, $z_2 = x^2$, $z_3 = x^3$

defined on $\mathbb{C}[z]$ *with* $z = (z_1, z_2, z_3)$ *and consider the following set of equations*

$$\begin{aligned} 0 &= z_1^2 - z_2 \\ 0 &= z_1^3 - z_3 \\ 0 &= z_1 z_2 - z_3. \end{aligned} \tag{2.11}$$

The above "binomial equations" are the toric ideal associated with polynomial equation (2.10). Notice that if $x^* = \{x \,|\, x - 2x^2 + x^3 = 0\}$ *is a solution to equation (2.10) then* $z^* = \Psi(x^*)$ *is also a solution to (2.11). For example,* $x = 1$ *is a solution of (2.10) and one may verify that* $z = (\psi_1(1),\ \psi_2(1),\ \psi_3(1)) = (1, 1, 1)$ *is also a solution to (2.11). This observation suggests that we can solve polynomial equation (2.10) indirectly in the following steps: (i) compute the kernel of* c *which satisfies* $c\Psi(x) = 0$*, (ii) compute the solution of the binomial equations in (2.11), (iii) compute the intersection of the solutions from steps (i) and (ii). For our example, it is straightforward to verify that* $z^* = (1, 1, 1)$ *is a solution to the binomial system (2.11). On the other hand,* $v^* = (1, 1, 1)$ *is a kernel of vector* c *(i.e.* v^* *satisfies* $cv* = 0$*). Obviously, the intersection between* z^* *and* v^* *is given by* $z^* \cap v^* = (1, 1, 1)$ *which is satisfied for* $x = 1$*. The key point in this approach is that there are algorithms (with less computational complexity than the Buchberger algorithm) that can be used to compute the solution (or the Gröbner basis) of toric ideal (2.11) (i.e. step (ii)) [106, see also chapter 3]. This approach would then provides more efficient computation methods for solving general polynomial equations of the form (2.10).*

2.2 SOS Optimization

A fundamental problem that arise in many applications is that of proving the global nonnegativity of some functions in several variables. More specifically, given a function $f(x)$ in variables $x = (x_1, \ldots, x_n)$, one is often required to check the validity

of the proposition $f(x) \geq 0$ for all x. From a computational stand point, this problem is in general NP-hard (Non-deterministic Polynomial-time hard) which means that the validity of the proposition cannot be decided in polynomial time. However, if function $f(x)$ is a *multivariates polynomial*, a checkable condition for proving the validity of such proposition is available through the use of SOS decomposition technique [87, 88]. This section presents a brief introduction to SOS decomposition techniques and its connection with semidefinite programming (SDP). In particular, a fundamental result introduced in [87, 88] on the equivalence between SDP and SOS optimization for proving the nonnegativity of multivariate polynomials is discussed. The SOS optimization technique discussed in this section is the main computational approach that will be used in our proposed methods to forecast the onset of regime shifts (chapters 4 - 5).

The presented materials are mainly drawn from [87, 88] and so interested readers are encouraged to consult these references for more detailed expositions and proofs.

2.2.1 SOS decomposition

Throughout this section, the polynomial $f(x)$ is defined over the reals, $\mathbb{R}$.

A polynomial $f(x, k)$ is said to be *nonnegative* or *positive semidefinite* (psd) if $f(x, k) \geq 0$ for all $x \in \mathbb{R}^n$. A necessary condition which guarantees a polynomial to be psd is that its total degree is even. A class of polynomial systems for which this condition is always satisfied is the SOS polynomials.

Definition 3. *We say that the polynomial $f(x)$ is SOS if it can be rewritten as $f(x) = \sum_{i=1}^{\ell} q_i^2(x)$ for some set ℓ of polynomials $q_i(x), i = 1, \ldots, \ell$.*

Clearly, an SOS polynomial $f(x)$ is also psd. We use the symbol $\mathcal{P}_n^{2d}$ to denote the set of SOS polynomials in n unknown variables with degree less than or equal to $2d$.

Now consider polynomial $f(x, k) = \sum_{|\alpha| \leq 2d} k_\alpha x^\alpha \in \mathbb{R}(k)[x]$ where $f \in \mathcal{P}_n^{2d}$. One

may verify that the number of coefficients of $f(x,k)$ equals $\binom{n+2d}{2d}$. Let

$$[x]_d \doteq [1, x_1, \ldots, x_n, x_1^2, x_1x_2, \ldots, x_n^d]^T,$$

be the vector of all $\binom{n+d}{d}$ monomials in x of degree less than or equal to d. Let Q be an $\binom{n+d}{d} \times \binom{n+d}{d}$ symmetric matrix and consider the equation

$$f(x,k) = [x]_d^T Q [x]_d. \tag{2.12}$$

The following theorem states that $f(x,k)$ is SOS if it can be decomposed as in (2.12).

Theorem 2.2.1 ([87]). *A polynomial $f(x,k) = \sum_{|\alpha|\leq 2d} k_\alpha x^\alpha$ of degree $2d$ in n variables is SOS if and only if there exists $Q \in \mathcal{S}_{\geq 0}^{\binom{n+d}{d}}$ satisfying (2.12).*

The symmetric psd matrix Q is known as Gram matrix and it satisfies the decomposition $Q = V^T V$. This implies that the decomposition (2.12) can be written as

$$f(x,k) = [x]_d^T Q [x]_d = [x]_d^T V^T V [x]_d = (V[x]_d)^T (V[x]_d),$$

which satisfies the condition in definition 3. Thus, any polynomials that can be decomposed as in (2.12) is always a psd function.

Now consider the decomposition in (2.12) and let's index the elements of matrix Q in this decomposition by the $\binom{n+d}{d}$ monomials in $[x]_d$. One may verify that the following relationship between the coefficients of $f(x,k)$ and the elements of Q holds.

$$k_\alpha = \sum_{i+j=\alpha} Q_{ij}, \quad Q \succeq 0. \tag{2.13}$$

Equation (2.13) is a system of $\binom{n+2d}{2d}$ linear equations relating the entries of matrix Q and the coefficients k_α of $f(x,k)$. This relationship therefore suggests that the problem of finding an SOS decomposition of a polynomial in (2.12) boils down to the

problem of searching a psd matrix Q for which equality (2.13) holds. This is a well established problem which can be solved using SDP.

2.3 SDP and SOS optimization

An SDP is an optimization problem of the form

$$\begin{aligned} \min \quad & \langle c, x \rangle \\ \text{subject to} \quad & \langle A_i, x \rangle = b_i \quad \text{for } i = 1, \ldots, m, \\ & x \succeq 0, \end{aligned} \tag{2.14}$$

where $x \in \mathcal{S}^n_{\geq 0}$ is the decision variable, $b \in \mathbb{R}^m$, $c, A_i \in \mathcal{S}^n_{\geq 0}$ are given symmetric positive semidefinite matrices, and $\langle X, Y \rangle \doteq Tr(X^T Y) = \sum_{ij} X_{ij} Y_{ij}$. The first constraint in (2.14) defines an affine subspace whereas the second constraint defines a positive semidefinite cone $\mathcal{S}^n_{\geq 0}$ of x. Both of these sets are convex and so their intersection (i.e. the set of feasible solution x) is also a convex set. Since the objective in (2.14) is a linear function, one may view an SDP as an optimization of a linear functional over a convex set. Such convex property of SDP implies that the *primal* formulation in (2.14) has a *weak dual* formulation of the form

$$\begin{aligned} \max \quad & \langle b, y \rangle \\ \text{subject to} \quad & \Sigma_{i=1}^m y_i A_i \quad \text{for } i = 1, \ldots, m, \end{aligned} \tag{2.15}$$

where $y \in \mathbb{R}^m$. One advantage of this duality is that any feasible solution of the dual problem (2.15) gives a lower bound on the achievable value of the primal problem (2.14). Conversely, any feasible solutions of the primal formulation (2.14) provide upper bounds for the dual formulation in (2.15). Depending on the level of problem complexities, one can therefore use either the primal or the dual formulations of the SDP. In term of computational implementation, there exist efficient numerical

softwares for solving SDPs (2.14)-(2.15) such as Sedumi [105], SDPT3 [113], etc.

Remark 2.3.1. Note that SDP can be viewed as a generalization of linear programming (LP). Recall that the standard formulation of an LP problem is given by [6]

$$\begin{aligned} \min \quad & c \cdot x \\ \text{s.t.} \quad & a_i \cdot x = b_i, \qquad i = 1, \ldots, m \\ & x \in \mathbb{R}^n_{\geq 0} \end{aligned} \tag{2.16}$$

where x is a *vector* of n variables and $\mathbb{R}^n_{\geq 0} \equiv \{x \in \mathbb{R}^n \mid x \geq 0\}$ is an n dimensional nonnegative orthant. On the other hand, variables x in SDP formulation is a *matrix* which can be viewed as "vector" in the cone of symmetric positive semidefinite matrix $\mathcal{S}^n_{\geq 0}$. This implies that if the condition $x \in \mathbb{R}^n_{\geq 0}$ in the LP formulation states that each element of vector x should be nonnegative, then the condition $x \in \mathcal{S}^n_{\geq 0}$ in the SDP formulation can be viewed as stating that each of the *eigenvalues* of matrix x should be nonnegative. An LP formulation can therefore be viewed as a special case of an SDP formulation and so many computational properties of LP problem can be extended to SDP problem. Some of the LP properties that do not extend to SDP are mentioned below [60].

- A feasible solution of an LP problem always achieve its optima. On the other hand, the solutions of SDP problem may or may not achieve their optima and so there may be a finite/ infinite duality gap between the solutions of the primal and the dual formulation.
- While there exist finite algorithms (such as simplex) for solving an LP problem, there is no finite algorithm for solving an SDP problem. In other words, SDP formulations do not have direct analog of the "basic feasibility problem" [6] found in LP.

The connection between the feasibility of SOS decomposition (2.12) and the SDP formulation arise from the simultaneous requirements for matrix Q to satisfy both the positive definiteness condition and the linear equalities in (2.13). One can readily see that such requirement in fact is equivalent with the primal formulation (2.14) of

an SDP. This observation then suggests that the search of an SOS decomposition of a polynomial function can be formulated as an SDP. This is the fundamental result proved in [87, 88].

Theorem 2.3.2 ([87])**.** *The existence of SOS decomposition of a polynomial in n variables of degree $2d$ can be decided by solving an SDP feasibility problem.*

The result in theorem 2.3.2 is the basis for the formulation of SOS program or SOS optimization. An SOS optimization is a convex optimization with SOS polynomials constraints. In general, an SOS optimization takes the form

$$\begin{array}{ll} \min & c^T a \\ \text{subject to} & q_0 + \sum_{i=1}^{\ell} a_i q_i(x) \quad \text{is SOS.} \end{array} \tag{2.17}$$

Using the SOS decomposition in (2.12) one may see that the SOS constraints in (2.17) can be formulated as constraints in either the primal or the dual formulations of SDPs (2.14)-(2.15). It is therefore clear that the SOS optimization (2.17) is equivalent with the SDPs (2.14)-(2.15). There are various SOS programming tools that can be used to solve the SOS optimization (2.17) including SOSTOOLS [90], GloptiPoly [55], and YALMIP [75]. In general, these softwares are parser codes which transform the SOS optimization (2.17) into SDP formulations (2.14)-(2.15) and then use the available SDP solver codes such as Sedumi [105] and SDPT [113]to obtain the optimal solution. The SOS optimization method therefore provides a means to simplify a non standard optimization problem into a more solvable SDP problem.

CHAPTER 3

EQUILIBRIUM PARAMETERIZATION OF NONNEGATIVE SYSTEMS WITH KINETIC REALIZATION

This chapter discusses a method for computing a parameterization of system's equilibrium in a class of *nonnegative systems with kinetic realization*. A dynamical system

$$\dot{x}(t) = f(x, k), \quad x(0) = x_0,$$

whose state $x(t)$ depends on parameter k is said to be *nonnegative* if and only if $f(x, k) \geq 0$ for all x and $t \geq 0$. This system is said to have a kinetic realization if there exists a constant matrix N and a vector of monomials $v(x, k)$ such that $f(x, k) = Nv(x, k)$. Dynamical systems with kinetic realization originate from differential equation models of chemical reaction networks (CRN) [114, 17, 35]. One important property of kinetic realization is that their special structure allows one to compute a parameterization of the system's equilibria as a rational function of the system parameters and some convex parameters. This parameterization method was first proposed in [43, 44] and is based on the concept of *toric variety* from algebraic geometry [3, 4]. The main advantage of such parameterization is that it helps simplify the analysis of the system's properties (stability, bifurcation, etc.).

The first two sections of this chapter review the equilibrium parameterization method proposed in [43, 44] using a CRN model. At the end of the chapter, we show that this parameterization can also be applied to a larger class of systems other than that arising from CRN. We denote this class of systems as *nonnegative systems with*

kinetic realization and present an example application of computing their equilibrium parameterization using a tritrophic foodweb model from ecology [54]. We point out that the subject discussed in this chapter will be central for the discussion of our proposed method to forecast the occurence of bifurcation-induced regime shifts in chapter 4. More specifically, the equilibrium parameterization discussed here is the stepping stone from which the simplification of the distance-to-bifurcation problem is achieved. This chapter should therefore be viewed as an essential part of chapter 4.

The remainder of this chapter is structured as follows. Section 3.1 discusses backgrounds on CRN models and the property of their kinetic realization. Section 3.2 describes the the method introduced in [43, 44] for computing equilibrium parameterization of CRN's kinetic realization. Section 3.3 presents the method for computing an equilibrium parameterization of nonnegative systems with kinetic realization. Discussions and some remarks are given in section 3.4.

3.1 Kinetic Realization of Chemical Reaction Network

3.1.1 CRN model and kinetic realization

The dynamics of reactant and product species involved in a CRN are governed by the law of *mass action kinetic* which states that the velocity/rate of each elementary reaction in the network is directly proportional to the product of the reactant concentrations [35]. This law is the basis from which differential equation models of CRN are derived.

Consider a set of r elementary reactions $\mathcal{R}_i$ $(i = 1, \ldots, r)$ between $s \geq 1$ chemical *species* $X_1, X_2, \ldots, X_s$ described in the following CRN

$$\mathcal{R}_i : \quad \sum_{j=1}^{s} a_{ij} X_j \xrightarrow{k_i} \sum_{j=1}^{s} b_{ij} X_j, \quad i = 1, 2, \ldots, r, \tag{3.1}$$

where for $i = 1, 2, \ldots, r$, the quantity k_i is the *rate constant* of the ith reaction between *reactant species* $\sum_{j=1}^{s} a_{ij} X_j$ and *product species* $\sum_{j=1}^{s} b_{ij} X_j$. Let $x_j(t)$ denotes the concentration of species X_j at time t and let $x(t) = [x_1(t), \ldots, x_s(t)]^T$. We define a *complex* as an object at the head or the tail of each reaction arrow in (3.1). The complex at the tail of an arrow is called the *reactant complex* and is denoted by $\mathcal{C}_j^R = \sum_{j=1}^{s} a_{ij} X_j$ for $i = 1, \ldots, r$, whereas the complex at the head of an arrow is called the *product complex* and is denoted by $\mathcal{C}_j = \sum_{j=1}^{s} b_{ij} X_j$.

Let $\mathcal{C} = \{\mathcal{C}_1, \mathcal{C}_2, \ldots, \mathcal{C}_m\}$ denotes the union set of complexes appeared in heads and tails of reaction arrows of CRN (3.1), i.e.

$$\mathcal{C}_i = \sum_{j=1}^{s} c_{ij} X_j, \quad i = 1, \ldots, m,$$

where $c_{i,j} = a_{i,j} \cup b_{i,j}$. The association of all s species to m complexes define a *bipartite graph* from X_i $(i = 1, \ldots, s)$ to $\mathcal{C}_j$ $(j = 1, \ldots, m)$ whose weights are given by the coefficients a_{ij} or b_{ij}. Corresponding to all complexes in $\mathcal{C}$, we define an $(s \times m)$ matrix Y with entries $[Y]_{ij} = c_{ji}$ for $i = 1, 2, \ldots, s$ and $j = 1, 2, \ldots, m$. By denoting the jth column of Y as $Y(j)$, we also define a monomial vector $\psi(x)$ such that

$$\psi_j(x) = x^{Y(j)}. \tag{3.2}$$

Then for $i = 1, 2, \ldots, r$, and $j, l = 1, 2, \ldots, m$ with $j \neq l$, the ith elementary reaction, $\mathcal{R}_i$, in CRN (3.1) may be rewritten as

$$\mathcal{R}_i : \quad \mathcal{C}_j \xrightarrow{k_i} \mathcal{C}_l, \tag{3.3}$$

where k_i is the rate constant of the ith reaction $\mathcal{R}_i$.

The representation of CRN (3.1) in term of complexes as given in (3.3) defines a directed graph $G(V, E)$ with a set of vertices $V = \mathcal{C}$ and a set of directed edges

$E = \mathcal{R}$. The weight of each edge in this graph is given by the rate constant k_i that corresponds to the ith reaction from $\mathcal{C}_j$ to $\mathcal{C}_l$. Using this graph representation, we may construct an $(m \times r)$ *incidence matrix* I_a such that for each $(\mathcal{C}_j, \mathcal{C}_l) \in \mathcal{R}_i$ in (3.3), the ith column of I_a satisfies

$$I_a(i) \doteq \begin{cases} I_a(j,i) = -1, \\ I_a(l,i) = 1, \\ 0, \text{ otherwise.} \end{cases} \tag{3.4}$$

Corresponding to matrix I_a, we also construct an $(r \times m)$ *weighting matrix* I_k such that for each $(\mathcal{C}_j, \mathcal{C}_l) \in \mathcal{R}_i$ in (3.3), the ith row of matrix I_k is defined as

$$I_k^T(i) \doteq \begin{cases} I_k^T(j,i) = k_i, \\ 0, \text{ otherwise.} \end{cases} \tag{3.5}$$

Using matrices Y, I_a, I_k and vector $\psi(x)$, define a constant matrix $N = YI_a$ and a vector of monomials $v(x,k) = I_k\psi(x)$. The dynamics of CRN (3.1) is then governed by the following differential equation.

$$\begin{aligned} \dot{x} &= YI_aI_k\psi(x) \\ &= Nv(x,k) \\ &= N \text{ diag}(k)x^Z \end{aligned} \tag{3.6}$$

where $N \in \mathbb{Z}^{n\times m}$ is known as *stoichiometric matrix* and $v(x,k) \in \mathbb{R}_+^m$ is called *flux vector* which satisfies a decomposition $v = \text{ diag}(k)x^Z$ where k is the set of reaction constants and $Z \in \mathbb{Z}_{\geq 0}^{n\times m}$ is a matrix of nonnegative integers whose ith column denotes the multi-index of the ith monomial $v_i(x,k)$. We call differential equation (3.6) the *kinetic realization* of CRN (3.1). An example which illustrates the construction of kinetic realization (3.6) from a CRN of the form (3.1) is given in example 3.1.

3.1.2 Properties of kinetic realization

It is well known that the trajectories of kinetic realization (3.6) lie in an affine subspace of the positive orthant [35, 43]. This can be verified by observing that for differential equation $\dot{x}(t) = Nv(x(t), k)$ in (3.6) and any time $t_1 < t_2 \in [0, t]$, the vector difference $x(t_2) - x(t_1)$ is an element of $im(N)$, where $im(N)$ denotes the image of N. By integrating this vector difference along the solution of $x(t)$, we have

$$x(t_2) = x(t_1) + \int_{t_1}^{t_2} Nv(x(t), k)dt,$$

which implies

$$x(t_2) - x(t_1) = N \int_{t_1}^{t_2} \text{diag}(k)\psi(x(t))dt.$$

The above equation shows that the difference $x(t_2) - x(t_1)$ is a linear combination of the column of matrix N with coefficients $c_i = k_i \int_{t_1}^{t_2} x(t)^{\alpha_i} dt$ and α is the multi-index of the monomials $\psi(x)$. Thus for any initial condition $x_0 \in \mathbb{R}^n_{\geq 0}$, the trajectory $x(t)$ at time $t \geq 0$ will stay in an affine space $\mathbb{S} = (x_0 + im(N)) \cap \mathbb{R}^n_{\geq 0}$ known as the *stoichiometric compatibility class* [35].

Let $w = w_1, \ldots, w_m$ be a basis vector of the orthogonal complement of $im(YI_a)$. This means w is a basis for $ker((YI_a)^T)$ with dimension $d = dim(ker((YI_a)^T)) = m = rank(YI_a)$. Let $x(0) = x_0$ be an initial condition and define $c_i = w_i^T x_0$. We then have

$$x_0 + im(YI_a) = \{x \in \mathbb{R}^n \mid w_i^T x - c_i = 0 \quad \text{for } i = 1, \ldots, d\}. \tag{3.7}$$

Equation (3.7) is often called the *conservation relation* and it shows how mass or energy are conserved within the system. The kinetic realization (3.6) therefore generally

takes the form

$$\begin{aligned} \dot{x} &= Nv(x,k), \qquad x(0) = x_0, \\ w_i^T x &= c_i, \qquad \text{for } i = 1, \ldots, n - rank(YI_a). \end{aligned} \tag{3.8}$$

Given a differential equation as in (3.8), one is often interested in computing the system's equilibria, x^*, defined as

$$x^* = \{x \in \mathbb{Q}^n(k) : Nv(x,k) = 0\}, \tag{3.9}$$

such that x^* is a vector in $\mathbb{R}^n$ for fixed k, and is a continuum otherwise. Computing the analytical expression of equilibria (3.9) in high dimensional systems usually requires the use of symbolic methods. One of such methods is based on the techniques from algebraic geometry which uses the Gröbner basis of equations $Nv(x,k) = 0$ [20, see also chapter 2]. This method originated from the fact that the zeros of polynomial equations are equivalent with the zeros of its basis [20]. Gröbner bases of polynomial equation can be computed using Buchberger algorithm [9, 20] which have been implemented in many computer algebra softwares [22]. The standard Buchberger algorithm, however, has a drawback in that (in the worst case) the degree of the computed bases grow doubly exponential with respect to the number of unknown variables [31, see also the discussion in chapter 2].

One alternative approach for computing equilibria (3.9) is by studying the solution of system (3.8) in a projective space [43]. By considering contionuous mapping functions $v : \mathbb{R}^n \to \mathbb{R}^m$ and $g : \mathbb{R}^m \to \mathbb{R}^n$, then the following statements for model (3.8) are equivalent [42, 43].

$$\begin{gathered} \exists x \in \mathbb{R}^n \text{ with } g(v(x,k)) = 0, \\ \exists v \in \mathbb{R}^m \text{ with } v \in im(v(x,k)) \text{ and } g(v) = 0. \end{gathered}$$

For the case of model (3.8), function $v(\cdot)$ is given by $v(x,k) = \text{diag}(k)x^Z$ and function $g(\cdot)$ is given by matrix N. From the discussion in the previous section, we know that $v(x,k) \geq 0$ and so the above equivalence can be rewritten as

$$\begin{gathered} \exists x \in \mathbb{R}^m_{\geq 0} \text{ with } Nv(x,k) = 0. \\ \exists v \in \mathbb{R}^m_{\geq 0} \text{ with } v \in im(v(\mathbb{R}^n_{\geq 0})) \text{ and } Nv = 0. \end{gathered} \tag{3.10}$$

By the nonnegativity of v, the *equilibrium fluxes* $v^* = \{v \in \mathbb{R}^m \mid g(v) = 0\}$ is then given by

$$\exists v^* \in \mathbb{R}^m \text{ with } v^* \in im(v(\mathbb{R}^n_{\geq 0})) \text{ and } v^* \in ker(N) \cap \mathbb{R}^m_{\geq 0}, \tag{3.11}$$

where $ker(N)$ denotes the null space of N. This observation suggests two important consequences that will be useful for computing the parameterization of equilibrium state x^* (3.9).

First: it means that the equilibrium fluxes are non-negative vectors lying in the null space of N. In particular, any equilibrium flux must lie in a convex polyhedral cone [17, 67, 43]

$$v^* \in \mathcal{K}_v = \ker(N) \cap \mathbb{R}^m_{\geq 0} = \left\{ v \in \mathbb{R}^m_{\geq 0} : v = \Sigma_{i=1}^q \lambda_i E_i \right\}. \tag{3.12}$$

The cone, $\mathcal{K}_v$, in equation (3.12) is finitely generated by a set of extreme rays, $E_i \in \mathbb{R}^m_{\geq 0}$ for $i = 1, 2, \ldots, q$. Such rays are routinely computed using tools such as CellNetAnalyzer [67]. Every equilibrium flux in $\mathcal{K}_v$ can therefore be parameterized with respect to these rays. In equation (3.12), the parameters $\lambda = (\lambda_1, \lambda_2, \ldots, \lambda_q)$ are called *convex parameters* [17] and so any equilibrium flux can be written as $v^*(\lambda)$ a linear function of the convex parameters.

Second: any flux, v, in the system must satisfy the equation

$$v_i = k_i x^{z_i}, \quad i = 1, 2, \ldots, m. \tag{3.13}$$

Equations (3.13) are *binomials* in $\mathbb{R}(k)[x, v]$ and this system's zeros characterize both the equilibrium fluxes, v^*, and the equilibrium state x^*. The ideal generated by these binomials is a *toric ideal* [4, 43] for which efficient algorithms for computing a Gröbner basis are available [106, 47]. One can therefore solve for the equilibria of the system in terms of its equilibrium fluxes and system parameters.

The preceding two consequences of kinetic realization can be summarized as

(i) any equilibrium flux can be expressed as a function $v^*(\lambda)$ in terms of convex parameters (λ), and

(ii) any equilibrium state can be expressed as a rational function $x^*(v^*, k)$ of the equilibrium fluxes (v^*) and the system parameters (k).

Using the expression $v^*(\lambda)$ of equilibrium flux in term of the convex parameters, one can then parameterize the equilibrium state as $x^*(\lambda, k) \in \mathbb{Q}^n(k, \lambda)$. Detailed discussion on this equilibrium parameterization is given in the next section.

Another property of kinetic realization is that the system's Jacobian matrix J can be parameterized as [43, 44]

$$J(\lambda, k) = N\mathrm{diag}(v^*(\lambda))Z^T\mathrm{diag}(1/x^*(\lambda, k)). \tag{3.14}$$

One can therefore use the Jacobian matrix (3.14) as an alternative to study the steady state properties of the system (see chapter 4).

3.2 Equilibrium Parameterization of Kinetic Realization

This section presents detailed discussion of method for computing the equilibrium parameterization of kinetic realization (3.6). This parameterization essentially

consists of two main steps. The first step aims to compute a Gröbner basis for the toric ideal induced by the binomial system (3.13). In particular, this basis is defined only with respect to the flux variable, v, and so its computation involves the elimination of unknown variables x from binomial system (3.13). The variety of this basis therefore defines the equilibrium flux v^*. The second step aims to extend the obtained equilibrium flux v^* for solving the equilibrium state x^* using the relationships in (3.12)-(3.13). This extension will be established through a transformation using Hermite normal form [108, chapter 3.2]. We point out that these two steps essentially correspond to the elimination and extension steps for computing of the Gröbner basis of binomial ideal (3.13).

3.2.1 Computation of equilibrium flux

Let $R(k)[x]$ and $R(k)[v]$ be polynomial rings in the unknowns $x = (x_1, \ldots, x_n)$ and $v = (v_1, \ldots, v_m)$, respectively. The mapping $v(x, k)$ from the state $x \in \mathbb{R}^n$ to the flux $v \in \mathbb{R}^m$ in (3.6) satisfies

$$v(x,k) : \mathbb{R}^n_{\geq 0} \mapsto \mathbb{R}^m_{\geq 0}, \qquad x \mapsto v(x,k),$$

and the image of $v(x, k)$ is given by

$$v_1(x,k) = k_1 x^{Z_1},\ v_2(x,k) = k_2 x^{Z_2},\ \ldots,\ v_m(x,k) = k_m x^{Z_m}.$$

From the above relation, one may see that an equilibrium flux $v^* \in \mathbb{R}^m_{\geq 0}$ will correspond to an equilibrium state $x^* \in \mathbb{R}^n_{\geq 0}$ if and only if v^* lies on the image the function $v(x^*, k)$, i.e. if

$$v^* \in im(v(x^*, k)).$$

The above condition can be enforced by requiring that

$$v_i - v_i(x,k) = 0, \quad \text{for } i = 1, \ldots, m. \tag{3.15}$$

The expression on the left hand side of (3.15) is binomial ideal over $\mathbb{R}(k)[x,v]$. Since $v = \text{diag}(k)x^Z$ and $Z \in \mathbb{Z}_{\geq 0}^{n\times m}$, one may conclude that matrix Z induces a substitution homomorphism on $v(x,k)$ and that $v \in \mathbb{R}(k)[v]$ is a toric ideal associated with the function $v(x,k)$ [4]. This implies that the equilibrium flux v^* lies on the affine toric variety $V(\mathcal{I})$ of the toric ideal $\mathcal{I} = \langle v_i - v_i(x,k)\rangle \cap \mathbb{R}(k)[v]$. In particular, one may use the Elimination Theorem to compute the Gröbner basis of $\mathcal{I}$. This Gröbner basis will be the defining ideal of the toric variety $\mathbb{V}(\mathcal{I})$ and therefore can be used to compute the equilibrium flux v^*. In the following, we describe the procedure to compute the equilibrium flux v^*.

First, we define ideal $I \in \mathbb{R}(k)[x,v]$ which corresponds to binomial system (3.15)

$$I = \langle v_1 - k_1 x^{Z_1}, \ldots, v_m - k_m x^{Z_m}\rangle \subseteq \mathbb{R}(k)[x,v]. \tag{3.16}$$

The associated toric ideal $\mathcal{I} \subseteq \mathbb{R}(k)[v]$ (note the difference of the ring) is given by

$$\begin{aligned} \mathcal{I} &= \langle v_1 - k_1 x^{Z_1}, \ldots, v_m - k_m x^{Z_m}\rangle \cap \mathbb{R}(k)[v], \\ &= I \cap \mathbb{R}(k)[v]. \end{aligned} \tag{3.17}$$

By the Hilbert's Basis Theorem [20], we know I is generated by a finite number of basis where one choice of such basis is the Gröbner basis [20]. Since $I \in \mathbb{R}(k)(x,v)$ is a binomial ideal, its Gröbner basis will also be binomial ideal defined on $\mathbb{R}(k)(x,v)$ [78].

Let $\mathbb{G}$ denotes the Gröbner basis of I with respect to elimination ordering (such as lex order) that eliminates variable x. Now notice that the toric ideal $\mathcal{I}$ in (3.17),

obtained from the intersection $I \cap \mathbb{R}(k)[v]$, is the nth elimination ideal of I (as it is obtained by eliminating n variables x from I) defined on the ring $\mathbb{R}(k)[v]$. By using the Gröbner basis $\mathbb{G}$ of ideal I, the Elimination Theorem discussed in chapter 2 implies that the basis

$$\mathbb{G}_n(v) = \mathbb{G} \cap \mathbb{R}(k)[v]$$

is a Gröbner basis for $I \cap \mathbb{R}(k)[v] = \mathcal{I}$. This means that one of the Gröbner basis for toric ideal $\mathcal{I}$ is those bases in $\mathbb{G}$ which contains only indeterminates v. Since the variety of an ideal is equivalent to the variety of its basis [20], the toric variety $\mathbb{V}(\mathcal{I})$ is then given by

$$\mathbb{V}(\mathcal{I}) = \{v \in \mathbb{Q}^m(k) : \mathbb{G}_n(v) = 0\} \subseteq \mathbb{R}(k)[v]. \tag{3.18}$$

The equilibrium flux v^* can then be obtained from the toric variety (3.18), i.e.

$$v^*(k) \in \mathbb{V}(\mathcal{I}). \tag{3.19}$$

3.2.2 Computation of equilibrium state

By the Ideal-Variety Correspondence theorem [20], we know that any variety $\mathbb{V}(I) \in \mathbb{R}(k)[x, v]$ of binomial ideal (3.15) will vanish on toric variety $\mathbb{V}(\mathcal{I})$ (3.19). Since $v^*(k) \in \mathbb{V}(\mathcal{I}) \subseteq \mathbb{R}(k)[v]$, then $v^*(k)$ defines only a partial solution to $\mathbb{V}(I)$ and we need to extend it to obtain the remaining solution $x^* \in \mathbb{R}[x, v]$. If such solution x^* exists, then both x^* and v^* will then define the total solution $\mathbb{V}(I) \subseteq \mathbb{R}(k)[x, v]$ for binomial system (3.15).

The Extension Theorem [20] can be used to show that the partial solution $v^*(k)$ can be extended to obtain x^*. In particular, let us rewrite the ideal in (3.13) as

$$v = \text{diag}(k)x^Z. \tag{3.20}$$

Now note that for a given nonzero solution $v^*(k)$, the above representation satisfies the condition on Extension Theorem 2.6 for $g_i(\cdot) = \text{diag}(k)$ (with the second term on the right hand side in (2.6) equals to zero) and thereby guarantees the existence of the extended solution x^*.

Now we show that x^* can be computed using the Hermite normal form [44, 78]. Let's introduce a coordinate transformation $x^* = \omega^U$ with $\omega \in \mathbb{R}^n$ and U is a unimodular matrix. Recall from linear algebr that the Hermite normal form H of a matrix Z is given by $H = UZ$ [108]. Evaluating (3.20) at (state and flux) equilibrium gives $v^*(k) = \text{diag}(k)(x^*)^Z$ which implies

$$\text{diag}(k)(x^*)^Z = \text{diag}(k)\omega^{UZ} = \text{diag}(k)\omega^H = v^*(k). \tag{3.21}$$

For given $v^*(k)$, solving the equation $\text{diag}(k)\omega^H = v^*(k)$ for ω and then followed by computing x^* using the relation $x^* = \omega^U$, the solution $x^*(k) \in \mathbb{R}(k)[x]$ can be obtained. Both $x^*(k)$ and $v^*(k)$ then define the total solution to binomial ideal I in (3.15).

Now recall from (3.12) that the equilibrium flux v^* is defined on the convex cone $\mathcal{K}_v$ and satisfies a parameterization of the form

$$v^*(\lambda) \in \mathcal{K}_v. \tag{3.22}$$

This implies that v^* is given by the intersection of (3.19) and (3.22), i.e.

$$v^*(\lambda, k) = \{v^* \in \mathbb{V}(\mathcal{I})\} \cap \{v^* \in \mathcal{K}_v\} \subseteq \mathbb{R}(\lambda, k)[v]. \tag{3.23}$$

By substitution of (3.23) to (3.21), then the equilibrium state $x^*(v^*, k)$ from transformation (3.21) can now be rewritten as $x^*(\lambda, k)$ a parameterization of λ and k.

The complete algorithm to compute parameterizations of $v^*(\lambda, k)$ and $x^*(\lambda, k)$ is

depicted in figure 3.1. The following example of the Brusselator dynamics will be used to illustrate the equilibrium parameterization discussed in this section.

Example 7. *Consider the dynamics of the Brusselator generated by species X, Y with concentration $[X], [Y]$, respectively, according to the following CRN. [35]*

$$2X + Y \xrightarrow{k_1} 3X$$

$$\emptyset \underset{k_3}{\overset{k_4}{\rightleftarrows}} X \xrightarrow{k_2} Y$$

We use x_1, x_2 to denote $[X], [Y]$, respectively. There are five complexes in this CRN namely $\mathcal{C} = \{x_1^2 x_2, x_1^3, x_1, x_2, 1\}$.

Matrix Y and vector $\psi(x)$ which satisfy (3.2) are given by

$$Y = \begin{bmatrix} 2 & 3 & 1 & 0 & 0 \\ 1 & 0 & 0 & 1 & 0 \end{bmatrix}, \quad \psi^T(x) = [\ x_1^2 x_2, \ \ x_1^3, \ \ x_1, \ \ x_2, \ \ 1, \ ].$$

Using the rules in equations (3.4) and (3.5), matrices I_a and I_k are then defined as

$$I_a = \begin{bmatrix} -1 & 0 & 0 & 0 \\ 1 & 0 & 0 & 1 \\ 0 & -1 & -1 & 1 \\ 0 & 1 & 0 & 0 \\ 0 & 0 & 1 & -1 \end{bmatrix}, \quad I_k = \begin{bmatrix} k_1 & 0 & 0 & 0 & 0 \\ 0 & 0 & k_2 & 0 & 0 \\ 0 & 0 & k_3 & 0 & 0 \\ 0 & 0 & 0 & 0 & k_4 \end{bmatrix}.$$

The kinetic realization of the system is then given by

$$\dot{x} = Y I_a I_k \psi(x) = N v(x, k),$$

1: **Input**: kinetic realization, $v(x,k) = (k_1 x^{Z_1}, \ldots, k_m x^{Z_m})^T$ and matrix N
2: **Output**: equilibrium flux, $v^*(\lambda, k)$, and equilibrium state $x^*(\lambda, k)$

3: Construct the binomial ideal $I \subseteq \mathbb{R}(k)[x, v]$ of (3.18).

$$I = \langle v_1 - k_1 x^{Z_1}, \ldots, v_m - k_m x^{Z_m} \rangle \in \mathbb{R}(k)[x, v]$$

4: Compute a Gröbner basis $\mathbb{G}$ of $I \in \mathbb{R}(k)[x, v]$ with respect to lex ordering that eliminate indeterminates x, i.e.

$$x_1 \succ \cdots \succ x_n \succ v_1 \cdots \succ v_m$$

5: Use $\mathbb{G}$ and Elimination Theorem to compute the Gröbner basis $\mathbb{G}_n \in \mathbb{R}(k)[v]$ for the nth elimination ideal of I according to

$$\mathbb{G}_n = \mathbb{G} \cap \mathbb{R}(k)[v]$$

- The Gröbner basis $\mathbb{G}_n$ will be formed by those basis in $\mathbb{G}$ that contain only the indeterminate v.
- The toric ideal (3.20) is then given by $\mathcal{I}\langle \mathbb{G}_n \rangle \subseteq \mathbb{R}(k)[v]$ and its variety is given by $\mathbb{V}(\mathcal{I}) = \{v \in \mathbb{R}(k)^m \, : \, \mathbb{G}_n = 0\} \subset \mathbb{R}(k)[v]$.

6: The equilibrium flux defined by toric variety is given by $v^*(k) \in \mathbb{V}(\mathcal{I})$.
7: Compute the convex parameterization of equilibrium flux $v^*(\lambda) \in \mathcal{K}_v$.
8: The equilibrium flux is

$$v^*(\lambda, k) = \{v^* \in \mathbb{V}(\mathcal{I})\} \cap \{v^* \in \mathcal{K}_v\}.$$

9: Use transformation (3.21) to obtain $x^*(\lambda, k)$.

Figure 3.1. Algorithm for computing parameterization of equilibrium flux and equilibrium state.

where matrix N and vector $v(x,k)$ are defined as

$$N = \begin{bmatrix} 1 & -1 & -1 & 1 \\ -1 & 1 & 0 & 0 \end{bmatrix}, \quad v(x) = [\ k_1 x_1^2 x_2, \quad k_2 x_1, \quad k_3 x_1, \quad k_4\ ],$$

and matrices diag(k) and Z such that $v(x,k) = diag(k)x^Z$ are given by

$$diag(k) = \begin{bmatrix} k_1 & 0 & 0 & 0 \\ 0 & k_2 & 0 & 0 \\ 0 & 0 & k_3 & 0 \\ 0 & 0 & 0 & k_4 \end{bmatrix}, \quad Z = \begin{bmatrix} 2 & 1 & 1 & 0 \\ 1 & 0 & 0 & 0 \end{bmatrix}.$$

The differential equation governing the Brusselator dynamics is then given by

$$\begin{aligned} \dot{x}_1 &= k_1 x_1^2 x_2 + k_4 - k_2 x_1 - k_3 x_1, \\ \dot{x}_2 &= -k_1 x_1^2 x_2 + k_2 x_1. \end{aligned} \tag{3.24}$$

Now we illustrate the parameterization of equilibrium flux and equilibrium state for this system using the method described in section 3.2.

Step 1: We first compute the convex parameterization of equilibrium flux in (3.12). For the Brusselator system (3.24), the extreme rays of $ker(N) \cap \mathbb{R}^m_{\geq 0}$ computed using CellNetAnalyzer [67] is given by

$$E = \begin{bmatrix} E_1 \\ E_2 \end{bmatrix}^T = \begin{bmatrix} 1 & 1 & 0 & 0 \\ 0 & 0 & 1 & 1 \end{bmatrix}^T.$$

Thus, the parameterization of equilibrium flux (3.16) in term of the convex parameters λ is given by

$$v^*(\lambda) = \sum_{i=1}^{2} \lambda_i E_i = \begin{bmatrix} \lambda_2 \\ \lambda_2 \\ \lambda_1 \\ \lambda_1 \end{bmatrix}. \tag{3.25}$$

Step 2: *Next, we compute the equilibrium flux defined by toric variety $\mathcal{I}$ in (3.17). The ideal I formed by the flux vector v_i and each monomial in $v(x,k)$ is given by*

$$I \;=\; \langle v_1 - k_1 x_1^2 x_2,\; v_2 - k_2 x_1,\; v_3 - k_3 x_1,\; v_4 - k_4 \rangle.$$

The Groebner basis of I computed using Singular [22] is given by

$$\mathbb{G}(I) \;=\; \{v_4 - k_4,\; k_3 v_2 - k_2 v_3,\; k_1 x_2 v_3^2 - k_3^2 v_1,\; k_3 x_1 - v_3\}.$$

Using the Elimination Theory, the Gröbner basis of toric ideal $\mathcal{I}$ in (3.17) is given by those elements of $\mathbb{G}$ which contain only indeterminate v, i.e.

$$\mathbb{G}_n(\mathcal{I}) = \{v_4 - k_4,\; k_3 v_2 - k_2 v_3\}.$$

The toric ideal, $\mathcal{I}$, is therefore given by $\mathcal{I} = \langle \mathbb{G}_n \rangle$ and the toric variety is defined as $\mathbb{V}(\mathcal{I}) = \{\mathbb{G}_n(\mathcal{I}) = 0\}$. The equilibrium flux obtained from $\mathbb{V}(\mathcal{I})$ then satisfy

$$v_4^* - k_4 = 0, \quad k_3 v_2^* - k_2 v_3^* = 0. \tag{3.26}$$

Step 3: *We now compute the intersection of $v^*(k)$ and $v^*(\lambda)$. From the parameterization of equilibrium flux $v^*(\lambda)$ in (3.25), we have*

$$v_1^* = v_2^* = \lambda_2, \;\; \textit{and} \;\; v_3^* = v_4^* = \lambda_1.$$

Substitution of (3.25) to (3.26) gives the following relation

$$\begin{aligned} \lambda_1 - k_4 &= 0, \\ k_3\lambda_2 - k_2\lambda_1 &= 0, \end{aligned}$$

which implies that the equilibrium flux can be parameterized either in term of convex parameters or the system parameters as follows.

$$v^*(\lambda, k) = \begin{bmatrix} \lambda_2 \\ \lambda_2 \\ \lambda_1 \\ \lambda_1 \end{bmatrix} = \begin{bmatrix} k_2k_4/k_3 \\ k_2k_4/k_3 \\ k_4 \\ k_4 \end{bmatrix}. \tag{3.27}$$

Step 4: *Finally we use the Hermite transformation (3.21) to compute the parameterization of equilibrium state $x^*(\lambda, k)$ from $v^*(\lambda, k)$ in (3.27). The unimodular matrix U and Hermite normal form H that correspond to matrix Z in (3.21) such that $UZ = H$ are*

$$UZ = H \quad \Leftrightarrow \quad \begin{bmatrix} 0 & 1 \\ 1 & -2 \end{bmatrix} Z = \begin{bmatrix} 1 & 0 & 0 & 0 \\ 0 & 1 & 1 & 0 \end{bmatrix}.$$

Using the transformation (3.21), the relation $diag(k)w^H = v^*(\lambda, k)$ with $v^*(\lambda, k)$ in (3.27) becomes

$$diag(k)w^H = \begin{bmatrix} k_1w_2 \\ k_2w_1 \\ k_3w_1 \\ w_3 \end{bmatrix} = v^*(\lambda, k).$$

Solving the above equation for w and then using the relation $x^* = w^U$ in (3.21), the

parameterization of the equilibrium state $x^*(\lambda, k)$ is given by

$$x_1^* = \frac{\lambda_2}{k_3}, \quad x_2^* = \frac{k_3^2 \lambda_1}{k_1 \lambda_2^2}. \tag{3.28}$$

Notice that the above equilibrium is an explicit function of the system's parameters and so for given values of the system's parameters, one may directly evaluate system's equilibria without having to solve the differential equations in the system's model.

3.3 Kinetic Realization of Nonnegative Systems

As discussed in the previous sections, the special structure of kinetic realization (3.6) allows one to compute a parameterization of the system's equilibria as a rational polynomial of the system parameters and some convex parameters. Notice that this analytical expression of the system's equilibrim is very useful for analyzing the dynamical properties (e.q. stability, bifurcation, etc.) of the system. It is therefore reasonable to ask whether the kinetic realization (3.6) can be constructed for larger classes of systems other than that arise from CRN.

As described in [53], there are in fact many systems from which the kinetic realization (3.6) can be constructed. In particular, the necessary and sufficient conditions which guarantee the existence of a system's kinetic realization (3.6) is given in the following lemma from [53].

Lemma 3.3.1 ([53])**.** *An m polynomial systems $f_1, \ldots, f_m$ in n variables $x = (x_1, \ldots, x_n)$ is a mass action kinetic systems if and only if for $i = 1, \ldots, n$, there exist real polynomials $g_i(x), h_i(x)$ with nonnegative coefficients such that $f_i = g_i(x) - x_i h_i(x)$.*

Lemma 3.3.1 essentially states that a system modeled as differential equation $\dot{x}_i = f_i(x, k)$ will have a kinetic realization if: (i) $f_i(x, k)$ is polynomial function and (ii) $f_i(x, k)$ satisfies $f_i(x, k) = g_i(x, k) - x_i h_i(x, k)$ where $g(\cdot)$ and $h(\cdot)$ are polynomials with nonnegative coefficients. The first condition which requires the system's vector

fields to be polynomial functions is not too restrictive since any differential equation models can be approximated as polynomial systems using Taylor or higher order polynomials approximation methods [104]. On the other hand, the second condition which essentially requires the system to be nonnegative [52] is also not restrictive because many systems (such as biological, ecological, or compartmental system) satisfy this property. These facts therefore suggest that there exist a large class of systems (other than that arising from models of CRN) which satisfies the conditions in lemma 3.3.1. As a result, the kinetic realization (3.6) for these systems can be extracted and that the equilibrium parameterization discussed in chapter 2 can also be applied to them. In the rest of this proposal, we call this class of systems as *nonnegative systems with kinetic realization.* An example computation of the kinetic realization (3.6) and equilibrium parameterization $x^*(\lambda, k)$ for this class of system will be presented in example 8 using a tritrophic food web model from ecology [54].

Remark 3.3.2. Although would not be pursued here, we point out that there exist a large literature in chemical reaction networks on the problem of computing optimal elementary reactions of the form (3.1) from a given differential equation [53, 109–111, 62, 61]. This problem is often called *inverse* or *minimal realization* problems. In fact, lemma 3.3.1 is one of the important results in this problem. In particular, lemma 3.3.1 can be used to realize a set of elementary reactions of the form (3.1) for polynomial system

$$\begin{aligned} \dot{x}_i &= f_i(x,k), \quad i = 1, \ldots, n, \\ &= \sum_{j=1}^{z_i} k_{ij} x^{[\alpha^{ij}]}, \end{aligned} \tag{3.29}$$

where α is the multi-index associated to monomials x^α and $f(x) = \sum_{k=1}^{z} c_k x^{[\alpha^k]}$ is a representation of polynomial $f(x)$ as linear combination of z monomials with coefficient k. The basic idea in this realization is to construct an equivalent elementary

Algorithm 1 Realization of elementary reaction for given monomial

procedure ELEMENTARYREACTION(kx^α)
  if ($kx^\alpha \in f_i$) and (sign(kx^α) is *positive*) **then**
    build reaction $\mathcal{R}$: $\sum_{i=1}^{n} \alpha_i x_i \xrightarrow{k} (\sum_{i=1}^{n} \alpha_i x_i) + x_i$
  else
    if ($kx^\alpha \in f_i$) and (sign(kx^α) is *negative*) **then**
      build reaction $\mathcal{R}$: $\sum_{i=1}^{n} \alpha_i x_i \xrightarrow{k} (\sum_{i=1}^{n} \alpha_i x_i) - x_i$
    end if
  end if
  Return $\mathcal{R}$
end procedure

reaction to each monomial in $f_i(x)$ according to the *sign of each monomial* and *in which polynomial* f_i that monomial appear. These rules are summarized in Algorithm 1 which outputs a set of elementary reactions of the form (3.1).Given polynomial system (3.29) which consist of z_i monomials, Algorithm 1 will produces at most $n(\mathcal{R}) = \sum_{i=1}^{n} z_i$ elementary reactions of the form (3.1). It is possible that the output of agorithm 1 is not optimal in the sense that the number of constructed reactions exceed a minimal number of reactions required to construct the corresponding differential equation. In this case, one may use, for example, the method in [110] to obtain a minimal realization of the algorithm 1's output. This combination would then provides an algorithmic method for constructing optimal set of elementary reactions for given polynomial systems.

Example 8. *This example illustrates the method for computing the kinetic realization and equilibrium parameterization of nonnegative systems with kinetic realization described in sections 3.2-3.3 using a tritrophic food web model from [54]. The scaled*

differential equation governing the dynamics of the system is given by

$$\begin{aligned}\dot{x}_1 &= x_1(1-x_1) - \frac{k_1 x_1 x_2}{k_2 + x_1} \\ \dot{x}_2 &= \frac{k_3 x_1 x_2}{k_2 + x_1} - k_4 x_2 x_3 - k_5 x_2 \\ \dot{x}_3 &= k_6 x_2 x_3 - k_7 x_3\end{aligned}$$

where x_1, x_2, x_3 denote the biomasses of producers, consumers, and top predators, respectively, and k_i, $(i = 1, \ldots, 7)$ are some positive parameters. Notice that this system does not satisfies the first condition in lemma 3.3.1 due to the rational polynomials appear in the first and the second state equations. However, we can introduce an augmented state x_4 of the form

$$x_4 = (k_2 + x_1)^{-1} \quad \rightarrow \quad \dot{x}_4 = (\partial x_4/\partial x_1)\dot{x}_1 = x_1 x_4^2 (x_1 - 1) + k_1 x_1 x_2 x_4^3,$$

so that the original differential equation can be rewritten as

$$\begin{aligned}\dot{x}_1 &= x_1(1-x_1) - a x_1 x_2 x_4 \\ \dot{x}_2 &= k_3 x_1 x_2 x_4 - k_4 x_2 x_3 - k_5 x_2 \\ \dot{x}_3 &= k_6 x_2 x_3 - k_7 x_3 \\ \dot{x}_4 &= x_1 x_4^2 (x_1 - 1) + k_1 x_1 x_2 x_4^3\end{aligned} \tag{3.30}$$

which now satisfies the condition in lemma 3.3.1. One may verify that matrix N and vector $v(x,k)$ that correspond to kinetic realization $\dot{x} = Nv(x,k)$ of system (3.30) are

$$N = \begin{bmatrix} 1 & -1 & 1 & 0 & 0 & 0 & 0 & 0 & 0 & 0 & 0 \\ 0 & 0 & 0 & 1 & -1 & 1 & 0 & 0 & 0 & 1 & 0 \\ 0 & 0 & 0 & 0 & 0 & 0 & 1 & -1 & 0 & 0 & 0 \\ 0 & 0 & 0 & 0 & 0 & 0 & 0 & 0 & 1 & -1 & 1 \end{bmatrix},$$

$v(k,x) = \ [x_1, x_1^2, k_1x_1x_2x_4, k_3x_1x_2x_4, k_4x_2x_3, k_5x_2, k_6x_2x_3, k_7x_3, x_1^2x_4^2, x_1x_4^2, k_1x_1x_2x_4^3]^T,$

and matrix Z *which satisfies* $v(x,k) = diag(k)x^Z$ *for* $k = k_i,\ (i = 1, \ldots, 7)$ *is*

$$Z = \begin{bmatrix} 1 & 2 & 1 & 1 & 0 & 0 & 0 & 0 & 2 & 1 & 1 \\ 0 & 0 & 1 & 1 & 1 & 1 & 1 & 0 & 0 & 0 & 1 \\ 0 & 0 & 0 & 0 & 1 & 0 & 1 & 1 & 0 & 0 & 0 \\ 0 & 0 & 1 & 1 & 0 & 0 & 0 & 0 & 2 & 2 & 3 \end{bmatrix}.$$

Now we proceed with the computation of the equilibrium parameterization.

Step 1: First, we compute the convex parameterization of equilibirium flux. For system (3.30), the following seven extreme rays $(E_i, i = 1, \ldots, 7)$ *are identified using* CellNetAnalyzer*[67].*

$$\begin{bmatrix} E_1 \\ E_2 \\ E_3 \\ E_4 \\ E_5 \\ E_6 \\ E_7 \end{bmatrix} = \begin{bmatrix} 1 & 1 & 0 & 0 & 0 & 0 & 0 & 0 & 0 & 0 & 0 \\ 0 & 1 & 1 & 0 & 0 & 0 & 0 & 0 & 0 & 0 & 0 \\ 0 & 0 & 0 & 1 & 1 & 0 & 0 & 0 & 0 & 0 & 0 \\ 0 & 0 & 0 & 1 & 0 & 1 & 0 & 0 & 0 & 0 & 0 \\ 0 & 0 & 0 & 0 & 0 & 0 & 1 & 1 & 0 & 0 & 0 \\ 0 & 0 & 0 & 0 & 0 & 0 & 0 & 0 & 1 & 1 & 0 \\ 0 & 0 & 0 & 0 & 0 & 0 & 0 & 0 & 0 & 1 & 1 \end{bmatrix}.$$

The convex parameterization (3.12) of equilibrium flux is then given by

$$v^*(\lambda) = [\lambda_1, \lambda_1 + \lambda_2, \lambda_2, \lambda_3 + \lambda_4, \lambda_3, \lambda_4, \lambda_5, \lambda_5, \lambda_6, \lambda_6 + \lambda_7, \lambda_7]^T. \tag{3.31}$$

Step 2: Next we compute the equilibrium flux from the toric variety $\mathbb{V}(\mathcal{I})$ *defined in*

(3.18). The ideal I formed by the flux vector v_i and the monomials $v(x,k)$ is

$$\begin{aligned} I &= \langle\, v_1 - x_1, v_2 - x_1^2, v_3 - k_1x_1x_2x_4, v_4 - k_3x_1x_2x_4, v_5 - k_4x_2x_3, v_6 - k_5x_2, \\ &\quad v_7 - k_6x_2x_3, v_8 - k_7x_3, v_9 - x_1^2x_4^2, v_{10} - x_1x_4^2, v_{11} - k_1x_1x_2x_4^3 \,\rangle. \end{aligned}$$

By computing the Groebner basis of I using Singular [22] and applying the Elimination Theorem to eliminates variable x, the Gröbner basis for toric ideal $\mathcal{I}$ is given by

$$\begin{aligned} \mathbb{G}_n(\mathcal{I}) = \{\, & k_6v_7v_8 - k_5k_7v_7, k_6v_5 - k_4v_7, k_5^2v_4^2 - k_3^2v_6^2v_9, k_3v_3 - k_1v_4, \\ & k_5^2v_2 - v_6^2, v_1v_{11} - v_3v_{10}, v_1v_{10} - v_9 \,\}. \end{aligned}$$

The toric ideal is then defined as $\mathcal{I} = \langle \mathbb{G}_n \rangle$ and the toric variety is given by $\mathbb{V}(\mathcal{I}) = \{\mathbb{G}_n = 0\}$. The equilibrium flux obtained from $\mathbb{V}(\mathcal{I})$ then satisfy

$$v^*(k) = \{v : \mathbb{G}_n(\mathcal{I}) = 0\}. \tag{3.32}$$

Step 3: By computing the intersection of $v^*(k)$ in (3.32) and $v^*(\lambda)$ in (3.31), one may verify that the equilibrium flux is given by

$$\begin{aligned} v^*(\lambda,k) = [& v_1^*, v_2^*, v_3^*, \lambda_3+\lambda_4, \lambda_3, \lambda_4, k_6\lambda_3/k_4, k_6\lambda_3/k_4, \lambda_6, \\ & \lambda_6(1+\lambda_2/(\lambda_1-\lambda_2)), \lambda_2\lambda_6/(\lambda_1-\lambda_2)]^T, \end{aligned}$$

where

$$\begin{aligned} v_1^* &= (k_7/k_6)^2 - (k_1/k_6)(\lambda_3 + k_5k_7/k_6), \\ v_2^* &= (k_7/k_6)^2 - (k_1/k_6 - k_1/k_3)(\lambda_3 + k_5k_7/k_6), \\ v_3^* &= (k_1/k_3)(\lambda_3 + k_5k_7/k_6). \end{aligned}$$

Note that we have used $\mu = (k_1, k_5, k_6, \lambda_3, \lambda_4, \lambda_5, \lambda_6, \lambda_7)$ to parameterize the equilibrium flux.

Step 4: Finally, we use Hermite transformation (3.25) to compute the equilibrium

$x^*(\lambda, k)$ from $v^*(\lambda, k)$. The unimodular matrix U that satisfies (3.25) for the given matrix Z of system (3.30) is

$$U = \begin{bmatrix} 1 & 0 & 0 & -1 \\ 0 & 1 & 0 & -1 \\ 0 & 0 & 0 & 1 \\ 0 & 0 & 1 & 0 \end{bmatrix}.$$

Using the relation in (3.25), the parameterized equilibrium state x^* is then given by

$$x_1^* = \frac{\lambda_6}{\lambda_6 + \lambda_7}, \quad x_2^* = \frac{\lambda_4}{\lambda_5}, \quad x_3^* = \frac{k_5\lambda_5}{k_6\lambda_4}, \quad x_4^* = \frac{k_5\lambda_7}{k_1\lambda_4(\lambda_6 + \lambda_7)}. \tag{3.33}$$

3.4 Remarks and Proposed Research

This chapter presented method for computing equilibrium parameterization of nonnegative systems with kinetic realization. As will be shown in the next chapter, this equilibrium parameterization is useful to help simplify the minimum distance-to-bifurcation problem.

Proposed research: We are currently developing a software toolkit that performs all computations in the equilibrium parameterization method described in this chapter. In particular, this toolkit will be integrated with another software toolkit that implements the method for predicting bifurcation-induced regime shifts discussed in chapter 4. Thus, one of the expected outputs of the proposed research is an integrated software toolkit that can performs both equilibrium parameterization described in this section and the method for predicting regime shifts described in chapter 4. We plan to evaluate the performance of this toolkit in an experiment for predicting ecological regime shifts which will be discussed in chapter 6.

CHAPTER 4

FORECASTING BIFURCATION-INDUCED REGIME SHIFTS

4.1 Introduction

This chapter presents our proposed methods to forecast the bifurcation-induced regime shifts. We recall that bifurcation-induced regime shifts occur because the system undergoes a bifurcation as a result of variation on system's parameters that exceeds a critical threshold. We formulate the problem of predicting the onset of bifurcation-induced regime shifts as a minimum *distance-to-bifurcation* problem [25] and then propose a method to solve this problem in a class of *nonnegative systems with kinetic realization*. Our proposed method consist of two main steps:

- First, we use the equilibrium parameterization discussed in chapter 3 to simplify the optimization problem for computing the minimum distance-to-bifurcation. In particular, the use of such parameterization allows us to express the constraints of optimization only in term of system's parameters rather than the system's parameters and equilibria.
- Second, by rewriting the constraints of optimization as semialgebraic sets in the parameter space, we show that the optimization problem for computing the minimum distance-to-bifurcation can be recasted as an SOS optimization problem. This SOS optimization can then be solved using the available SOS programming softwares [90, 75, 55].

4.1.1 Backgrounds and prior works

To motivate the discussion, recall the lake eutrophication model in chapter 1

$$\dot{x} = a - bx + \frac{x^2}{1 + x^2}$$

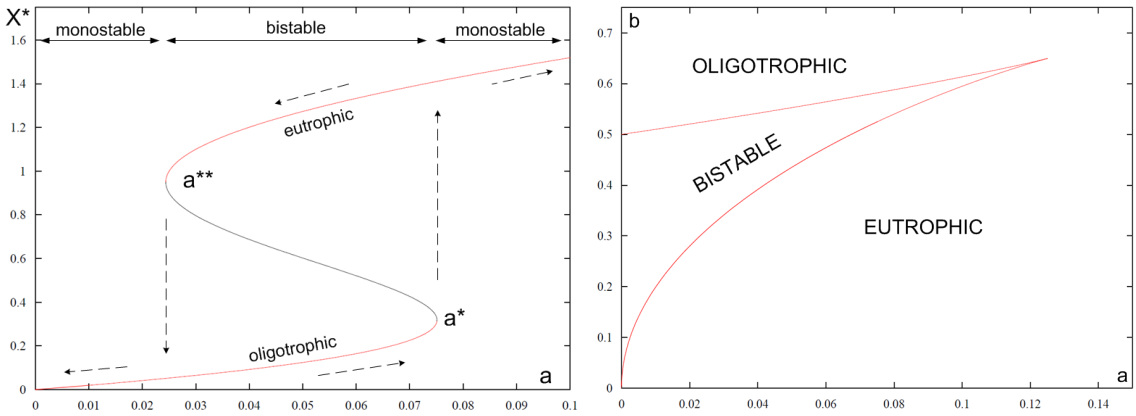

(a) One-parameter bifurcation diagram. (b) Two-parameters bifurcation diagram.

Figure 4.1. Bifurcation diagrams of the lake model.

where the state x denotes the concentration of Phosporus (P) in the lake water column and $a, b \geq 0$ are parameters denoting the rate of inflow and outflow of P into and out of the lake, respectively. Recall from chapter 1 that the equilibria of this system is given by those values of x at the intersections of the curves $f(x)$ and $g(x)$ defined below

$$\underbrace{a + \frac{x^2}{1+x^2}}_{f(x)} = \underbrace{bx}_{g(x)}.$$

First, let us consider the characteristic of these equilibria when parameter b is held fixed while parameter a is varied. The values of equilibria for different a can be traced from the one-parameter bifurcation diagram in figure 4.1a which is obtained using XPPAUT [33]. One may see that the number of equilibria changes as the value of a increase and that these changes are followed by the change on the qualitative dynamics (i.e. stability) of the system. When a increases from zero up to a critical value a^*, then further increase on a will induces a regime shift in which the system's equilibria flip from low to high P levels. Once the system stays in the high P level equilibrium, the return to a low P level requires a decrease on parameter a down to the critical value a^{**} due to hysteresis property of the bifurcation diagram. One

may further analyze how the equilibria bifurcates when both parameters a and b are simultaneously varied. The two-parameters bifurcation diagram in figure 4.1b [33] clearly shows the partition of the parameter space into regions where the system may have single (oligotrophic or eutrophic) or multiple equilibria (bistable). The curve which encapsulates the bistable region in figure 4.1b is known as the *bifurcation manifold* and it contains all critical parameter values k^* at which transitions or regime shifts between different dynamics of the system occur. Thus for any nominal parameter k^0, the minimum distance-to-bifurcation

$$\gamma = \inf_k |k^* - k^0| \tag{4.1}$$

is defined as the shortest distance between k^0 and the bifurcation manifold.

The computation of γ, however, is generally difficult since the bifurcation set is usually not known. In particular, the standard numerical bifurcation methods illustrated in the above example are limited to systems having at most two unknown parameters. For dynamical system

$$\dot{x}(t) = f(x(t), k), \quad x(t) = x_0, \tag{4.2}$$

whose vector fields depend on parameter k, the bifurcation manifold consists of those critical parameters k^* that satisfy the bifurcation conditions in Table 4.1 [73]. The first row of the table shows necessary and sufficient conditions for a Hopf bifurcation. The transversality condition requires that the partial derivative (with respect to parameter k) of the real part of the characteristic polynomial's roots be not equal to zero. The other transversality conditions in this table are conditions on the various derivatives of the vector field in which w and v are the left and right eigenvectors, respectively, associated with the zero eigenvalue of the Jacobian matrix (see [73] for details). Each of these transversality conditions essentially describes an instance

TABLE 4.1

Local bifurcation condition [73].

Type	Jacobian Eigenvalue	Transversality
Hopf	simple 0	$D_k\{Re(s)\} \neq 0$
Saddle-node	simple imaginary pair	$w\left(D_k f\big\|_{x^*,k^*}\right) \neq 0, \quad w\left(D_x^2 f\big\|_{(v,v)}\right) \neq 0$
Transcritical	simple imaginary pair	$w\left(D_k f\big\|_{x^*,k^*}\right) \neq 0, \quad w\left(D_{x,k}^2 f\big\|_{v,v}\right) \neq 0$
Pitchfork	simple imaginary pair	$w\left(D_k f\big\|_{x^*,k^*}\right) \neq 0, \quad w\left(D_x^3 f\big\|_{x^*,k^*}\right) \neq 0$

where the system undergoes change on its stability properties at the critical parameter k^*. Prior works have proposed several methods for computing γ in the context of robust stability analysis [69, 80, 84, 115] and voltage collapse problem in power systems [26, 26]. In general, these methods use numerical optimization techniques to search for the minimum γ subject to the constraints that the critical parameter k^* satisfy the condition in table 4.1. These methods, however, are computationally demanding since the search for the minimum γ requires the computation of system's equilibrium x^* *numerically* for each values of the parameter and at every iteration.

4.1.2 Approach and Contribution

This chapter presents the use of SOS optimization [87, 88] to bound the distance-to-bifurcation, γ, in a class of *nonnegative systems with kinetic realization*. We recall from chapter 3 that a polynomial systems in (4.2) is said to have a kinetic realization if there exists a matrix N and a vector of monomials $v(x,k)$ such that $f(x,k) = Nv(x,k)$. As discussed in chapter 3, the special structure of these systems allows one to compute an analytical parameterization of their equilibria in terms of the

system parameters. This equilibrium parameterization can therefore simplifies the distance-to-bifurcation problem because the constraints that define the bifurcation conditions can now be expressed only in terms of the system's parameters, rather than the system's parameters and equilibria. By rewriting the bifurcation conditions in table 4.1 as semialgebraic set description in the parameter space, we show that the SOS relaxation techniques [87, 88] can be used to recast the computation of the globally minimum distance-to-bifurcation as an SOS optimization problem.

The remainder of this chapter is structured as follows. Section 4.2 reviews some backgrounds on local bifurcation theory. Section 4.3 describes the necessary bifurcation conditions which will be used in section 4.4 to recast the distance-to-bifurcation problem as an SOS optimization problem. Section 4.5 illustrates an application of the proposed method to study the resilience of a tritrophic food chain from ecology. Remarks and suggestion for future works are given in section 4.6.

4.2 Local Bifurcation and Distance-to-Bifurcation Problem

4.2.1 General systems

Consider dynamical system (4.2) and assume that the parameters are fixed real numbers such that differential equation (4.2) can be rewritten as

$$\dot{x} = f(x), \qquad x(0) = x_0. \tag{4.3}$$

Let $\varphi(t) : \mathbb{R}^n \mapsto \mathbb{R}^n$ denotes an *evolution operator* which transforms the initial state $x_0 \in \mathbb{R}^n$ into some state $x(t) \in \mathbb{R}^n$ at time $t \in [0, T]$

$$x(t) = \varphi(t)x_0.$$

The family of operators $\varphi(t)$ for $t \in [0, T]$ is often called the *flow* of system (4.3) and it characterize the evolution of the state $x(t)$ of the system at any time t when initialized at x_0. For a dynamical system whose evolution is governed by the flow $\varphi(t)$, two basic geometric objects can be associated with it namely its *orbits* in the state space and its *phase portrait* in the state space formed by these orbits. An orbit of a system that starts at x_0 is an ordered subset of the state space at which the evolution operator $\varphi(t)x_0$ is defined. Examples of orbits includes fixed points (equilibria), cycles, etc. On the other hand, the phase portrait of a system is a partitioning of the state space into orbits and thereby provides a topological description about the qualitative dynamics of the system. Two dynamical systems are said to be *topologically equivalent* if their phase portrait are qualitatively similar, namely if one phase portrait can be obtained from another by continuous transformations [48, 73].

The dynamics of a system is usually studied locally in some bounded region $\mathcal{X} \subset \mathbb{R}^n$ of the state space. This is particularly helpful for topological classification of the phase portrait near the equilibrium points because the local behaviors of a system near its equilibrium points can be studied from its linearization. Let x^* be an equilibrium of (4.3) such that $f(x^*) = 0$ and let $J = \frac{\partial f}{\partial x}\big|_{x^*}$ denotes its Jacobian matrix evaluated at the equilibrium x^*. Let n_-, n_0, and n_+ be the number of eigenvalues of J with negative, zero, and positive real part, respectively. An equilibrium is called *hyperbolic* if $n_0 = 0$, that is, if there are no eigenvalues on the imaginary axis [73]. In the neighborhood of a hyperbolic equilibriums x^* of (4.3), the Grobman-Hartman Theorem [73] states that the qualitative dynamic of nonlinear system (4.3) is guaranteed to be *locally topologically equivalent* to its linearization $\dot{\xi} = J\xi$. One can then study the local topological equivalence of dynamical systems by analyzing the local phase portrait of its linearization around the equilibrium points.

Now let the vector fields of system (4.2) depend on its parameters $k \in \mathbb{R}^p$ and consider the phase portrait of this system. If k vary in the parameter space $\mathbb{R}^p$ then the

equilibrium x^* and the phase portrait of the system will also vary in the state space $\mathbb{R}^n$. The phase portrait can either remain topologically equivalent to the original one or it can change to something else. The appearance of a topologically nonequivalent phase portrait under variation of the parameters is called a *bifurcation* and the value of the parameters at which a bifurcation occurs is called the bifurcation (critical) parameter [73]. Since the behavior of nonlinear systems with hyperbolic equilibrium is locally topologically equivalent with its linearization around the equilibrium, one can then study the bifurcation using its linearization. In this case, topological equivalence of the system under parameter variation can be studied by analyzing the impact of such variation on the topology of the equilibrium. Let x^* be a nominal equilibrium of the systems and let y^* be the equilibrium when the parameter vary. The following theorem provides conditions under which the the linearized system is locally topologically equivalent.

Theorem 4.2.1 ([73])**.** *The phase portrait of a system near two hyperbolic equilibria, x^* and y^* are locally topologically equivalent if and only if these equilibria have the same number n_- and n_+ of eigenvalues with negative and positive real part, respectively.*

Theorem 4.2.1 is the basic result from which the necessary and sufficient bifurcation conditions in table 4.1 is constructed [73]. Searching for the parameter set which satisfy these conditions, however, is not a trivial task since their evaluation requires the knowledge of system's equilibria. In particular, the standard numerical softwares [24, 33] used for bifurcation analysis is limited to study at most two parameters simultaneously. As a result, computing the minimum distance-to-bifurcation (4.1) for more than two parameters is also become increasingly complex (see [26] for a review of this method).

4.2.2 Nonnegative systems with kinetic realization

The computation of minimum distance-to-bifurcation, however, can be simplified for nonnegative *polynomial systems* that have kinetic realization. Note that system (4.2) with polynomial vector fields $f(x,k) \in \mathbb{R}^n(k)[x]$ is said to be *nonnegative* if and only if $x(t) \in \mathbb{R}^n_{\geq 0}$ for all $x_0 \in \mathbb{R}^n_{\geq 0}$, $t \geq 0$ [52]. A necessary and sufficient condition for system (4.2) to be nonnegative is that $f_i(x,k) \geq 0$ for all x in which $x_i = 0$ [52, 51]. We recall that system (4.2) has a *kinetic realization* if there exists an $n \times m$ integer matrix, N, and an $m \times 1$ vector of monomials, $v(x,k) \in \mathbb{R}(k)[x]$ such that

$$\dot{x}(t) = f(x,k) = Nv(x,k), \quad x(0) = x_0, \tag{4.4}$$

where N is generally a sparse matrix and the flux vector $v(x,k)$ satisfies a decomposition of the form $v(x,k) = \mathrm{diag}(k)x^Z$, with $Z \in \mathbb{Z}^{n\times m}_{\geq 0}$ is a matrix whose ith column denotes the multi-index of the ith monomial in $v(x,k)$.

Nonnegative systems exist for a large number of real world systems including compartmental, biological, and ecological systems [52, 51]. The restriction to polynomial systems with kinetic realizations is not overly restrictive since 1) any smooth function can be approximated arbitrarily closely with a polynomial [104], 2) systems with rational vector fields can be transformed into polynomial systems [34], and 3) there exist a number of methods for extracting kinetic realizations from polynomial systems [53, 110, 111, 61–63].

As discussed in chapter 3, the special structure of nonnegative systems with kinetic realization has two major consequences, namely

(i) any equilibrium flux can be expressed as a function $v^*(\lambda)$ in terms of the convex parameters (λ), and

(ii) any equilibrium state can be expressed as a rational function $x^*(v^*,k)$ of the equilibrium fluxes (v^*) and the system parameters (k).

Using the convex parameterization of equilibrium fluxes v^*, one can then parameterize

the equilibrium state as $x^*(k,\lambda) \in \mathbb{Q}^n(k,\lambda)$ a rational function of system's parameters and convex parameters. This algebraic equation characterizes all system equilibria as a function of the system and convex parameters and it provides a critical starting point for characterizing the bifurcation constraints in the distance-to-bifurcation problem.

Another property of kinetic realization is that the system's Jacobian matrix J can be parameterized as [43, 44]

$$J(\lambda,k) = N\mathrm{diag}(v^*(\lambda))Z^T\mathrm{diag}(1/x^*(\lambda,k)). \tag{4.5}$$

This implies that the bifurcation condition in table 4.1 can be evaluated directly in term of the parameters (λ,k) without having to directly compute the equilibrium x^* for different k. Earlier work on the distance-to-bifurcation problem [25, 26, 10] always required that one solve for the equilibrium as part of the optimization; this increases the number of decision variables in the problem.

4.3 Necessary Bifurcation Conditions

Consider the Jacobian matrix in (4.5). Let $p(s) = |sI - J|$ be the characteristic polynomial of J defined as

$$p(s) = a_0 s^n + a_1 s^{n-1} + \cdots + a_{n-1}s + a_n, \tag{4.6}$$

where the coefficients $a_i(\lambda,k)$ are functions of the parameters (λ,k). For notational convenience, we denote these parameters as $\mu = (\lambda,k)$. The eigenvalues of J are given by the roots of $p(s)$ and one says the matrix J is asymptotically stable if and only if all its eigenvalues have negative real parts and it is unstable otherwise. For

$z = 1, \ldots, n$, the zth Hurwitz determinant, $\triangle_z$, associated with $p(s)$ is

$$\triangle_z = \begin{vmatrix} a_1 & a_3 & a_5 & \ldots & a_{2z-1} \\ a_0 & a_2 & a_4 & \ldots & a_{2z-2} \\ 0 & a_1 & a_3 & \ldots & a_{2z-3} \\ \vdots & \vdots & \vdots & \ddots & \vdots \\ 0 & 0 & 0 & a_{z-2} & a_z \end{vmatrix}$$

such that

$$\triangle_1 = |a_1|, \quad \triangle_2 = \begin{vmatrix} a_1 & a_3 \\ a_0 & a_2 \end{vmatrix}, \quad \triangle_3 = \begin{vmatrix} a_1 & a_3 & a_5 \\ a_0 & a_2 & a_4 \\ 0 & a_1 & a_3 \end{vmatrix}, \quad \ldots.$$

The following proposition gives the conditions for J to have simple zero eigenvalue.

Proposition 4.3.1. *Consider matrix J in (4.5) with characteristic polynomial $p(s)$ in (4.6). If the coefficients of $p(s)$ satisfies the conditions $a_n = 0$ and $a_{n-1} \neq 0$, then matrix J will have zero eigenvalue with multiplicity not greater than one.*

Proof. That $a_n = 0$ implies one of the roots of $p(s)$ is zero is clear. Now notice that $p(s)$ will have zero eigenvalue with multiplicity not greater than one if $\frac{\partial p(s)}{\partial s}|_{s=0} \neq 0$, which will be satisfied when $a_{n-1} \neq 0$. □

The following lemma from [18] gives the condition for J to have a simple pair of imaginary eigenvalues. The proof is based on the Orlando formula [39].

Lemma 4.3.2 ([18])**.** *Consider matrix J in (4.5) with characteristic polynomial $p(s)$ in (4.6). If the $(n-1)$th Hurwitz determinant of $p(s)$ satisfies $\triangle_{n-1} = 0$, then matrix J will have a pair of imaginary eigenvalues with multiplicity not greater than one.*

Now let us express the necessary conditions in table 4.1 in term of the coefficients of $p(s)$ in (4.6). Let q denotes the number of parameters in μ. Let Ω^{SN} be the parameter set where a saddle-node (also pitchfork and transcritical) bifurcation occurs. Using the conditions in proposition 4.3.1, one has

$$\Omega^{SN} = \left\{ \mu \in \mathbb{R}^q_{\geq 0} \mid a_n(\mu) = 0,\ a_{n-1}(\mu) \neq 0 \right\}. \tag{4.7}$$

In a similar way, lemma 4.3.2 can be used to describe the following parameter set Ω^H where Hopf bifurcation occurs.

$$\Omega^H = \left\{ \mu \in \mathbb{R}^q_{\geq 0} \mid \triangle_{n-1}(\mu) = 0 \right\}. \tag{4.8}$$

If a bifurcation occurs, then one may denote the parameter set Ω for which at least one type of bifurcation occurs as

$$\Omega = \Omega^{SN} \cup \Omega^H. \tag{4.9}$$

The sets in (4.7)-(4.9) are algebraic sets characterizing those parameters for which a bifurcation may occur. Thus, system (4.4) will *not* have a bifurcation if the set Ω is empty. A method for checking whether these sets are empty is discussed in the next section.

Remark 4.3.3. Note that we only characterize the necessary conditions for the existence of Hopf and saddle-node bifurcations. This is because the necessary conditions for the existence of pitchfork and transcritical bifurcations are the same with that in the saddle-node bifurcation (see table 4.1). Moreover, we do not characterize the semialgebraic descriptions of the transversality condition in table 4.1 because it will not be used in the optimization formulation for computing the minimum distance-to-bifurcation γ. Thus, the satisfaction of the transversality conditions will be checked

after the critical parameter k^* from the optimization is obtained.

4.4 Distance-to-Bifurcation Problem

From the previous section, it should be clear that the non-existence of a particular bifurcation is equivalent to the emptiness of the corresponding bifurcation set. In general, checking the emptiness of the set Ω^{SN}, for example, can be difficult. In recent years, however, it has proven fruitful to consider convex relaxations of this problem in which one checks for the emptiness of the set $\tilde{\Omega}(\gamma) \cap \Omega^{SN}$, where $\tilde{\Omega}(\gamma)$ is a semi-algebraic set defined by a psd *certificate* function $V(\mu)$.

In particular, let $\gamma > 0$ be a real-valued constant and let $\alpha(|\mu - \mu_0|)$ be a class $\mathcal{K}$ function in which μ is the parameter set with known initial parameter μ_0. We define the *certificate* set as

$$\tilde{\Omega}(\gamma) = \{\, \mu \in \mathbb{R}^q \mid \alpha(|\mu - \mu_0|) \leq \gamma \,\}. \tag{4.10}$$

For given a specific $\gamma > 0$, if the intersection of the certificate set $\tilde{\Omega}(\beta)$ with the bifurcation set Ω^{SN} is empty, then the distance-to-bifurcation cannot be less than $\alpha^{-1}(\gamma)$. The key point in formulating the problem in this way is that the conditions which specify whether the intersection set $\tilde{\Omega}(\beta) \cap \Omega^{SN}$ is empty or not can be relaxed into SOS condition [90, 75]. This fact is formally stated in the following proposition.

Proposition 4.4.1. *For a constant $\gamma > 0$, let $\tilde{\Omega}(\gamma)$ be a certificate set in (4.10). Consider the set Ω^{SN} in (4.7). If there exist polynomials $V(\mu)$ and $r(\mu)$ such that*

$$a_{n-1}^2(\mu)(V(\mu) - \gamma) + r(|\mu|)a_n(\mu) \quad \text{is SOS}, \tag{4.11}$$

then $\Omega^{SN} \cap \tilde{\Omega}(\gamma) = \varnothing$.

Proof. Verifying the condition $\Omega^{SN} \cap \tilde{\Omega}^{SN} = \varnothing$ amounts to check the emptiness of

the set

$$\{\, \mu \mid a_n = 0,\, a_{n-1} \neq 0,\, V(\mu) - \gamma \neq 0,\, -(V(\mu) - \gamma) \geq 0 \,\}.$$

Using the *positivstellensatz* (p-satz) theorem [103, 5, see also chapter 2], this set is empty if there exist SOS polynomials s_0, s_1 and polynomials $V(\mu)$, $t(\mu)$ such that

$$s_0 - s_1(V(\mu) - \gamma) + a_{n-1}^{2m} \left(V(\mu) - \gamma\right)^{2m} + t(\mu)a_n = 0.$$

Letting $s_0 = 0$, $m = 1$, and $t(\mu) = (V(\mu) - \gamma)r(\mu)$, the above equation becomes

$$s_1(V(\mu) - \gamma) = (V(\mu) - \gamma)\left(a_{n-1}^2(V(\mu) - \gamma) + r(\mu)a_n\right),$$

which implies the SOS condition in (4.11). Now consider any $\mu \in \Omega^{SN}$ for which $a_n(\mu) = 0$ holds. Upon substitution with the SOS condition in (4.11), we have

$$a_{n-1}^2(\mu)(V(\mu) - \gamma) \geq 0.$$

Since $a_{n-1}^2 > 0$, we have $V(\mu) - \gamma \geq 0$ which implies that any $\mu \in \Omega^{SN}$ will lie outside the level set defined by $V(\mu) \leq \gamma$. □

In a similar way, an SOS condition for the non-existence of a Hopf bifurcation can be stated in the following proposition.

Proposition 4.4.2. *For a constant $\gamma > 0$, let $\tilde{\Omega}(\gamma)$ be a certificate set (4.10) and consider Ω^H in (4.8). If there exist polynomials $V(\mu)$, $r(\mu)$ such that*

$$V(\mu) - \gamma + r(\mu)\triangle_{n-1}(\mu) \quad \text{is SOS}, \tag{4.12}$$

then $\Omega^H \cap \tilde{\Omega}(\gamma) = \varnothing$.

Proof. Verifying the condition $\Omega^H \cap \tilde{\Omega}(\gamma) = \varnothing$ amounts to check the emptiness of the

set

$$\{\, \mu \mid \triangle_{n-1} = 0,\ V(\mu) - \gamma \neq 0,\ -(V(\mu) - \gamma) \geq 0 \,\}.$$

Using the p-satz theorem, this set is empty if there exist SOS polynomials s_0, s_1 and polynomials $V(\mu)$, $t(\mu)$ such that

$$s_0 - s_1(V(\mu) - \gamma) + (V(\mu) - \gamma)^{2m} + t(\mu)\triangle_{n-1} = 0.$$

Let $s_0 = 0$, $m = 1$, $t(\mu) = (V(\mu) - \gamma)r(\mu)$, then

$$s_1(V(\mu) - \gamma) = (V(\mu) - \gamma)\left[(V(\mu) - \gamma) + r(\mu)\triangle_{n-1}\right],$$

as given in the SOS condition (4.12). Now consider any $\mu \in \Omega^H$ for which $\triangle_{n-1}(\mu) = 0$ holds. Upon substitution with the SOS condition in (4.12) we have $V(\mu) > \gamma$ which implies that any $\mu \in \Omega^H$ will lie outside the level set defined by $V(\mu) \leq \gamma$. □

The results in Propositions 4.4.1 and 4.4.2 characterize those γ for which the associated certificate set $\tilde{\Omega}(\gamma)$ is bifurcation free. Clearly, if one were to identify the maximum value of γ for which, say, proposition 4.4.1 held, then this γ could be used to bound the minimum distance-to-bifurcation. In particular, let μ_0 be a known initial parameter. Define the certificate function as $V(\mu) = \alpha(|\mu - \mu_0|)$ where α is class $\mathcal{K}$, and let $\overline{\gamma}$ denotes the largest real constant for which, say, Proposition 4.4.1 holds. Then the distance-to-bifurcation, γ, can be bounded below as $\gamma = |\mu^* - \mu_0| \geq \alpha^{-1}(\overline{\gamma})$. One obvious choice for α is to let it be $|\mu - \mu_0|$. This observation suggests that we can formulate an SOS optimization to compute the minimum γ. This is formalized in the following proposition which is stated for the saddle-node bifurcation in Proposition 4.4.1. Clearly a similar result would hold for the Hopf bifurcation using the SOS condition given in equation (4.12).

Proposition 4.4.3. *Consider system (4.4) and its Jacobian matrix in (4.5). Let* μ_0

be the initial parameters and let μ^* denotes the critical parameters at which a saddle-node bifurcation occurs. If there exist a constant $\bar{\gamma} > 0$, polynomials $\bar{V} = |\mu^* - \mu_0|$ and $r(\mu)$ such that the following SOS optimization

$$\begin{aligned} &max \quad \bar{\gamma} \\ &s.t. \quad a_{n-1}^2(\mu)(\bar{V}(\mu) - \gamma) + r(\mu)a_n(\mu) \quad \text{is SOS,} \end{aligned}$$

has a feasible solution, then the distance-to-bifurcation is defined as $|\mu^* - \mu_0| \geq \overline{\gamma}$.

Proof. From the proposition's assumption, we know a saddle-node bifurcation exists and therefore the set Ω^{SN} is not empty. Since no bifurcation takes place at μ_0, one can take the infimum of this set, say $\inf(\Omega^{SN})$. Note that the sets $\tilde{\Omega}(\gamma)$ are compact sets, so there exists $\overline{\gamma} = \inf(\Omega^{SN})$ such that for any $\gamma < \overline{\gamma}$ we know from Proposition 4.4.1 that no saddle-node bifurcation occurs. □

As discussed in chapter 3, an SOS program defined in proposition 4.4.3 can be solved efficiently using the SOS programming tools [90, 75] combined with semidefinite programming solver [105].

4.5 Examples

This section present example uses of the method discussed in the preceedings sections for computing the minimum distance-to-bifurcation in different applications. The first two examples illustrate the computation of distance to Hopf bifurcation for the brusselator and the tritrophic foodweb models analyzed in chapter 3. The last example presents the computation of the minimum distance to saddle-node bifurcation in an example from voltage collapse problem which was examined previously in [10].

4.5.1 The Brusselator model

The model of this system is given in (3.24) and its equilibrium parameterization is given in (3.29). Note that this model has four parameters and so the standard numerical bifurcation softwares would be difficult to use for bifurcation analysis.

The Jacobian matrix (4.5) for this system is given by

$$\begin{aligned} J(\lambda, h) &= N\text{diag}(E\lambda)Z^T\text{diag}(h), \\ &= \begin{bmatrix} (\lambda_1 - \lambda_2)h_1 & \lambda_1 h_2 \\ -\lambda_1 h_1 & -\lambda_1 h_2 \end{bmatrix}, \end{aligned}$$

with $h_i = (1/x_i^*)$ and x_i^* $(i = 1, 2)$ are given in (3.29). The characteristic polynomial of J satisfies

$$p(s) = s^2 + (\lambda_1 h_2 + \lambda_2 h_1 - \lambda_1 h_1)s + \lambda_1 \lambda_2 h_1 h_2.$$

Using the equilibrioum parameterization in (3.29), one may verify that the above characteristic polynomials can be rewritten in term of systems parameters below

$$p(s) = s^2 + (k_2 - k_1 - k_3)s + k_1 k_3.$$

It is easy to see that $p(s)$ will have a simple pair of imaginary eigenvalues if $k_1 k_3 > 0$ and $k_2 - k_1 - k_3 = 0$. Since $k_i \geq 0,\ (i = 1, \ldots, 4)$, the condition for Hopf bifurcation can be reduced to a single algebraic condition $k_2 - k_1 - k_3 = 0$. By defining $F(k) = \Sigma_{i=1}^4 (k_i^* - k_i^0)^2$ where k_i^0 denotes the initial paramater values, the minimum distance-to-bifurcation can be computed using the following SOS optimization.

$$\begin{aligned} &\max \quad \gamma, \\ &\text{s.t.} \quad F(k) - \gamma - \sigma(k)(k_2 - k_1 - k_3) \quad \text{is SOS.} \end{aligned}$$

Let's consider an initial parameter $k_i^0 = 1$ for $i = (1, \ldots, 4)$ and initial states $x_1(0) =$

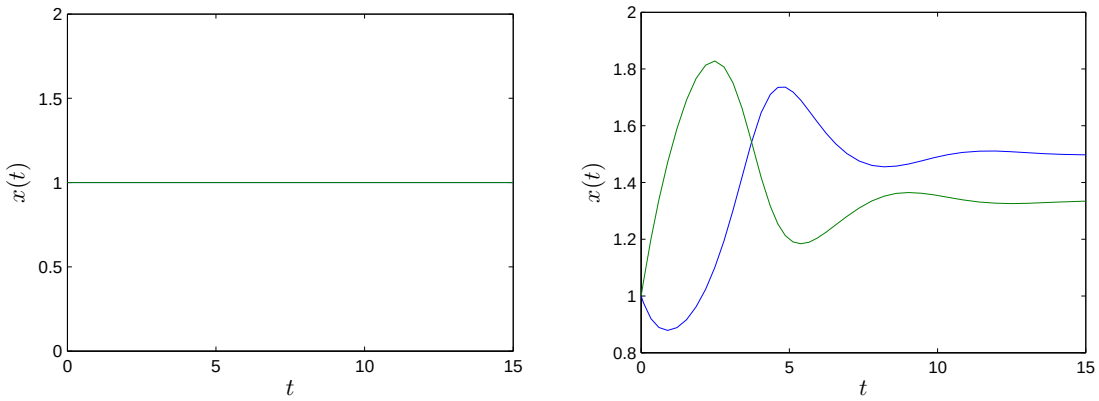

(a) Initial parameter k^0.

(b) Critical parameter k^*.

Figure 4.2. Hopf bifurcation in the Brusselator model.

$x_2(0) = 1$ for which the system has an asymptotically stable equilibrium at $x_1^* = x_2^* = 1$ (see figure 4.2a). We use SOSTOOLS [90] to solve the above SOS optimization and found a minimum distance of $\gamma = 0.33$ which corresponds to parameter $k = [2/3, 4/3, 2/3, 1]$. The trajectories of the states for this parameter k^* are plotted in figure 4.2b and confirm that a simple Hopf bifurcation occurs.

4.5.2 Tritrophic foodweb model

The model of this system is given in (3.31) and its equilibrium parameterization is given in (3.33). The Jacobian matrix (4.5) is therefore given by

$$\begin{aligned} J(\lambda, h) &= N\mathrm{diag}(E\lambda)Z^T\mathrm{diag}(h) \\ &= \begin{bmatrix} -h_1(\lambda_1+\lambda_2) & \lambda_2 h_2 & 0 & h_4\lambda_2 \\ h_1(\lambda_3+\lambda_4) & 0 & -\lambda_3 h_3 & (\lambda_3+\lambda_4)h_4 \\ 0 & \lambda_5 h_2 & 0 & 0 \\ \lambda_6 h_1 & \lambda_7 h_2 & 0 & \lambda_7 h_4 \end{bmatrix} \end{aligned}$$

with $h_i = (1/x_i^*)$ and x_i^* $(i = 1, \ldots, 4)$ is given in (3.33). The characteristic equation of J is given by

$$p(s) = s^4 + a_3 s^3 + a_2 s^2 + a_1 s + a_0,$$

where

$$\begin{aligned}
&a_0 = 0, \qquad a_2 = k_6\lambda_3\lambda_4(\lambda_6 + \lambda_7) - k_5, \\
&a_1 = k_5 k_6 \lambda_3(\lambda_6 + 2\lambda_7) - k_1 k_6 \lambda_4 \lambda_6 \lambda_7 - 2k_1 k_5(\lambda_3 + \lambda_4)(\lambda_6 + \lambda_7)^2, \\
&a_3 = k_5(\lambda_6 + 2\lambda_7) - k_1\lambda_4(\lambda_6 + \lambda_7)^2.
\end{aligned}$$

The Hurwitz determinant that corresponds to the above $p(s)$ is given by

$$\triangle = \begin{vmatrix} a_3 & a_1 & 0 & 0 \\ 1 & a_2 & a_0 & 0 \\ 0 & a_3 & a_1 & 0 \\ 0 & 1 & a_2 & a_0 \end{vmatrix},$$

such that the first three hurwitz determinant are given by $\triangle_1 = a_3$, $\triangle_2 = a_3 a_2 - a_1$, and $\triangle_3 = a_1(a_2 a_3 - a_1) - a_0 a_3^2$. By the criterion in proposition 4.3.1, a Hopf bifurcation will occur if the following conditions are satisfied

$$\triangle_1 = a_3 > 0, \quad \text{and} \quad \triangle_2 = a_3 a_2 - a_1 = 0.$$

One may verify that these conditions are equivalent with the requirement

$$a_1 > 0, \quad a_2 > 0, \quad a_3 > 0, \quad a_3 a_2 - a_1 = 0.$$

Note that $a_i (i = 0, \ldots, 3)$ contain only parameters (k_1, k_5, k_6) and so the minimum distance-to-bifurcation is defined by the following optimization problem

$$\begin{aligned} \min \quad & (k_1^* - k_1^0)^2 + (k_5^* - k_5^0)^2 + (k_6^* - k_6^0)^2 \\ \text{s.t.} \quad & a_2 a_3 - a_1 = 0, a_1 > 0, a_2 > 0, a_3 > 0 \end{aligned}$$

The corresponding SOS optimization is then given by

$$\begin{aligned} \max \quad & \gamma \\ \text{s.t.} \quad & F(k) - \gamma - \sigma(k)(a_2 a_3 - a_1) - \textstyle\sum_{i=1}^{3} g_i(k) a_i \quad \text{is SOS} \end{aligned}$$

with $F(k) = (k_1^* - k_1^0)^2 + (k_5^* - k_5^0)^2 + (k_6^* - k_6^0)^2$. Let $x_0 = (0.7, 0.8, 1.4)$ be the initial condition and $k^0 = (0.4, 0.4, 0.25, 0.1, 0.02, 0.25, 0.2)$ be the initial parameter. One may verify that the pair (x^0, k^0) results in an asymptotically stable trajectory of the system (see figure 4.3a).

For initial pair (x^0, k^0), we use the above SOS optimization problem to compute the critical parameters $k^* = (k_1^*, k_5^*, k_5^*)$ at which a Hopf bifurcation occurs. Using k^0 and the equilibrium parameterization x^* in (3.33), we have $(\lambda_3, \lambda_4, \lambda_6, \lambda_7) = (0.084, 0.016, 0.1, 0.4)$. Thus, the corresponding coefficients in the constraint of the above SOS optimization are

$$\begin{aligned} a_1 &= -0.05 k_1 k_5 - 0.000672 k_1 k_6 + 0.0756 k_5 k_6, \\ a_2 &= -k_5 + 0.000672 k_6, \\ a_3 &= -0.004 k_1 + 0.9 k_5. \end{aligned}$$

Solving the above optimization problem, we get the minimum value $\gamma = 0.1447$ that corresponds to parameter $k^* = (k_1^*, k_5^*, k_6^*) = (0.0220, 0.0002, 0.2766)$. The trajectory of the system for this k^* is plotted in figure 4.3b which shows sustained oscillation and verify the appearance of a Hopf bifurcation.

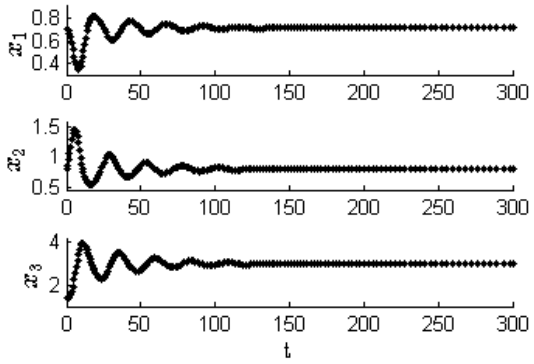

(a) Stable trajectory for k^0.

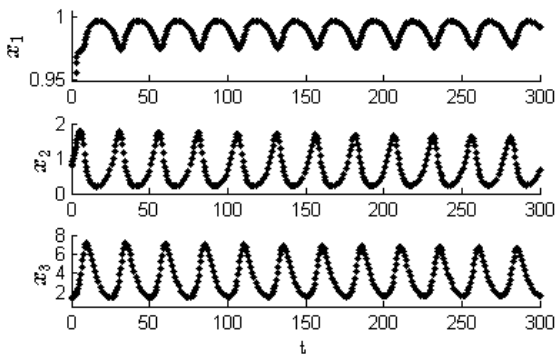

(b) Oscillation for k^*.

Figure 4.3. Comparison of foodweb model trajectories for k^0 and k^*.

As a comparison, we use XPPAUT [33] to search for the closest bifurcation parameters k^* at which a Hopf bifurcation occurs when the initial parameters are set to k^0. We get a closest Hopf bifurcation in the one parameter case at $k_1^* = 0.0184$ which corresponds to $\gamma = 0.1456$. A smaller γ obtained in our method (using three parameters) compared to that obtained using XPPAuto (one parameter) illustrates the sensitivity of the system to correlated variations of the parameters. In other words, considering only individual parameter variation in the standard numerical bifurcation analysis may result in a conservative estimate about the minimum distance to bifurcation. Our proposed method avoid such conservativeness by considering simultaneous parameter variations when searching for the minimum distance-to-bifurcation.

4.5.3 Voltage collapse problem

This example considers a two-buses generator-line-load model of a power network model which was previously used in [10] to study the voltage collapse problem. The

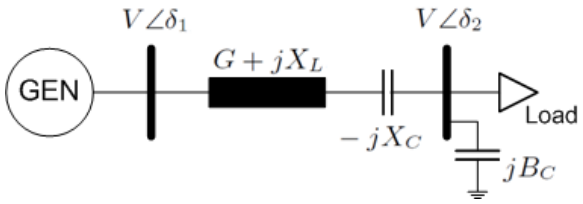

Figure 4.4. A simple power network [10].

differential equation governing the system dynamics is given by

$$\begin{aligned}
\dot{\omega} &= \frac{1}{M}[P_m - P_{e1}(\delta, V) - D_G\omega], \\
\dot{\delta} &= \omega - \frac{1}{D_L}[P_{e2}(\delta, V) - P_d], \\
\dot{V} &= \frac{1}{\tau}[Q_e(\delta, V) - Q_d],
\end{aligned} \tag{4.13}$$

where $\delta = \delta_1 - \delta_2$ and

$$\begin{aligned}
&P_{e1} = G - V(G\cos\delta - B\sin\delta), \qquad P_{e2} = -V^2G + V(G\cos\delta + B\sin\delta), \\
&Q_e = -V^2(B - B_c) - V(G\sin\delta - B\cos\delta), \\
&G = R/[R^2 + (X_L - X_x)^2], \qquad B = (X_L - X_x)/[R^2 + (X_L - X_x)^2.
\end{aligned}$$

We will use the methods in previous section to determine the minimum distance to saddle-node bifurcation (i.e. voltage collapse). We pose the problem in term of parameters $k = (P_d, Q_d)$ (the load powers) and compute the minimum $\gamma = |k^* - k^0|$ such that the equilibrium and the bifurcation conditions are satisfied. Let's assume $\omega = 0, X_c = B_c = 0, R = 0.1, X_L = 0.5$ and define $x = \sin\delta$ and $y = \cos\delta$. One can

verify that the equilibria of (4.13) satisfy

$$\begin{aligned} 0 &= -V^2G + VGy + VBx - P_d, \\ 0 &= -V^2B - VGx + VBy - Q_d, \\ 0 &= x^2 + y^2 - 1. \end{aligned} \tag{4.14}$$

On the other hand, system (4.13) will have a saddle node bifurcation if its Jacobian matrix is singular (i.e. has zero determinant) which in this case is defined as

$$0 = B^2 + G^2 - 2B^2Vy - 2G^2Vy. \tag{4.15}$$

Note that equations (4.14)-(4.15) define a set of polynomial equation. If we directly compute a Gröbner basis for this polynomial equation, it is interesting to find that the following single Gröbner basis $\mathcal{G}$ in term of parameters P_d and Q_d is obtained

$$\begin{aligned} \mathcal{G} = B^2 &\left(B(B - 4Q_d) + 2(G^2 - 2GP_d - 2P_d^2)\right) \\ &+ G^2\left(G(G - 4P_d) - 4Q_d(B + Q_d)\right) + 8BGP_dQ_d. \end{aligned}$$

The Gröbner basis $\mathcal{G}$ thus defines the bifurcation manifolds at which a saddle-node bifurcation occurs and so the computation of the minimum distance to saddle-node bifurcation can simply be defined as

$$\begin{aligned} &\text{maximize:} \quad \gamma \\ &\text{such that:} \quad (P_d^* - P_d^0)^2 + (Q_d^* - Q_d^0)^2 - \gamma + r(\mu)\mathcal{G} \quad \text{is SOS.} \end{aligned}$$

We use SOSTOOLS [88] to solve the above SOS optimization and found a minimum $\gamma = 0.2404$ which corresponds to $k^* = (0.0961, 0.4808)$. These are the same results obtained in [10], but the underlying optimization problem is much simpler as it only uses a single constraint. Figure 4.5 plots the bifurcation manifold of the power

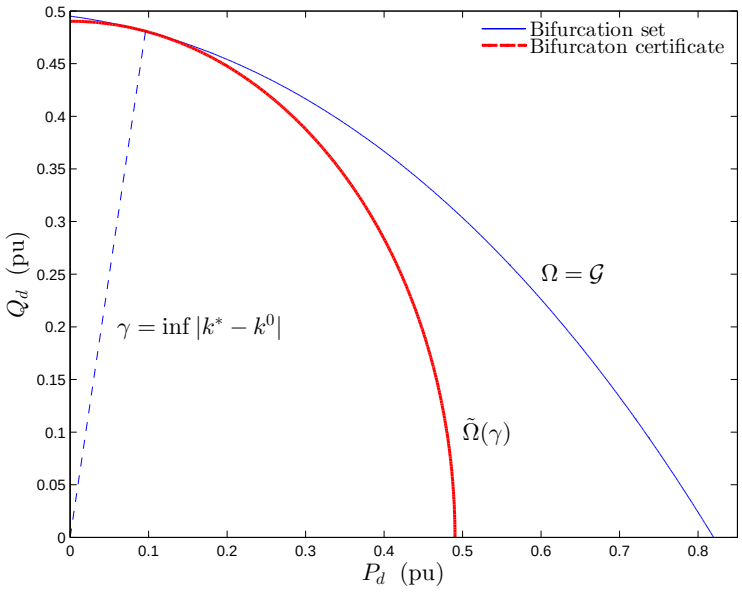

Figure 4.5. Bifurcation set and bifurcation certificate of system (4.13).

system (4.13) which is defined by the curve of the Gröbner basis $\mathcal{G}$. The certificate $\tilde{\Omega}(\gamma)$ plotted in this figures indicates that the obtained γ is the shortest distance from the initial parameter to the point of intersection between curves $\mathcal{G}$ and $\tilde{\Omega}(\gamma)$.

4.6 Remarks and Proposed Research

This chapter proposed a method to predict the bifurcation-induced regime shifts in the framework of minimum distance-to-bifurcation problem. We presented SOS optimization method to compute a lower bound on the minimum distance-to-bifurcation in nonnegative systems with kinetic realizations. Applications of the proposed method in several examples showed that the proposed approach was able to detect how correlated variations in system rate constants could lead to smaller distance-to-bifurcations than are usually found with the conventional one or two parameters bifurcation tools.

Proposed Research: We identify the following two research tasks that will be

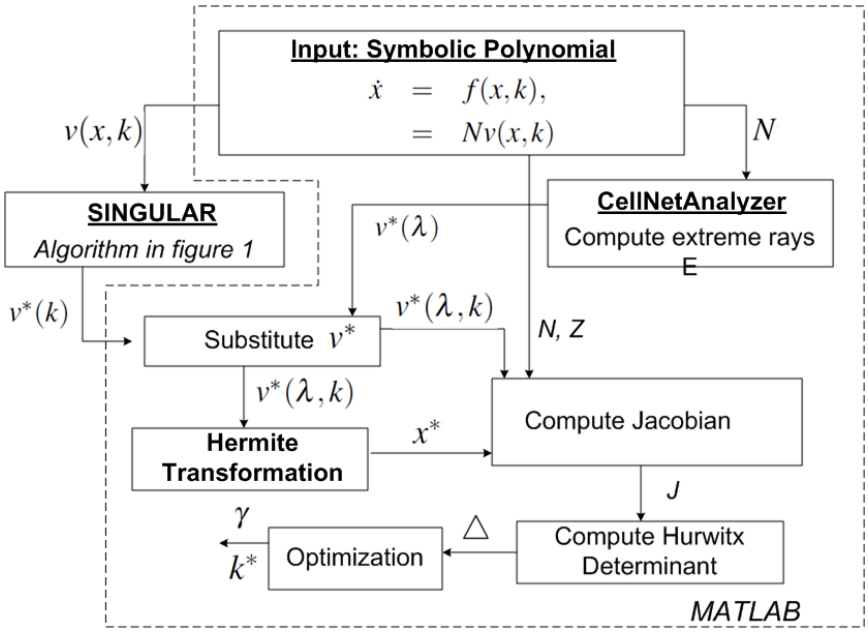

Figure 4.6. Block diagram of the software toolkit.

pursued to complete the results presented in this chapter.

- *Development of software toolkit:* This research task aims to develop a software toolkit which implements the method presented in this chapter. In particular, this toolkit will be integrated with the software toolkit that performs equilibrium parameterization method discussed in chapter 3. A block diagram of the currently developed toolkit is shown in figure 4.6. The toolkit will combine several freely available software codes to perform various computations discussed in this chapter. We plan to evaluate the performance of this toolkit in an experiment for predicting ecological regime shifts described in chapter 6.

- *Performance comparison and evaluation:* This research task aims to compare the performance of the proposed method with the currently established regime shifts methods such as those in [26, 10]. This comparison will be performed using the model of predator-prey system cultured in the chemostat as described in chapter 6. An alternative model that will be used for this evaluation is the two-are power system model described in [68]. The expected output of this research task is a clear evaluation about the strength and weakness of each method.

Suggestion for future works:

- The current approach requires the analyzed systems to be nonnegative and

have kinetic realization. Note that the role of nonnegativity requirement in the current approach is that it helps reduce the space $ker(N) \cap \mathbb{R}^n$ into a convex cone $ker(N) \cap \mathbb{R}^n_+$ which can be characterized in term of the convex parameter λ. It would be interesting to investigate efficient methods for computing the intersection $ker(N) \cap \mathbb{R}^n$. If such computation method exist, then the nonnegativity requirement can be dropped and the proposed method can be applied to larger classes of systems.

- The proposed method is currently applied only for local bifurcations of co-dimension 1. Further explorations may includes application of the proposed methods to study global bifurcation or local bifurcation of co-dimension 2 [73].

CHAPTER 5

FORECASTING NOISE-INDUCED REGIME SHIFTS

5.1 Introduction

This chapter discusses our proposed methods to forecast noise-induced regime shifts. We recall that a noise-induced regime shift occurs because the underlying system have multiple stable equilibria and the perturbation from external noises pushes the system's sample paths from the region of attraction (ROA) of one stable equilibrium to the ROA of alternative equilibrium. We present two probabilistic quantities that can be used to predict the onset of such noise-induced regime shifts namely the *mean first passage time* (MFPT), which quantify the average time required by the process' sample paths to cross the boundary of an ROA, and the *reachability probability* which quantifies the probability that, starting from the ROA of one stable equilibrium, the process' sample paths eventually reach the ROA of an alternative equilibrium in finite time period.

5.1.1 Backgrounds and prior works

To motivate the discussion, let's revisit the stochastically perturbed lake eutrophication model described in chapter 1. The model of the system is given by the following stochastic differential equation (SDE)

$$\begin{aligned} dx(t) &= f(x)dt + g(x)dw(t), \\ &= \left(a - bx + \frac{x^2}{1+x^2}\right)dt + \sigma dw(t), \end{aligned}$$

where $f(x)$ and $g(x)$ are the *drift* and *diffusion*, respectively, $\{w(t)\}$ is a Wiener process with constant variance σ. One may verify that this scalar SDE can be written as a *stochastic gradient system* [40]

$$dx = -\nabla V(x)dt + \sigma dw(t),$$

where $\nabla V(x) = \frac{dV(x)}{dx}$ and $V(x) = -\int f(x)dx$ is a *potential function* governing the dynamics of the deterministic part of the system. One may therefore view the state x as a particle moving in a potential landscape defined by $V(x)$. In our example, this potential function is given by

$$V(x) = -\int \left(a - bx + \frac{x^2}{1+x^2}\right) dx = \frac{bx^2}{2} + \arctan(x) - (a+1)x.$$

Let us consider the parameters $a = 0.06$ and $b = 0.525$ for which the deterministic part of the system have two stable equilibria separated by one unstable equilibrium. The plot of $V(x)$ for this parameter values depicted in figure 5.1a shows that it has two local minima x_L^* and x_H^* which are separated by one local maxima x_U^*. One may verify that the points x_L^* and x_H^* correspond to the two stable equilibria of the system whereas the point x_U^* corresponds to the unstable equilibrium. In particular, the potential $V(x)$ also defines the ROAs 'Low ROA' and 'High ROA' of the stable equilibria x_L^* and x_H^*, respectively. These ROAs are separated by a *separatrix* defined by the unstable equilibrium point x_U^* . Thus, any trajectory of the deterministic system which starts inside one of the ROAs will be confined within that ROA and eventually goes to the equilibrium point of that ROA.

In the presence of external noises $\{w(t)\}$, the sample paths of the system can no longer be guaranteed to always stay within a particular ROA. The presence of external noise, in particular, brings a consequence that *there is a positive probability* for the sample paths of the process to eventually reach the separatrix of the competing

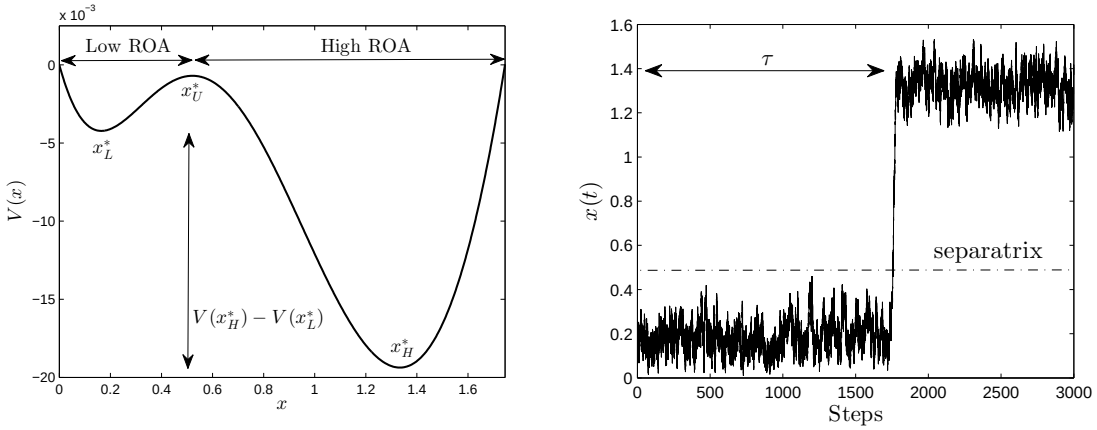

(a) Potential function $V(x)$.

(b) Noise-induced regime shifts ($\sigma = 0.05$).

Figure 5.1. Potential function and sample path of lake eutrophication model.

ROAs *in a finite time*. Once the sample path gets closer to the separatrix, further perturbation from external noise may forces the sample path to cross the separatrix and then reach the ROA of an alternative equilibrium. Such *noise-induced* regime shifts is illustrated in figure 5.1b when the variance of the noise is $\sigma = 0.05$. This example illustrates that even small noise intensity may drives the process' sample paths to shift from the ROA of equilibrium x_L^* to the ROA of alternative equilibrium x_L^*.

The statistics of process $\{x(t)\}$ can be studied from its probability density function, $\varphi(x,t)$, whose evolution satisfies the *Chapman-Kolmogorov* or *Fokker-Planck* (FP) equations of the form [40]

$$\frac{\partial \varphi(x,t)}{\partial t} = -\frac{\partial}{\partial x}\left(f(x)\varphi(x,t)\right) + \frac{1}{2}\frac{\partial^2}{\partial x^2}\left(\sigma^2\varphi(x,t)\right).$$

For a stochastic gradient system as in our example, the above FP equation can be solved explicitly. One may then, for example, computes the average time τ required by $\{x(t)\}$ to reach the point x_U^* when started from point x_L^* (i.e. MFPT). For our

example, this τ is given by [40]

$$\tau(x_L^* \to x_U^*) = \frac{\pi}{(|\nabla^2 V(x_U^*)|\, \nabla^2 V(x_L^*))^{1/2}} exp\left\{ \frac{V(x_U^*) - V(x_L^*)}{\sigma^2} \right\}.$$

The time τ would then indicates the expected time at which the system undergoes regime shifts. One may also compute the probability that the sample paths of $\{x(t)\}$ which start in the ROA of equilibrium point x_L^* will eventually reach the ROA of equilibrium point x_H^* in a finite time $t \leq \tau(x_L^* \to x_U^*)$. For the above lake model, this probability is given by [40]

$$\mathbb{P}\{x(t) = x_U^* | x(0) = x_L^*\} = \frac{\int_{x_L^*}^{x_U^*} \psi(x)dx}{\int_0^{x_U^*} \psi(x)dx}, \quad \text{where} \quad \psi(x) = exp\left(\int_0^{x_L^*} \frac{-\nabla V(x)}{\sigma^2} dx \right),$$

and it can be used to measure the likelihood of regime shifts occurence.

The above example suggests that the task of predicting the onset of regime shifts can be formulated either as an MFPT or as a stochastic reachability problems which are formally stated below.

- *MFPT problem:* Let $\{x(t)\}$ be a stochastic process whose state $x(t)$ at time $t \geq 0$ taking values on a bounded open subsets $\mathcal{X} \subseteq \mathbb{R}^n$ of the Euclidean space with smooth boundary $\partial\mathcal{X}$. Let $\mathcal{X}_0 \subset \mathcal{X}$ be an initial set such that $x(0) = x_0 \in \mathcal{X}_0$. The time at which the sample paths of $\{x(t)\}$ hits the set $\partial\mathcal{X}$ is a random variable τ called the first passsage time and is defined as

$$\tau \equiv \inf_t \{ t \geq 0 \,|\, x(t) \in \partial\mathcal{X} \}. \tag{5.1}$$

  Thus, the MFPT problem concerns with the computation of the expected value $\mathbb{E}\{\tau\}$ of τ.

- *Stochastic reachability problem:* Let $\{x(t)\}$ be a stochastic process whose state $x(t)$ at time $t \geq 0$ taking values on a bounded open subsets $\mathcal{X} \subseteq \mathbb{R}^n$ of the Euclidean space. Let $\mathcal{X}_0 \subset \mathcal{X}$ be an initial set such that $x(0) = x_0 \in \mathcal{X}_0$ and let $\mathcal{X}_u \subset \mathcal{X}$ denotes an arbitrary set such that $\mathcal{X}_u \cap \mathcal{X}_0 = \emptyset$. The stochastic reachability problem concerns with the computation of the probability that, starting from the initial set $\mathcal{X}_0$, the sample paths of the process will reach the set $\mathcal{X}_u$ in a finite time $t \in [0, T]$. More formally, this problem seeks to compute

a constant $\beta \in [0, 1]$ such that

$$\mathbb{P}\{x(t) \in \mathcal{X}_u, \text{ for some } 0 \leq t \leq T \mid x(0) \in \mathcal{X}_0\} \leq \beta. \tag{5.2}$$

One should notice that the approach described in the above example do not scales up to systems with dimensionality greater than one due to its reliance on the solution of the FP equation. It is widely acknowledged that solving the FP equation for systems with dimensionality greater than one is generally difficult as it involve the task of solving a set of partial differential equations with appropriate boundary conditions [93, 37, 40]. Another approach commonly used to compute (5.1)-(5.2) is based on the stochastic simulations using Monte Carlo methods [70]. This approach, however, is computationally expensive as it requires exhaustive simulations of a large number of the process' sample paths.

5.1.2 Approach and Contribution

One alternative approach to compute (5.1)-(5.2) which do not rely on the solution of FP equation and do not require exhaustive simulations of the process' sample paths is based on the Lyapunov-like method commonly used in stochastic stability analysis [91, 72]. This method essentially search for a positive semidefinite function $V(x(t))$, called *barrier certificate*, from which the upper bounds for (5.1)-(5.2) can be deduced. In particular, if the drift and diffusion terms of the process are polynomial functions then the computation of these bounds can be formulated and solved using SOS optimization [91]. This SOS optimization approach is recently introduced in [91] to solve the reachability problems in stochastic process driven by simple Brownian motion.

One should realize that many cases of noise-induced regime shifts occur due to the presence of jumps or discontinous changes on the system's states as a result of extreme or abnormal events. Examples of these include natural storm events

that wash organisms out of the lakes or rivers [99], abnormal variations of the stock market prices that leads to market crash [2], or the collapse of an ecosystem due to natural disaster or human exploitation [99]. These events are no longer suitable to be modeled by Wiener process but are better characterized as stochastic renewal process. Forecasting regime shifts that are induced by these 'shock' noises is also important and so it is valuable to extend the basic approach in [72, 91] to systems modeled as jump diffusion process.

This chapter presents an extension of the methods introduced in [72, 91] to compute upper bounds of (5.1)-(5.2) for systems modeled as jump diffusion processes. As in [72, 91], the proposed method is also based on searching for a barrier certificate, $V(x(t))$, that generates a supermartingale from which the bounds can be deduced. The main contribution in this chapter is a polynomial characterization of the jump diffusion process' infinitesimal generators which allows the use of SOS optimization technique to search for the appropriate barrier certificate.

The remainder of this chapter is structured as follows. Section 5.2 gives background on jump diffusion process. Section 5.3 presents the characterization of upper bounds for (5.1)-(5.2) in systems modeled as jump diffusion processes. Formulation of the SOS optimization problem for computing these bounds are also discussed. Section 5.4 illustrates an example use of the proposed method for managing fish population in freshwater ecosystem. Remarks and suggestions for future works are given in section 5.5.

Notational Conventions: Let $\{x(t)\}$ denotes a random process whose state $x(t) \in \mathcal{X}$ at time $t \in \mathbb{R}_+$ taking values in an open subset $\mathcal{X} \subseteq \mathbb{R}^n$ of the Euclidean space. The expected value of $\{x(t)\}$ is denoted as $\mathbb{E}\{x\}$ and the probability of an event is denoted as $\mathbb{P}\{\cdot\}$. If $\{x(t)\}$ has distribution $F(x)$, then its nth moment is denoted as $\mathbb{M}_x^n = \int_0^\infty x^n dF(x)$.

For given n-dimensional multi-indices α and β, their binomial coefficient is defined as

$$\binom{\alpha}{\beta} = \binom{\alpha_1}{\beta_1} \cdots \binom{\alpha_n}{\beta_n} = \frac{\alpha!}{\beta!(\alpha-\beta)!}.$$

Given n-dimensional vectors $x, y \in \mathbb{R}^n$ and n-dimensional multi-indices α and β, the multi-index binomial theorem states

$$(x+y)^{[\alpha]} = \sum_{0 \leq \beta \leq \alpha} \binom{\alpha}{\beta} x^{[\alpha-\beta]} y^{[\beta]}.$$

It can be shown that

$$\partial^{[\alpha]} x^{[\beta]} = \begin{cases} \frac{\beta!}{(\beta-\alpha)!} x^{[\beta-\alpha]}, & \text{if } \alpha \leq \beta, \\ 0, & \text{otherwise.} \end{cases}$$

Given a bounded real-valued function $V(x) : \mathbb{R}^n \to \mathbb{R}$ and an n-dimensional multi-index α, the αth order partial derivative of V is defined as $\partial^{[\alpha]} V = \frac{\partial^{\alpha_1} V}{\partial x_1^{\alpha_1}} \frac{\partial^{\alpha_2} V}{\partial x_2^{\alpha_2}} \cdots \frac{\partial^{\alpha_n}}{\partial x_n^{\alpha_n}}$.

5.2 Jump Diffusion Processes

Let $\{\Omega, \mathcal{F}, \mathbb{P}\}$ be a complete probability space and let $\{\mathcal{F}_t\}_{t \geq 0}$ be a filtration over $\{\Omega, \mathcal{F}, \mathbb{P}\}$ which satisfies the conditions [112, 85]: (i) $\mathcal{F}_t$ contains the $\mathbb{P}-$negligible sets for all t, (ii) $\mathcal{F}_t$ is right continuous, i.e. $\mathcal{F}_{t^+} = \mathcal{F}_t$, for all t (i.e. the totality of information are observable by time t). Consider a jump diffusion process (JDP)

$$dx(t) = f(x(t))dt + \sigma(x(t))dw(t) + dJ(t), \quad x(0) = x_0, \tag{5.3}$$

where $f(\cdot) : \mathbb{R}^n \to \mathbb{R}^n$ and $\sigma(\cdot) : \mathbb{R}^n \to \mathbb{R}^n$ are Lipschitz continuous functions, $\{x(t)\}$ is a stochastic process, $\{w(t)\}$ is a Wiener process and $\{J(t)\}$ is a shot noise process

defined as

$$J(t) = \sum_{\ell=1}^{N(t)} y_\ell e^{-\delta(t-\tau_\ell)}, \quad \ell \in \mathbb{Z}_+. \tag{5.4}$$

In equation (5.4), $N(t)$ is a Poisson process with intensity ρ, $\{\tau_\ell\}$ are the event times of Poisson jumps, $\{y_\ell\}$ is an i.i.d. random process with distribution $F(y)$ describing the ℓ-th jump's size, and δ is a real positive constant representing the rate of exponential decay after a jump. The JDP in (5.3) is understood in Itô's sense and processes $\{w(t)\}$ and $\{J(t)\}$ are assumed to be independent from each other.

Let $Y(\tau_\ell, y_\ell) = y_\ell e^{\delta\tau_\ell}$, then $J(t)$ in (5.4) may be written as

$$J(t) \;\; = \;\; e^{-\delta t} \int_0^t \int_{\mathbb{R}^n} Y(\tau, y) N(d\tau, dy), \tag{5.5}$$

where $N(d\tau, dy)$ is a Poisson random measure with $\mathbb{E}\{N(dt, dy)\} = \rho dt F(dy)$. We define the increment of $J(t)$ as $dJ(t) = J(t + dt) - J(t)$ where dt is an infinitesimal time increment. Using equation (5.5) to expand out $dJ(t)$ and retaining the first order terms in dt, one finds the jump process increment can be written as

$$dJ(t) = -\delta J(t) dt + \int_{\mathbb{R}^n} y N(dt, dy), \tag{5.6}$$

where the second term in (5.4) is known as the compound Poisson process. Using the expression for the jump increment in (5.4), the JDP in (5.3) can be rewritten as

$$dx(t) = (f(x(t)) - \delta J(t))\, dt + \sigma(x(t)) dw(t) + \int_{\mathbb{R}^n} y N(dt, dy), \quad x(0) = x_0. \tag{5.7}$$

Since $\{J(t)\}$ in (5.6) and $\{w(t)\}$ are Markov processes, one may conclude that the solution of (5.7) is also a Markov process [92].

Now consider a Markov process $\{x(t)\}$ with right continuous sample path and

consider any function $V(x(t)) : \mathbb{R}^n \to \mathbb{R}$ that generate some statistics of $\{x(t)\}$. The (infinitesimal) *generator* of $\{x(t)\}$ is an operator, $\mathcal{L}$, whose action on $V(x(t))$ is defined by

$$\mathcal{L}V(x(t)) = \lim_{h \downarrow 0_+} \frac{\mathbb{E}\{V(x(h))|V(x_0)\} - V(x_0)}{h} \qquad \text{(if the limit exists)},$$

where $\downarrow$ means that the limit is taken from the right. For a diffusion process $\{x(t)\}$ that satisfies stochastic differential equation $dx(t) = f(x(t))dt + \sigma(x(t))dw(t)$ and a function $V(x(t)) \in C^2(\mathbb{R}^n)$ that is twice continuously differentiable in x and bounded for all $x \in \mathbb{R}^n$ (denote this class of functions as $C^2(\mathbb{R}^n)$), its generator, $\mathcal{L}_{DP}$, is given by [94]

$$\mathcal{L}_{DP}V(x(t)) = \frac{\partial V(x(t))}{\partial x} f(x(t)) + \frac{1}{2}\mathrm{Tr}\left(\sigma^T(x(t))\frac{\partial^2 V(x(t))}{\partial x^2}\sigma(x(t))\right). \tag{5.8}$$

For the jump process $\{x(t)\}$ in (5.7) and a function $V(x(t)) \in C^2(\mathbb{R}^n)$, one can show that its generator, $\mathcal{L}_{JP}$, is [112, 85]

$$\mathcal{L}_{JP}V(x(t)) = \rho \int_0^\infty (V(x+y) - V(x))\, dF(y) - \frac{\partial V(x(t))}{\partial x}\delta J(x). \tag{5.9}$$

Combining the above generators of diffusion and jump diffusion processes, one may conclude that the generator, $\mathcal{L}$, of JDP in (5.7) is given by

$$\begin{aligned}\mathcal{L}V(x(t)) &= \frac{\partial V(x(t))}{\partial x}\left(f(x(t)) - \delta J(t)\right) + \frac{1}{2}\mathrm{Tr}\left(\sigma^T(x(t))\frac{\partial^2 V(x(t))}{\partial x^2}\sigma(x(t))\right) \\ &\quad + \rho\int_0^\infty (V(x+y) - V(x))dF(y).\end{aligned} \tag{5.10}$$

The following Dynkin's formula for the JDP in (5.7) with generator in (5.10) can now be stated.

Lemma 5.2.1 (Dynkin's formula, [85]). *Consider the JDP in (5.5) defined on a*

bounded open set $\mathcal{X} \in \mathbb{R}^n$ *with smooth boundary* $\bar{\mathcal{X}}$. *Let* $V(x(t)) \in C^2(\mathbb{R}^n)$ *and let* $\tau < \infty$ *be a stopping time such that* $\tau \leq \tau_{\mathcal{X}} := \inf\{t : x(t) \notin \mathcal{X}\}$. *Suppose* $\mathbb{E}\left\{|V(x(\tau))| + \int_0^\tau |\mathcal{L}V(x(s))|ds\right\} < \infty$. *Then*

$$V(x(\tau)) = V(x_0) + \int_0^\tau \mathcal{L}V(s, x(s))ds. \tag{5.11}$$

Now recall [94] that a process $\{V(x(t))\}$ is said to be a *supermartingale* with respect to the filtration $\{\mathcal{F}_t\}_{t\geq 0}$ generated by the process $\{x(t)\}$ if: (i) $V(x(t))$ is $\mathcal{F}_t$-measurable for all $t \geq 0$, (ii) $\mathbb{E}\{|V(x(t))|\} < \infty$, and (iii) $\mathbb{E}\{V(x(t_2))|V(x(t_1))\} \leq V(x(t_1))$ for all $0 \leq t_1 \leq t_2 \leq \tau$. By the choice of $V(x(t)) \in C^2(\mathbb{R}^n)$ in (5.10) and the boundedness of $x \in \mathcal{X}$, it is known [85] that $V(x(t))$ will always satisfies conditions (i) and (ii), respectively. If $V(x(t))$ also satisfies $\mathcal{L}V(x(t)) \leq 0$, $\forall x \in \mathcal{X}$, then the Dynkin's formula (5.11) implies that condition (iii) will also be satistied. One may then conclude that a function $V(x(t)) \in C^2(\mathbb{R}^n)$ with $\mathcal{L}V(x(t)) \leq 0$, for all $x \in \mathcal{X}$ is a supermartingale with respect to $\{x(t)\}$. In this paper, we'll consider nonnegative supermartingale, i.e. $V(x(t)) \geq 0, \forall x \in \mathcal{X}$, for which the following inequality from [71] holds.

Lemma 5.2.2 ([71])**.** *Let* $\{V(x(t))\}$ *be a supermartingale with respect to the process* $\{x(t)\}$ *where* $x(t) \in \mathcal{X} \subseteq \mathbb{R}^n$ *and* $0 \leq t \leq \tau := \inf\{t : x(t) \notin \mathcal{X}\}$. *Let* $V(x(t))$ *be nonnegative in* $\mathcal{X}$. *Then for a constant* $\theta > 0$ *and any initial condition* $x_0 \in \mathcal{X}$,

$$\mathbb{P}\left\{\sup_{0\leq t\leq\tau} V(x(t)) \geq \theta \Big| x(0) = x_0\right\} \leq \frac{V(x_0)}{\theta}. \tag{5.12}$$

5.3 MFPT and Stochastic Reachability Analyses

Using the generator in (5.10), the Dynkin's formula in (5.11), and the supermartingale inequality in (5.12), we now present the method to compute upper bounds of (5.1)-(5.2) for JDP in (5.7).

5.3.1 Upper bound of MFPT

We first characterize an upper bound $\theta \geq 0$ for the MFPT of JDP (5.7).

Proposition 5.3.1. *Consider the JDP in (5.7) defined on a bounded open subset $\mathcal{X} \subset \mathbb{R}^n$ with smooth boundary $\partial\mathcal{X}$. Let the initial condition $x(0) = x_0$ be a random variable taking values in $\mathcal{X}_0 \subset \mathcal{X}$. If there exists a real-valued function $V(x(t)) \in C^2(\mathbb{R}^n)$ and a constant $\theta \geq 0$ such that*

$$\begin{aligned} V(x(t)) &\geq 0, \quad \forall x \in \mathcal{X}, \\ V(x(t)) &\leq 0, \quad \forall x \in \partial\mathcal{X}, \\ V(x(t)) &\leq \theta, \quad \forall x \in \mathcal{X}_0, \\ \frac{\partial V(x(t))}{\partial t} + \mathcal{L}V(x(t)) &\leq -1, \quad \forall x \in \mathcal{X}, \end{aligned}$$

where $\mathcal{L}V(x(t))$ is defined in (5.10), then $\mathbb{E}\{\tau\} \leq \theta$ with $\tau = \inf_t\{t \geq 0 : x(t) \in \partial\mathcal{X}\}$.

Proof. The technique of the proof is similar to that in [91]. Itô's lemma provides a stochastic differential equation for $V(x(t))$

$$dV(x(t)) = \left(\frac{\partial V(x(t))}{\partial t} + \mathcal{L}V(x(t))\right) dt + \sum_{k=1}^{m} \left(\sum_{i=1}^{n} \frac{\partial V(x(t))}{\partial x_i}\sigma_{ik}\right) dw_k(t).$$

Let $\tau \equiv \inf\{t \geq 0 : x(t) \in \partial\mathcal{X}\}$ and define $\tau \wedge t = \min\{\tau, t\}$. Integrating $dV(x(t))$ over the time interval $[0, \tau \wedge t]$ and taking the expectation yields

$$\mathbb{E}\left\{V(x(\tau \wedge t))\right\} = V(x(0)) + \mathbb{E}\left\{\int_0^{\tau\wedge t} \left(\frac{\partial V(x(s))}{\partial s} + \mathcal{L}V(x(s))\right) ds\right\}.$$

Taking the limit of the above equation as $t \to \infty$ and using the last condition in the proposition's statement, one finds

$$\mathbb{E}[V(x(\tau))] \leq V(x_0) - \mathbb{E}\left[\int_0^{\tau} ds\right] = V(x_0) - \mathbb{E}[\tau].$$

τ is the first time the state trajectory hits the boundary set $\partial\mathcal{X}$ and so the above equation implies that the MFPT satisfies

$$\mathbb{E}\{\tau\} \leq V(x_0) - \mathbb{E}[V(x(\tau))].$$

Boundary points of $\mathcal{X}$ are limit points of $\mathcal{X}$ and since $V(x(t)) \geq 0$ on $\mathcal{X}$, this means $V(x(t)) = 0$ on $\partial\mathcal{X}$. One may therefore conclude that $\mathbb{E}\{V(x(\tau))\} = 0$ which implies $\mathbb{E}\{\tau\} \leq V(x_0)$. By the third condition in the proposition, we know that $V(x_0) \leq \theta$ on $\mathcal{X}_0$ which implies $\mathbb{E}\{\tau\} \leq \theta$. □

Remark 5.3.2. From the proof of this proposition, we see that $\mathbb{E}\{V(x(t))|V(x_0)\} \leq V(x_0)$ for $0 \leq t \leq \tau$. Since $\mathcal{X}$ is a bounded set, this implies $\mathbb{E}\{V(x(t))\} < \infty$ which along with the requirement that $V(x(t)) \geq 0$ for all x implies the stochastic process generated by $V(x(t))$ is a supermartingale.

As stated below, the result in proposition 5.3.1 can be used to characterize an upper bound for the MFPT of diffusion process. The proof of this proposition is similar to that in proposition 5.3.1 except that we use the generator $\mathcal{L}_{DP}V(x(t))$ in (5.8).

Proposition 5.3.3. *Consider a diffusion process $dx(t) = f(x(t))dt + \sigma(x(t))dw(t)$ defined on a bounded open subset $\mathcal{X} \subset \mathbb{R}^n$ with smooth boundary $\partial\mathcal{X}$. Assume the initial condition satisfies $x(0) = x_0 \in \mathcal{X}_0 \subset \mathcal{X}$. If there exists a function $V(x(t)) \in C^2(\mathbb{R}^n)$ and a constant $\theta > 0$ such that*

$$\begin{aligned} V(x(t)) &\geq 0, \quad \forall x \in \mathcal{X}, \\ V(x(t)) &\leq 0, \quad \forall x \in \partial\mathcal{X}, \\ V(x(t)) &\leq \theta, \quad \forall x \in \mathcal{X}_0, \\ \frac{\partial V(x(t))}{\partial t} + \mathcal{L}_{DP}V(x(t)) &\leq -1, \quad \forall x \in \mathcal{X}, \end{aligned}$$

where $\mathcal{L}_{DP}V(x(t))$ is given in (5.8), then $\mathbb{E}\{\tau\} \leq \theta$ with $\tau = \inf_t\{t \geq 0 : x(t) \in \partial\mathcal{X}\}$.

5.3.2 Upper bound of finite time stochastic reachability

We now present the method to compute an upper bound for the probability (5.2).

Proposition 5.3.4. *Consider the JDP in (5.7) with $x_0 \in \mathcal{X}_0$. Let $\tau < \infty$ be a stopping time such that $T \leq \tau := \inf\{t : x(t) \notin \mathcal{X}\}$, and consider the stopped process $x(t)$ for $0 \leq t \leq T$. Assume the sets $\mathcal{X} \subset \mathbb{R}^n$, $\mathcal{X}_0 \subseteq \mathcal{X}$, and $\mathcal{X}_u \subseteq \mathcal{X}$ be given. Let $\phi(t)$ be a function of t such that $\Phi(T) = \int_0^T \phi(t)dt < \infty$ and define a function $\tilde{W}(x(t)) = V(x(t)) + \int_0^t \phi(t)dt$ with $V(x(t)) \in C^2(\mathbb{R}^n)$. If there exists a function $\tilde{W}(x(t))$ and positive constants β, β_1, β_2 with $\beta = \beta_1 + \beta_2$ such that*

$$\begin{aligned}
\tilde{W}(x(t)) &\geq 0, \quad \forall x \in \mathcal{X},\ t \in [0,T] \\
\tilde{W}(x(t)) &\leq \beta_1, \quad \forall x \in \mathcal{X}_0 \\
\int_0^T \phi(t)dt &\leq \beta_2, \quad \forall t \in [0,T] \\
\tilde{W}(x(t)) &\geq 1, \quad \forall x \in \mathcal{X}_u,\ t = T \\
\mathcal{L}\tilde{W}(x(t)) &\leq \phi(t), \quad \forall x \in \mathcal{X},\ t \in [0,T],
\end{aligned}$$

where $\mathcal{L}\tilde{W}(x(t)) = \mathcal{L}V(x(t)) - \frac{\partial}{\partial t}\int_0^T \phi(t)dt$, then the probability bound (5.2) holds.

Proof. Applying the Dynkin's formula to function $\tilde{W}(x(t))$ gives

$$\begin{aligned}
\mathbb{E}\{\tilde{W}(x(T \wedge \tau))\} &= V(x(0)) + \mathbb{E}\left\{\int_0^{T\wedge\tau} \mathcal{L}\tilde{W}(x(s))ds\right\} \\
&\leq V(x_0) + \mathbb{E}\left\{\int_0^T \phi(s)ds\right\} = V(x_0) + \Phi(T),
\end{aligned}$$

where the inequality is obtained using the last condition in the proposition. Using

the fourth condition in the proposition, the following inequality can be obtained

$$\begin{aligned}\mathbb{P}\{x(t) \in \mathcal{X}_u \text{ for } 0 \le t \le T \mid x(0) \in \mathcal{X}_0\} &= \mathbb{P}\{\sup_{0\le t\le T} W(x(t)) \ge 1 \mid x_0 \in \mathcal{X}_0\} \\ &\le V(x_0) + \Phi(T), \\ &\le \beta_1 + \beta_2 = \beta,\end{aligned}$$

where we have applied the supermartingale inequality in (5.12) to function $\tilde{W}(x(t))$ and use the second and the third conditions in the proposition to obtain the last inequality. □

5.3.3 SOS Optimization

As discussed in section 5.1, provided that the drift, diffusion and the jump terms in (5.7) are polynomial functions and the sets $\mathcal{X}, \partial\mathcal{X}, \mathcal{X}_0, \mathcal{X}_u$ in (5.1)-(5.2) are semi-algebraic, then the search for a barrier certificate, $V(x(t))$, can be formulated as an SOS optimization. In this SOS optimization, $V(x(t))$ is a polynomial function whose coefficients are the decision variables that will be determined in the optimization task. Thus, our goal is to formulate polynomial representations for the conditions (given in the previous section) that guarantee the process $\{V(x(t))\}$ to be a supermartingale. One issue in formulating such a representation comes from the integral term in the JDP's generator in (5.10). The following proposition shows how to address this issue.

Proposition 5.3.5. *Let $y \in \mathbb{R}^n$ be an n-dimensional independent random variable with distribution $F(y)$. Let $V(x) = \sum_{|\alpha|\le p} c_\alpha x^{[\alpha]}$ be a multi-index representation of polynomial function $V(x)$. Then*

$$\int (V(x+y) - V(x))\, dF(y) = \sum_{1\le|\beta|\le p} \frac{1}{\beta!} \partial^{[\beta]} [V(x)]\, \mathbb{M}^{|\beta|}, \tag{5.13}$$

and the generator in (5.10) can be rewritten as

$$\begin{aligned}\mathcal{L}^*V(x(t)) &= \frac{\partial V(x(t))}{\partial x}\left(f(x(t)) - \delta J(t)\right) + \frac{1}{2}\mathrm{Tr}\left(\sigma^T(x(t))\frac{\partial^2 V(x(t))}{\partial x^2}\sigma(x(t))\right) \\ &\quad + \sum_{1\le|\beta|\le p}\frac{1}{\beta!}\partial^{[\beta]}\left[V(x)\right]\mathbb{M}^{|\beta|}. \end{aligned} \tag{5.14}$$

Proof. We only need to show that equation (5.13) holds since its substitution to the integral term in equation (5.10) gives the generator in equation (5.14). Let's write

$$\begin{aligned} V(x+y) &= \sum_{|\alpha|\le p} c_\alpha (x+y)^{[\alpha]} = \sum_{|\alpha|\le p} c_\alpha \sum_{0\le|\beta|,\beta\le\alpha}\binom{\alpha}{\beta}x^{[\alpha-\beta]}y^{[\beta]}, \\ &= \sum_{|\alpha|\le p} c_\alpha\left[x^{[\alpha]} + \sum_{1\le|\beta|,\beta\le\alpha}\binom{\alpha}{\beta}x^{[\alpha-\beta]}y^{[\beta]}\right]. \end{aligned}$$

For notational convenience, let us denote the difference $V(x+y)-V(x)$ as $\Delta V(x,y)$. Using the above sum, one can write this difference as

$$\Delta V(x,y) = \sum_{|\alpha|\le p} c_\alpha \sum_{1\le|\beta|,\beta\le\alpha}\binom{\alpha}{\beta}x^{[\alpha-\beta]}y^{[\beta]},$$

and since

$$\partial^{[\beta]}\left[x^{[\alpha]}\right] = \begin{cases} \frac{\alpha!}{(\alpha-\beta)!}x^{[\alpha-\beta]} & \text{if } \beta\le\alpha, \\ 0 & \text{otherwise,}\end{cases}$$

the expression for $\Delta V(x,y)$ can be rewritten as

$$\Delta V(x,y) = \sum_{|\alpha|\le p} c_\alpha \sum_{1\le|\beta|,\beta\le\alpha}\frac{1}{\beta!}\partial^{[\beta]}\left[x^{[\alpha]}\right]y^{[\beta]}.$$

Expand out the first summation to obtain

$$\begin{aligned}\Delta V(x,y) &= \sum_{|\alpha|=1} c_\alpha \sum_{|\beta|=1} \frac{1}{\beta!}\partial^{[\beta]}\left[x^{[\alpha]}\right] y^{[\beta]} + \sum_{|\alpha|=2} c_\alpha \sum_{1\le|\beta|\le 2} \frac{1}{\beta!}\partial^{[\beta]}\left[x^{[\alpha]}\right] y^{[\beta]} + \cdots \\ &\quad + \sum_{|\alpha|=p} c_\alpha \sum_{1\le|\beta|\le p} \frac{1}{\beta!}\partial^{[\beta]}\left[x^{[\alpha]}\right] y^{[\beta]}.\end{aligned}$$

The order of the summations can now be interchanged since α and β are no longer directly coupled to yield

$$\begin{aligned}\Delta V(x,y) &= \sum_{|\beta|=1} \frac{1}{\beta!}\left[\sum_{|\alpha|=1} c_\alpha \partial^{[\beta]}\left[x^{[\alpha]}\right]\right] y^{[\beta]} + \sum_{1\le|\beta|\le 2} \frac{1}{\beta!}\left[\sum_{|\alpha|=2} c_\alpha \partial^{[\beta]}\left[x^{[\alpha]}\right]\right] y^{[\beta]} + \cdots \\ &\quad + \sum_{1\le|\beta|\le p} \frac{1}{\beta!}\left[\sum_{|\alpha|=p} c_\alpha \partial^{[\beta]}\left[x^{[\alpha]}\right]\right] y^{[\beta]}.\end{aligned}$$

Reordering the terms in the first summation yields,

$$\begin{aligned}\Delta V(x,y) &= \sum_{|\beta|=1} \frac{1}{\beta!}\left[\sum_{1\le|\alpha|\le p} c_\alpha \partial^{[\beta]}\left[x^{[\alpha]}\right]\right] y^{[\beta]} + \sum_{|\beta|=2} \frac{1}{\beta!}\left[\sum_{2\le|\alpha|\le p} c_\alpha \partial^{[\beta]}\left[x^{[\alpha]}\right]\right] y^{[\beta]} + \cdots \\ &\quad + \sum_{|\beta|=p} \frac{1}{\beta!}\left[\sum_{|\alpha|=p} c_\alpha \partial^{[\beta]}\left[x^{[\alpha]}\right]\right] y^{[\beta]}.\end{aligned}$$

Because $\partial^{[\beta]}\left[x^{[\alpha]}\right] = 0$ when $\alpha \le \beta$, the summation limits of the inner sums can be extended from 1 to p thereby yielding

$$\begin{aligned}\Delta V(x,y) &= \sum_{|\beta|=1} \frac{1}{\beta!}\left[\sum_{1\le|\alpha|\le p} c_\alpha \partial^{[\beta]}\left[x^{[\alpha]}\right]\right] y^{[\beta]} + \sum_{|\beta|=2} \frac{1}{\beta!}\left[\sum_{1\le|\alpha|\le p} c_\alpha \partial^{[\beta]}\left[x^{[\alpha]}\right]\right] y^{[\beta]} + \cdots \\ &\quad + \sum_{|\beta|=p} \frac{1}{\beta!}\left[\sum_{1\le|\alpha|\le p} c_\alpha \partial^{[\beta]}\left[x^{[\alpha]}\right]\right] y^{[\beta]}.\end{aligned}$$

Now note that

$$\partial^{[\beta]}V(x) \;=\; \partial^{[\beta]}\left[\sum_{|\alpha|\leq p} c_\alpha x^{[\alpha]}\right] = \sum_{1\leq|\alpha|\leq p} c_\alpha \partial^{[\beta]}\left[x^{[\alpha]}\right],$$

which is simply the inner sum in (5.15) and so the difference becomes

$$\Delta V(x,y) \;=\; \sum_{1\leq|\beta|\leq p} \frac{1}{\beta!}\partial^{[\beta]}\left[V(x)\right] y^{[\beta]}.$$

Integrating both sides with respect to $F(y)$, and since each component of y is independent, gives

$$\int \Delta V(x,y)dF(y) = \sum_{1\leq|\beta|\leq p} \frac{1}{\beta!}\partial^{[\beta]}\left[V(x)\right] \int y^{|\beta|}dF(y), = \sum_{1\leq|\beta|\leq p} \frac{1}{\beta!}\partial^{[\beta]}\left[V(x)\right] \mathbb{M}^{|\beta|},$$

where we have noticed that the integral $\int y^{|\beta|}dF(y) = \mathbb{M}^{|\beta|}$ is the $|\beta|$-th moment of y. Substitution of the above expression with the integral term in (5.10) gives the JDP generator in (5.14). □

Using the polynomial representation of the JDP's generator in (5.14), we now formulate the SOS optimizations for computing the upper bounds stated in propositions 5.3.1 - 5.3.4. The statement in proposition 5.3.6 below is an SOS optimization problem for searching a barrier certificate $V(x(t))$ which satisfies the conditions stated in proposition 5.3.1. Clearly, this SOS optimization can also be used for proposition 5.3.3 using an appropriate generator.

Proposition 5.3.6. *Consider the JDP in (5.7) with initial condition $x_0 \in \mathcal{X}_0$. Let the sets $\mathcal{X}$, $\mathcal{X}_0$, $\partial\mathcal{X}$ be described by $\mathcal{X} = \{x \in \mathbb{R}^n : g_{\mathcal{X}}(x) \geq 0\}, \mathcal{X}_0 = \{x \in \mathbb{R}^n : g_{\mathcal{X}_0}(x) \geq 0\}$, $\partial\mathcal{X} = \{x \in \mathbb{R}^n : g_{\partial\mathcal{X}}(x) = 0\}$, respectively, where the g's are polynomial functions. Consider the polynomial parameterization $\mathcal{V} \in C^2(\mathbb{R}^n)$ of $V(x(t))$, and define $\tau \equiv \inf\{t \geq 0 : x(t) \in \partial\mathcal{X}\}$. If there exist a function $V(x(t)) \in \mathcal{V}$, constants*

$\theta, \epsilon > 0$, *and SOS polynomials* $\sigma_{\mathcal{X}}(x), \sigma_{\mathcal{X}_0}(x), \sigma_{\partial\mathcal{X}}(x)$ *such that the SOS optimization*

$$
\begin{aligned}
\min \quad & \theta \\
\text{s.t.} \quad & V(x(t)) - \sigma_{\mathcal{X}}(x) g_{\mathcal{X}}(x) - \epsilon && \text{is SOS,} \\
& -V(x(t)) - \sigma_{\partial\mathcal{X}}(x) g_{\partial\mathcal{X}}(x) && \text{is SOS,} \\
& -V(x(t)) + \gamma - \sigma_{\mathcal{X}_0}(x) g_{\mathcal{X}_0}(x) && \text{is SOS,} \\
& -\tfrac{\partial V(x(t))}{\partial t} - \mathcal{L}^* V(x(t)) - \sigma_{\mathcal{X}}(x) g_{\mathcal{X}}(x) - 1 && \text{is SOS,}
\end{aligned}
$$

has a feasible solution, then $\mathbb{E}\{\tau\} \leq \theta$.

Proof. The conditions for $V(x(t))$ in the above SOS program is the SOS relaxation of the inequalities in Proposition 5.3.1. Such relaxation is accommodated using SOS multipliers $\sigma_{(\cdot)}(x)$. Also, θ (0th order SOS polynomial) is chosen as the objective function to be minimized since its minimum value obtained in the optimization will serve as the tightest upper bound for a given SOS polynomial parameterization. □

In a similar way, we can also formulate the following SOS optimization problem for searching a barrier certificate $V(x(t))$ that satisfies the conditions stated in proposition 5.3.4.

Proposition 5.3.7. *Consider the JDP in (5.7) with initial condition* $x_0 \in \mathcal{X}_0$. *Let* $\mathcal{X}, \mathcal{X}_0, \mathcal{X}_u, \mathcal{X}_T$ *be sets described be* $\mathcal{X} = \{x \in \mathbb{R}^n : g(x) \geq 0\}$, $\mathcal{X}_0 = \{x \in \mathbb{R}^n : g_0(x) \geq 0\}, \mathcal{X}_u = \{x \in \mathbb{R}^n : g_u(x) \geq 0\}, \mathcal{X}_T = \{t \in \mathbb{R}_+ : g_T(t) \geq 0\}$, *respectively, where the* g'*s are polynomial functions. Let the parameterizations of polynomials* $V(x(t)), \phi(t)$ *and SOS polynomials* $\sigma(x), \sigma_0(x), \sigma_u(x), \sigma_t(t)$ *be given. If there exist polynomials* $V(x(t))$

and $\phi(t)$ and positive constants β_1, β_2 such that the SOS optimization

$$\begin{aligned}
\min \quad & \beta = \beta_1 + \beta_2 \\
\text{s.t.} \quad & V(x(t)) + \textstyle\int_0^t \phi(s)ds - \sigma_{\mathcal{X}}(x)g_{\mathcal{X}}(x) - \sigma_t(t)g_T(t) \quad \text{is SOS}, \\
& \beta_1 - V(x(t)) - \sigma_0(x)g_0(x) \quad \text{is SOS}, \\
& \beta_2 - \textstyle\int_0^t \phi(s)ds - \sigma_t(t)g_T(t) \quad \text{is SOS}, \\
& V(x(t)) + \textstyle\int_0^T \phi(t)dt - \sigma_{\mathcal{X}}(x)g_{\mathcal{X}}(x) - 1 \quad \text{is SOS}, \\
& \phi(t) - \mathcal{L}^*V(x(t)) - \sigma_{\mathcal{X}}(x)g_{\mathcal{X}}(x) - \sigma_t(t)g_T(t) \quad \text{is SOS},
\end{aligned} \tag{5.15}$$

has a feasible solution, then the probability bound (5.2) holds.

As discussed in chapter 3, each of the above SOS optimization can be solved using the SOS programming softwares.

5.4 Example

This section illustrates the use of MFPT and stochastic reachability analyses discussed in the previous sections for ecosystems management. In particular, we consider the problem of choosing a harvesting strategy to manage the bass-crayfish population in freshwater lakes. Bass-crayfish interaction is an intraguild predation system in which both species compete for the same resource while also predate one another. The model presented in this section has two equilibria; one in which the bass dominate the ecosystem and the other in which the crayfish dominate the ecosystem. An outbreak of crayfish is undesirable as it can suppress the bass population. If such an outbreak occurs, management strategies are needed to shift the crayfish-dominated equilibrium point to the bass-dominated equilibrium point. One method to achieve this management objective is to permit the harvesting of crayfish by anglers. In general, this harvesting process can be modeled as a jump process in which the size

and the intensity of harvesting events are variables that the ecosystem manager needs to set.

This example is drawn from a paper [30] that used MFPT as a basis for management decisions. The underlying nondimensionalized model is given by the following state equations,

$$\begin{aligned} \dot{x}_1(t) &= x_1(k_1 - k_{11}x_1 - k_{12}x_2) - \frac{k_{12}^* x_2 x_1^2}{K_1^2 + x_1^2} - \sum_{i=1}^{N_t} y_i \delta(t - \tau_i), \\ \dot{x}_2(t) &= r_{21}x_2(k_2 - k_{22}x_2 - k_{21}x_1) + \eta \frac{k_{12}^* x_2 x_1^2}{K_1^2 + x_1^2}, \end{aligned} \tag{5.16}$$

where the biomass of the crayfish and bass are denoted as x_1 and x_2, respectively, k_i and k_{ii} are the intrinsic growth rate and the strength of density dependence of the ith species, respectively, k_{ij} is the competition rate on resource between species i and j, k_{ij}^* is the attack rates of species j on i, K_i is the carrying capacity, η is the conversion efficiency, and r_{ij} is the ratio of growth rate between species i and j. The parameter values are $k_i = k_{ii} = 1, k_{12} = 0.7, k_{21} = 0.9, k_{12}^* = 0.075, r_{21} = 1.5, \eta = 0.01, K_1 = 0.1$. The last term in the first equation of (5.16) models crayfish harvesting as a compound Poisson process in which the harvest size $\{y_i\}_{i=1}^{N_t}$ and the harvest times, $\{\tau_i\}_{i=1}^{N_t}$ are i.i.d with exponential distribution of intensity μ and λ, respectively, and N_t is the number of harvest events in the interval $[0, t]$.

Figure 5.2 plots the isoclines for equation (5.16), identifies the two stable equilibria and their regions of attraction (ROA), and marks the separatrix between the two ROAs. From the sample path of this system under a given harvesting policy, one sees that each harvesting event causes a step decrease in the crayfish population, after which the system begins relaxing back to the crayfish-dominated equilibrium. There is a finite probability that repeated harvesting events will drive the system state across the separatrix, whereupon the system's equilibrium state shifts to the bass-dominated equilibrium. Assuming the system's current state lies in the ROA

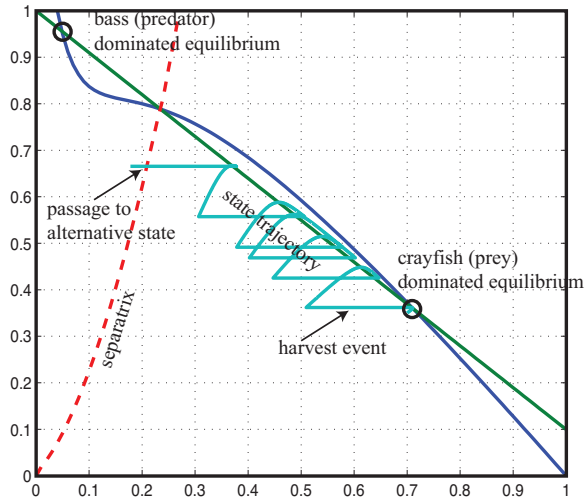

Figure 5.2. ROA in Bass-Crayfish Eco-system [29].

dominated by the crayfish, we're interested in specifying those harvesting parameters μ and λ that maximize the probability of a regime shift to the bass-dominated ROA in a specified time-interval subject to a constraint that limits the probability of driving the crayfish population to extinction.

To compute an upper bound for the MFPT using SOS program in proposition 5.3.6, we define the following sets.

$$\mathcal{X} = \left\{x \in \mathbb{R}^2_+,\ t \in \mathbb{R}_+ \,\middle|\, x_1(1-x_1) \geq 0,\ x_2(1-x_2) \geq 0, t(T-t) > 0\right\},$$

$$\mathcal{X}_0 = \left\{x \in \mathbb{R}^2_+ \,\middle|\, (x_1 - 0.72)^2 + (x_2 - 0.36)^2 \leq 10^{-4} \right\},$$

$$\partial\mathcal{X} = \{x \in \mathbb{R}^2_+ \big| 0.27x_1 - x_1^2 \geq 0,$$
$$x_2 - x_2^2 \geq 0, x_2 - 0.14x_1^3 - 9.5x_1^2 - 1.1x_1 + 3.10^{-4} = 0\}.$$

Region $\mathcal{X}$ characterizes a unit square in $\mathbb{R}^2_+$ over the time interval $[0, T]$. The initial region $\mathcal{X}_0$ is a disk of radius 0.01, centered at the crayfish-dominated equilibrium. The boundary region $\partial\mathcal{X}$ is the separatrix shown in Figure 5.2. figure 5.3a shows the MFPT approximation (circle) for $\mu = 0.1$ and $\lambda \in [0, 6]$ obtained using SOSTOOLS.

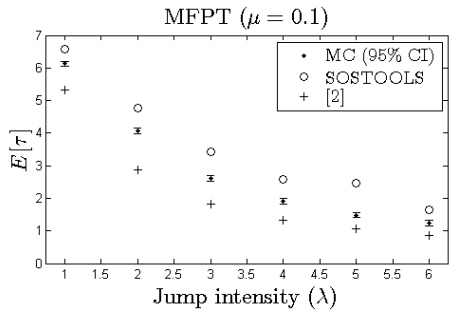

(a) MFPT comparison for various λ.

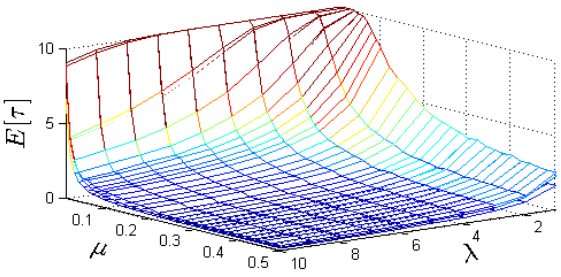

(b) MFPT as a function of μ and λ..

Figure 5.3. Result of MFPT approximation.

This plot also shows the MFPT obtained using a Monte Carlo (MC) simulation with a 95% confidence interval and estimates (plus) obtained in [29]. The estimates in [29] were based on a linearization and were only valid for small mean harvest sizes (μ). As a result, the estimates from [29] under approximate the actual MFPT seen in MC simulations, whereas our results provide reasonable upper bounds on the MFPT.

A more complete surface plot showing our MFPT approximations for a range of μ and λ is shown in Figure 5.3b. Clearly, one can maximize the likelihood of a regime shift by simply increasing the intensity of harvesting. In general, one would want to limit such harvesting intensity since large harvesting intensity may drive the crayfish population to extinction. While crayfish may be considered to be a "nuisance", the extinction of a species in the eco-system reduces overall bio-diversity and often makes such systems more prone to collapse from extreme events [58]. A reasonable choice on harvesting strategy involves limiting the harvesting rates λ and μ to minimize the likelihood of crayfish extinction while still achieving a regime shift over a specified time interval.

We use SOS programming to bound two probabilities. The first one is the probability of reaching a *controlled* region (i.e. $\partial\mathcal{X}$) which we denote as $\mathbb{P}_R$. The second one is the probability of reaching a small neighborhood of $x_1 = 0$ (crayfish near ex-

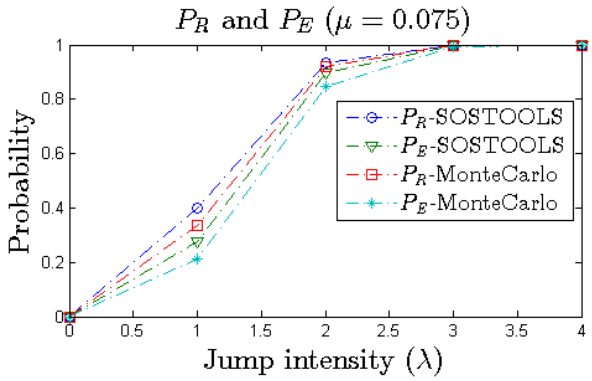

Figure 5.4. $\mathbb{P}_R$ and $\mathbb{P}_E$ for $\mu = 0.075$.

tinction) which we denote as $\mathbb{P}_E$. We use the same initial set, $\mathcal{X}_0$, and the domain set, $\mathcal{X}$, as before. For an upper bound β_R of $\mathbb{P}_R$, we define the target set

$$\mathcal{X}_F^R = \left\{ x \in \mathbb{R}_+^2 \middle| 0.27x_1 - x_1^2 \geq 0,\ x_2 - x_2^2 \geq 0, x_2 - 0.14x_1^3 - 9.5x_1^2 - 1.1x_1 + 3.10^{-4} = 0 \right\},$$

whereas for an upper bound β_E of $\mathbb{P}_E$, the target set is

$$\mathcal{X}_F^E = \left\{ x \in \mathbb{R}_+^2 \mid x_1(0.01 - x_1) \geq 0,\ \ x_2(1 - x_2) \geq 0 \right\}.$$

A plot of the SOS programming result is shown in Figure 5.4 for $\mu = 0.075$, $\lambda \in [0, 4]$, and time interval $T = 5$ unit.

One possible management strategy would be to determine those (μ, λ) pairs which minimize the probability of crayfish extinction ($\mathbb{P}_E$) subject to a constraint requiring the regime shift's MFPT to be less than a specified deadline, T. Let us set, for example, $T = 5$ unit as the deadline for regime shift's MFPT and search for that (μ, λ) that give the smallest upper bound, β_E, for $\mathbb{P}_E$. Using the surface plot in Fig. 5.3b, we first find all (μ, λ) pairs for which $\mathbb{E}[\tau] \leq 5$. Among these pairs, we then choose one that gives the smallest β_E. We find that the pair $(\mu = 0.075, \lambda = 1)$ gives $\mathbb{E}[\tau] \leq 4.31$ and $\mathbb{P}_E \leq \beta_E = 0.277$ (triangle in Figure 5.4). Using this pair in an MC

simulation, we find MFPT $= 4.6896 \pm 0.083$ and $\mathbb{P}_E = 0.243 \pm 0.104$. This confirms that our management approach minimizes the likelihood of an extinction event while assuring the regime shift's MFPT is less than the specified deadline of $T = 5$. One may also compare our proposed management framework with the method in [29] that uses a linearization of (5.16). Since [29] does not provide a way to compute $\mathbb{P}_E$ for a given (μ, λ), we ran an MC simulation to compute $\mathbb{P}_E$ for all possible parameter pairs and then singled out a pair that gives the smallest $\mathbb{P}_E$. The minimizing pair was $(\mu = 0.055, \lambda = 1)$ with MFPT $= 6.4008 \pm 0.083$ and $\mathbb{P}_E = 0.174$, which clearly violates the specified MFPT deadline.

5.5 Remarks and Future Works

This chapter presented a computational framework to predict the occurence of noise-induced regime shifts for system perturbed by jump/shock processes. Such predictions are formulated either as mean first passage time problem or as stochastic reachability problem whose solution can be obtained using SOS optimization. We illustrate an example use of the presented method in ecosystem regime shifts management.

Future works: One possible extension of the method discussed in this chapter is its application to predict large scale regime shifts or *phase transitions* in networks of interconnecting stochastic processes. The method presented in this chapter, however, cannot be applied directly to this large scale problem due to the limitation of the SOS optimization method which only capable of solving small to medium scale problems. A method to address this issue is by using the *devide-and-conquer* method to decompose the network into smaller subsystems. If an appropriate decomposition of the network can be obtained, the method presented in this chapter can then be used to analyze each subsystem.

To illustrate this approach, let us consider a hypothetical networked systems in

figure 5.5. This system is inspired by the lake eutrophication model discussed in section 5.1 in which the dynamic of each subsystem or site is governed by the SDE of the lake eutrophication model described in section 5.1. Thus, one may view this networked system as a spatial model for the Phosporus (P) concentration in three connected sites of a lake. The influx (u) of P from the environment enters the lake in site 1 and then distributed to other sites through inter-site fluxes of intensity α. The Wiener process $w_i(t),\ (i = 1, \ldots, 3)$ in the model of each site illustrates stochasticity that occurs due to small variation in the amount of input or inter-site fluxes that enter each site. We assume that the deterministic model of each site is bistable and that the intensity σ of the Wiener process in each site is relatively small such that each stable equilibria of the site is stochastically stable with probability 1. Moreover, the network is assumed to be *weakly coupled* so that the assumption that each subsystem is stochastically stable guarantees that the network system also stochastically stable [82, 83].

To analyze the system in figure 5.5, we view the network as an interconnection of *isolated subsystems* that are coupled through the inter-site fluxes. In this case, the dynamic of each site is governed by SDE of the form

$$dx_i(t) = [f_i(x_i(t)) + g(x_{-i}(t))]dt + \sigma dw_i(t), \quad (i = 1, 2, 3),$$

in which the subscript $-i \in \mathcal{N}_i$ denotes the ith site's nearest neighbors $\mathcal{N}_i$. This

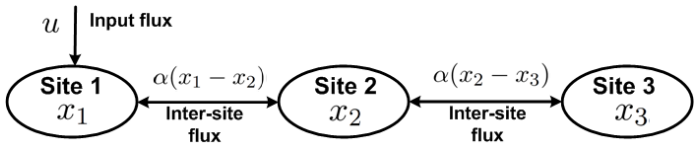

Figure 5.5. Network of lake systems.

modeling approach results in the following SDE model of system.

$$\begin{aligned} dx_1(t) &= \left(u - (1+\alpha)x_1 + \frac{x_1^3}{\theta^3 + x_1^3} + \alpha x_2 \right) dt + \sigma dw_1(t), \\ dx_2(t) &= \left(-(1+2\alpha)x_2 + \frac{x_2^3}{\theta^3 + x_2^3} + \alpha(x_1 + x_3) \right) dt + \sigma dw_2(t), \\ dx_3(t) &= \left(-(1+\alpha)x_3 + \frac{x_3^3}{\theta^3 + x_3^3} + \alpha x_2 \right) dt + \sigma dw_3(t). \end{aligned} \tag{5.17}$$

Notice in model (5.17) that the last term in the drift part of the ith site's is only a function of its nearest neighbors' states. This suggests that networked system (5.17) can be viewed as a random process evolving on a graph and the dynamics of the network can be studied using Markov Random Field (MRF) formalism [66, 7].

Let $G = (S, E)$ be an undirected graph of networked system in figure (5.5) which consists of a finite number of sites S whose edges $E \subset S \times S$ characterize the sites that are adjacent to each other. Consider a random process evolving on the graph G and let w_i be random variable describing the *configuration* of the ith site. In our case, the set of configurations are the two possible stable states that the system may have (i.e. oligotrophic and eutrophic states). Assume the probability of site ith configuration w_i taking some value can be specified as a conditional probability (or *local specification*) of the form

$$\mathbb{P}(w_i | w_j, j \in S) = \mathbb{P}(w_i | w_{-i}, -i \in \mathcal{N}_i) \tag{5.18}$$

The above relation suggests that the probability of site i taking a particular configuration w_i depends only on the configuration of its neighboring sites. In other words, the probability of the ith site's state to switch between the two possible configuration (i.e. from oligotrophic to eutrophic and vice versa) depends only on the size of the inter-site fluxes with its neighboring sites. This exactly the stochastic reachability problem discussed in the previous section and so the local specification in (5.18) can

be evaluated using the SOS optimization techniques discussed in section 5.3.

Figure 5.6 shows a preliminary result supporting the idea of using MRF *abstraction* to study the regime shifts in coupled SDEs. The sample trajectories of the coupled SDEs (5.17) generated using direct integration method is plotted in figure 5.6a. This figure is generated using an input flux $u = 0.1$ which is large enough to trigger regime shifts between the stable states of site 1. One may see from this figure that the shift from low to high P levels in site 1 is followed by the sma shifts in sites 2 and 3, causing a phase transition of the network from low to high P levels. Figure 5.6b plots the monte carlo (MC) simulation of the MRF model discussed previously. The transition probability (5.18) used in the MC simulation of the MRF is constructed based on the solution of the stochastic reachability problem discussed in section 5.3. One may see that the result from the MRF abstraction is capable of capturing the *qualitative* properties of the network's transition from low to high P level. The main advantage in using the MRF abstraction is that its required computation effort is less than that required by direct integration method (i.e. simulation time of the MRF abstraction is 1/100 th of the simulation time required by the direct integration method). The MRF abstraction method therefore provides a means to

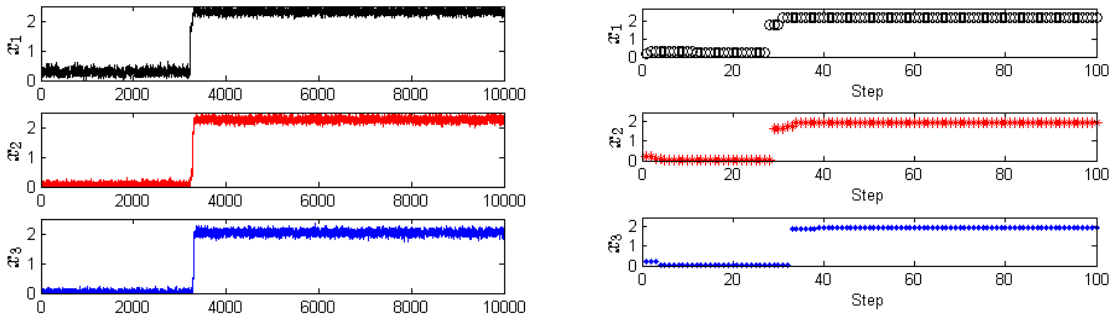

(a) Direct integration.

(b) MRF abstraction.

Figure 5.6. Simulation comparison of the coupled SDEs (5.17).

reduce the computation cost required in analyzing a large scale interconnected SDEs.

Future research directions that could be pursued includes the development of theoretical framework for explaining the large scale regime shifts phenomena in interconnected systems as well as the construction of efficient algorithm that connects the SOS optimization method and the sampling methods in MC simulation of MRF.

CHAPTER 6

FORECASTING REGIME SHIFTS IN MICROBIAL PREDATOR-PREYS SYSTEM

This chapter describes an experimental test bed which will be used to evaluate the methods described in the previous chapters to forecast ecological regime shifts. The proposed test bed is a microbial predator-prey system cultured in a chemostat which have been shown recently in [38, 116] to exhibits different alternative dynamics including population extinction, stable coexistence, sustained oscillation, and possibly chaos. Such diverse alternative dynamics and the ease of constructing its laboratory scale prototype are among the main motivations for choosing this system as a platform for evaluating our proposed method on forecasting ecological regime shifts.

This chapter is structured as follows. Section 6.1 presents the basic concepts of microbial dynamics cultured in the chemostat. Section 6.2 describes the materials and methods used for the experiments. Section 6.3 presents some hypothesis on microbial predator-prey dynamics that will be tested during experiments.

6.1 Modeling Microbial Growth in Chemostat

A chemostat is a well-mixed, continuous culture device which is often used in experiments to study the dynamics of nutrient-limited microorganisms or bacteria [56, 102]. In particular, it is a useful platform that can be used for hypothesis testing because many environmental factors which affect the microbial growth inside the chemostat can be controlled systematically during the experiments. This section

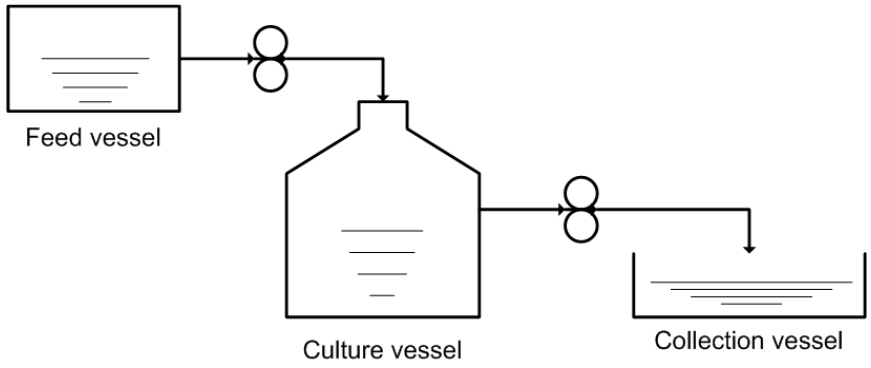

Figure 6.1. Basic schematic of a chemostat.

provides some backgrounds on the chemostat and the models of microbial growth cultured inside it.

6.1.1 Chemostat

Figure 6.1 illustrates the basic set up of a chemostat. It generally consists of three connected vessels namely the *feed*, *culture* and *collection*. The feed vessel contains all nutrients that are required for the growth of the bacteria. All of such nutrients are available in excess except one which is referred to as the *limiting nutrient*. The goal of the chemostat experiment is therefore to study how variation on the limiting nutrient affects the growth of the bacteria. The culture vessel is the media where bacteria grows with the supply of nutrients from the feed and other environmental factors such as light, air, or other minerals. The media in the culture is assumed to be well mixed in the sense that the content from the feed, the light illumination, and the air supply are uniformly dispersed throughout the media. The collection vessel is where the products of the culture are collected for measurement or other purposes.

The content of the feed is pumped into the culture at a steady state flow rate F and the content of the culture emerges from it at the same rate. The residence time of a particle in the culture is therefore determined by the *dilution rate* $\delta = F/V$

which is defined as the number of complete volume-changes/hour. This implies that the mean residence time of any particle in the culture is equal to $1/\delta$. Therefore if the concentration of organism in the culture is denoted by x then its *wash-out rate* from the vessel is defined as $dx/dt = -\delta x$.

6.1.2 Modeling microbial predator-prey system

Consider a single bacteria growing in a chemostat with constant inflowing media which contain one limiting nutrient N at concentration N_{in}. Assume all other minerals required for the growth of the bacteria are available in excess and that the chemostat is well aerated and sufficiently illuminated. Assume further that the experimenter can only controls the nutrient concentration of the feed and the dilution rate of the media into (out of) the culture. Using the law of mass conservation, the net rate of increase of the bacteria concentration in the culture satisfies

$$\begin{aligned} \text{increase rate} = &\ \text{growth - outflow} \\ \frac{dx}{dt} = &\ \mu x - \delta x, \end{aligned} \tag{6.1}$$

which implies that the growth rate of bacteria at steady state is determined by the dilution rate, δ, and the density of bacteria can be determined based on the nutrient concentration in the feed. On the other hand, the limiting nutrient is consumed by the bacteria in the culture according to the relation

$$\frac{dN}{dt} = -Y\frac{dx}{dt}, \tag{6.2}$$

where Y is known as the *yield constant* defined as

$$Y = \frac{\text{weight of the formed bacteria}}{\text{weight of the used substrate}}.$$

Using the law of mass conservation, the net rate of change of the nutrient concentration satisfies

$$\begin{aligned} \text{nutrient rate of change} &= \text{input - output} - \frac{\text{growth}}{\text{yield constant}} \\ \frac{dN}{dt} &= \delta(N_{in} - N) - \frac{\mu x}{Y}. \end{aligned} \tag{6.3}$$

Combining equations (6.1)-(6.3), the dynamics of the nutrient and bacteria concentrations are then governed by the following differential equation [56, 102].

$$\begin{aligned} \frac{dN}{dt} &= \delta(N_{in} - N) - \frac{\mu_m x}{Y}\left(\frac{N}{K_x + N}\right), \\ \frac{dx}{dt} &= x\left(\frac{\mu_m N}{K_x + N} - \delta\right). \end{aligned} \tag{6.4}$$

The single bacteria model (6.4) can be extended to model the dynamics of microbial predator-prey system. One example of such systems is the Brachionus-Chlorella interaction whose dynamics is given in the following model [38].

$$\begin{aligned} \frac{dN}{dt} &= \delta(N_{in} - N) - F_C(N)C, \\ \frac{dC}{dt} &= F_C(N)C - \frac{1}{\epsilon}F_B(C)B - \delta C, \\ \frac{dB}{dt} &= F_B(C)B - \delta C, \end{aligned} \tag{6.5}$$

where N, C and B denote the concentrations of limiting nutrient, Chlorella and Brachionus, respectively and

$$F_C(N) = \frac{b_C N}{K_C + N} \quad \text{and} \quad F_B(C) = \frac{b_B C}{K_B + C}$$

denote the Monod type response functions of Chlorella and Brachionus, respectively. The parameters b_C (b_B) and K_C (K_B) denote the maximum birth rate and half saturation constant of the Chlorella (Brachionus), respectively, whereas parameter ϵ

denotes the conversion efficiency of Chlorella on nutrient N.

6.2 Materials and Methods

The proposed experiment aims to (i) construct a laboratory scale chemostat that cultures microbial predator-prey system of the form (6.5), (ii) develop and validate the model of this system and (iii) use the developed model as a basis for predicting possible regime shifts of the system. The predator-prey system investigated in this experiment is formed by the Brachionus-Chlorella interaction previously studied in [38, 116]. The works in [38, 116] have shown that this system may exhibits different qualitative dynamics (population coexistence, oscillation or extinction) under different values of parameters δ and N_{in}. It is therefore reasonable to expect that this system is a suitable platform at which the proposed method for regime shifts prediction can be evaluated experimentally. This section describes the materials and methods used in the experiments.

6.2.1 Materials

Figure 6.2 shows the schematic of a laboratory scale chemostat that has been developed for the experiment. The set up consist of one feed vessel that pumps media containing limiting nutrients (i.e. nitrogen) into six 400-ml plastic cultures. A twelve hours light-dark cycle illumination and inflow of sterile air are provided to each culture to prevent light or CO_2 limitations on microbial growth. The dilution rate from the feed to each culture vessel is adjusted using peristaltic pumps. During the experiments, the concentration of limiting nutrients and the dilution rates to three (C1 - C3) of the six cultures will be varied to observe microbial responses to variations on these parameters. The remaining cultures (C4 - C6) will be used as references.

Two microorganisms namely green algae *Chlorella vulgaris* and rotifer *Brachionus*

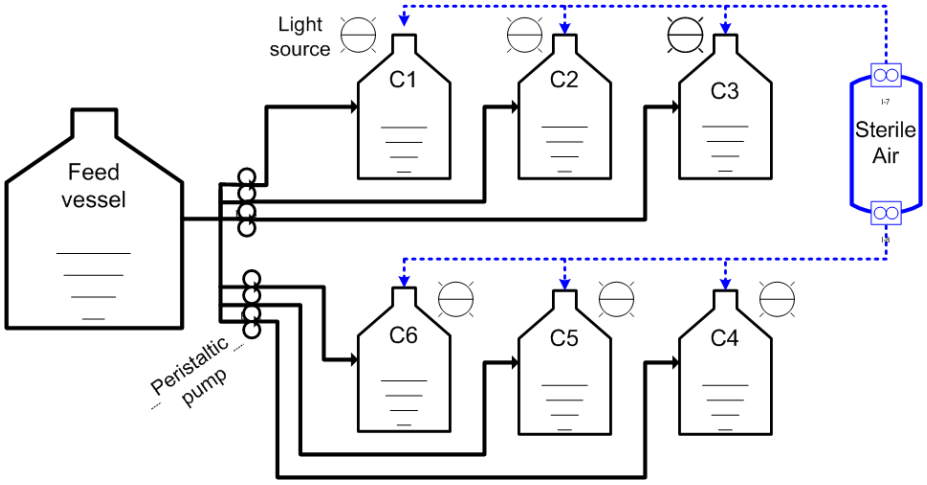

Figure 6.2. Schematic of the constructed chemostat.

calyciflorus will be cultured in the chemostat. Chlorella vulgaris is a unicellular green algae which grows and multiply through photosynthesis with the help of carbon dioxide, water, light, and some minerals. The rotifer Brachionus, on the other hand, is a freshwater zooplankton whose growth rate depends on the available concentration of primary producers such as Chlorella. Culturing Chlorella and Brachionus in a chemostat therefore sets a predator-prey system in which the growth of the producer (Chlorella) is limited by the available limiting nutrient whereas the growth of the predator (Brachionus) is limited by the available producer concentration.

6.2.2 Methods

6.2.2.1 Experiments and data measurement

Experiments will be conducted by adding Brachionus to the culture of Chlorella in the chemostat. According to the experiments in [38], the Brachionus-Chlorellay population interaction may last between 16-120 days. We expect to collect the data by sampling the outflow of the chemostat. In particular, the culture media is assumed to be well mixed such that the collected data is taken from a uniformly distributed

microbial density. For each sample, the number of rotifer cells will be counted using dissecting microscope whereas the chlorella population will be preserved on lugol's solution and then counted using compound microscope or particle counter. The obtained measurement would then indicate the temporal variation of the microbial densities and serve as a basis for model selection and parameter estimation.

6.2.2.2 Model selection

A basic model which can be used to describe the Brachionus-Chlorella system is the model in equation (6.5). Prior work in [38, 101], however, show that equation (6.5) is not adequate to model this system. In particular, they noted the following discrepencies between the prediction of model (6.5) and the observation on the experiments.

- Simulations of model (6.5) show that a low dilution rate δ produces higher oscillation amplitudes of bacteria densities. In contrast, the experiments show that low dilution rates result in a stable equilibrium fo the bacteria densities. This indicates that model (6.5) fails to predict the transitions between different qualitative behaviors of the system.
- The cycle periods of oscillation observed in experiments are longer than that predicted in simulations. In particular, the cycles observed in the experiments are almost out of phase (i.e. the maxima of Chlorella and the minima of Brachionus during the cycle occur almost at the same time).

To address these discrepencies, the following modification of model (6.5) is proposed in [101, 38].

$$\begin{aligned}
\frac{dN}{dt} &= \delta(N_{in} - N) - F_C(N)C, \\
\frac{dC}{dt} &= F_C(N)C - F_B(C)\frac{B}{\epsilon} - \delta C, \\
\frac{dR}{dt} &= F_B(C)R - (\delta + \mu + m)R, \\
\frac{dB}{dt} &= F_B(C)R - (\delta + m)B,
\end{aligned} \tag{6.6}$$

The main difference between these two models is that model (6.6) distinguishes the rotifer population into those that can reproduce (R) and those that cannot B. Such

classification is motivated by the experimental observations which suggest that the rotifers does not only suffer from the wash out but also from loss of fecundity while senescence. These additional loss effects are described in model (6.6) through parameters m and λ which denote the instantaneous mortality and senescence rate of the rotifers, respectively.

Although model (6.6) resolves the first discrepencies mentioned above, it still fails to capture the correct period and the phase of the population cycle. Further analyses of the experimental data indicate that such discrepencies are the result of Chlorella evolution in response to grazing pressure from the rotifers [116]. In particular, the Chlorella evolves to reproduce as a low-food quality clones as a defense mechanism against the grazing by the rotifers. Once the rotifers population crashed due to food shortage, the Chlorella density then increases; this increase, however, is not followed immediately by the increase on the rotifer population. Such delay in rotifer's response to return to higher population density is argued as the driving mechanism for the discrepencies in both period and phase between the Chlorella and the Brachionus population cycles [101]. By incoorporating this evolutionary effect to model (6.6), the following modified model proposed in [116] is shown to resolved the discrepencies found on the period and phase of the population cycles.

$$\begin{aligned}
\frac{dN}{dt} &= \delta(VN_{in} - N) - \sum_{i=1}^{k} F_{C,i}(N/V)C_i, \\
\frac{dC_i}{dt} &= \eta_C F_{C,i}(N/V)C_i - F_{B,i}(C/V)B - \delta C_i, \\
\frac{dR}{dt} &= \eta_B F_B(C_i/V)R - (\delta + m + \lambda)R, \\
\frac{dB}{dt} &= \eta_B F_B(C_i/V)R - (\delta + m)B,
\end{aligned} \tag{6.7}$$

The main difference of model (6.7) from model (6.6) is that the Chlorella population is now classified into k number of clones. Each of these clones is characterized by a parameter $p \in [0, 1]$ which indicates its relative food values to the rotifers. Clones

with low p are less prone to predation by the rotifers but are also less competitive (i.e. have higher carrying capacity) than clones with higher p in term of nutrient utilization. This characteristic threfore suggest a trade off between food value and competitive ability among clones in Chlorella population.

The proposed research experiment aims at using models (6.6) and (6.7) as candidates for the designed chemostat. The choice of model that is most suitable to our system will depends on the result from parameter estimation scheme explained in the next section. We point out that, depending on how well models (6.6) and (6.7) fit to our measurement data, further modification of these models are also possible.

6.2.2.3 Parameter estimation

For given candidate models (6.6) and (6.7), the values of all parameters need to be estimated based on the measurement data. Due to measurement errors that may occur in the experiments, we expect that the collected data will contain some uncertainties. To deal with these uncertainties, we choose the Bayesian Monte Carlo method as the framework for parameter estimation. In particular, our approach will be based on the Markov Chain Monte Carlo (MCMC) method.

Consider the problem of inferring a set of parameters, θ, from observation data, y. Bayesian inference provides a framework for recursively updating *prior* beliefs about the parameter distribution with information in the observation data. From the Bayes theorem, one knows that

$$p(\theta|y) = \frac{p(y|\theta)p(\theta)}{p(y)},$$

where $p(\theta|y)$ is the *posterior* probability distribution (belief function) about the parameters θ, conditioned on the observation data y. This formula has formed the basis of countless estimation and identification algorithms in which the underlying distributions are Gaussian. When one deviates from the Gaussian assumptions, however, a

major issue in the use of Bayesian inference lies in the computation of the probability $p(y)$ because it is usually an integral formed from the prior belief functions.

Markov Chain Monte Carlo methods bypass the issue associated with computing $p(y)$ by constructing a Markov chain whose stationary distribution is the posterior distribution $p(\theta|y)$. Construction of this chain, for instance using the Metropolis sampling [81], only requires the computation of the *ratio* of the target distribution in such a way that the normalizing constant $p(y)$ cancels out. If the constructed chain satisfies a suitable *detailed-balance* condition [65], then it is *reversible* with a stationary distribution equal to the posterior belief function $p(\theta|y)$. The main value of this Markov chain is that it can now be used to generate samples of the posterior distribution in a manner that allows one to estimate process parameters when the underlying prior distribution, $p(\theta|y)$, is no longer Gaussian.

The advantages provided by the Bayesian Monte Carlo methods have motivated its large applications for model calibration and data assimilation in ecological studies [16, 95, 76]. An MCMC method with adaptive Metropolis and delayed rejection samping techniques described in [77] is used to estimate 64 unknown parameters in a lake model of algae bloom. A Sequential Monte Carlo (SMC) method have recently used joint parameter and state estimation of a phytoplankton-zooplankton-nutrient-detritus (PZND) model [27, 28], and its extension to for moment (mean and variance) estimation of the parameter is described in [64]. Bayesian Monte Carlo methods, therefore, provide one of the only scalable methods for parameter estimation of nonlinear and high-dimensional systems. Our method to estimate the parameters of models (6.6)-(6.7) would be based on the MCMC method with combined delayed rejection and adaptive metropolis samplings introduced in [50, 77]. This method have been used previously to estimate models with highh number of parameters [**?** 77, 49] and we believe that it would perform well when applied to models (6.6)-(6.7).

6.3 Research & Experimental Plans

The main objective of this experiment with regard to regime shifts prediction is to characterize the impact of Chlorella evolution on the distance to hopf bifurcation of the Chlorella-Brachionus population. Early work in [38] have identified the hopf bifurcation diagram for model (6.6) in which the evolution of Chlorella was not included. This bifurcation diagram, however, has not been further investigated for model (6.7) in which the evolutionary mechanism of the Chlorella is included. The proposed experiment aims to investigate how the bifurcation diagram of model (6.6) changes with respect to the number of clones (i.e. genetic diversity) and the size of individuals in each clone of the Chlorella population. We hypothesize that both the number of clones and the size of individuals per clones will have significant impacts in modifying the bifurcation diagram of model (6.6) presented in [38]. What change in this bifurcation diagram actually take place is a question we wish to answer through this experiment.

Evaluation Method:

- *Model valiadation:* Evaluation of the developed model will be carried out by comparing computer simulations of models (6.6)-(6.7) and the data from experiments. In particular, computer simulation will be carried out using parameter values estimated from measurement data.
- *Regime shifts forecasting method:* We will evaluate the performance of the methods described in the previous chapters by directly comparing its prediction with the data from experiments. More specifically, the first evaluation will be carried out with regard to predicting the minimum dilution rate and nutrient concentration that are required to generate an oscillation (i.e.hopf bifurcation) in Chlorella-Brachionus populations when initialized from stable equilibrium population.

BIBLIOGRAPHY

1. F. Alvarado, Y. Hu, D. Ray, R. Stevenson, and E. Cashman. Engineering foundations for the determination of security costs. *Power Systems, IEEE Transactions on*, 6(3):1175–1182, 1991.

2. A. Ang and A. Timmermann. Regime changes and financial markets. Technical report, National Bureau of Economic Research, 2011.

3. F. D. Biase and R. Urbanke. An algorithm to calculate the kernel of certain polynomial ring homomorphisms. *Experimental Mathematics*, 4(3):227–234, 1995.

4. A. Bigatti and L. Robbiano. Toric ideals. *Matemática Contemporânea*, 21:1–25, 2001.

5. J. Bochnak, M. Coste, M.-F. Roy, et al. *Real algebraic geometry*, volume 95. Springer Berlin, 1998.

6. S. P. Boyd and L. Vandenberghe. *Convex optimization*. Cambridge university press, 2004.

7. P. Bremaud. *Markov chains: Gibbs fields, Monte Carlo simulation, and queues*, volume 31. springer, 1999.

8. W. A. Brock and S. R. Carpenter. Early warnings of regime shift when the ecosystem structure is unknown. *PloS one*, 7(9):e45586, 2012.

9. B. Buchberger. Bruno buchberger's phd thesis 1965: An algorithm for finding the basis elements of the residue class ring of a zero dimensional polynomial ideal. *Journal of symbolic computation*, 41(3):475–511, 2006.

10. C. A. Canizares. Calculating optimal system parameters to maximize the distance to saddle-node bifurcations. *Circuits and Systems I: Fundamental Theory and Applications, IEEE Transactions on*, 45(3):225–237, 1998.

11. S. Carpenter and W. Brock. Rising variance: a leading indicator of ecological transition. *Ecology letters*, 9(3):311–318, 2006.

12. S. Carpenter and W. Brock. Early warnings of unknown nonlinear shifts: a nonparametric approach. *Ecology*, 92(12):2196–2201, 2011.

13. S. R. Carpenter. Eutrophication of aquatic ecosystems: bistability and soil phosphorus. *Proceedings of the National Academy of Sciences of the United States of America*, 102(29):10002–10005, 2005.

14. S. R. Carpenter, N. F. Caraco, D. L. Correll, R. W. Howarth, A. N. Sharpley, and V. H. Smith. Nonpoint pollution of surface waters with phosphorus and nitrogen. *Ecological applications*, 8(3):559–568, 1998.

15. S. R. Carpenter, D. Ludwig, and W. A. Brock. Management of eutrophication for lakes subject to potentially irreversible change. *Ecological applications*, 9(3): 751–771, 1999.

16. J. S. Clark. Why environmental scientists are becoming bayesians. *Ecology letters*, 8(1):2–14, 2005.

17. B. L. Clarke. *Stability of complex reaction networks*. Wiley Online Library, 1980.

18. B. L. Clarke and W. Jiang. Method for deriving hopf and saddle-node bifurcation hypersurfaces and application to a model of the belousov–zhabotinskii system. *The Journal of chemical physics*, 99:4464, 1993.

19. R. Contamin and A. M. Ellison. Indicators of regime shifts in ecological systems: what do we need to know and when do we need to know it. *Ecological Applications*, 19(3):799–816, 2009.

20. D. A. Cox, J. Little, and D. O'Shea. *Ideals, varieties, and algorithms: an introduction to computational algebraic geometry and commutative algebra*, volume 10. Springer Verlag, 2007.

21. V. Dakos and A. Hastings. Editorial: special issue on regime shifts and tipping points in ecology. *Theoretical Ecology*, 6(3):253–254, 2013.

22. W. Decker, G.-M. Greuel, G. Pfister, and H. Schönemann. SINGULAR 3-1-6 — A computer algebra system for polynomial computations. 2012. http://www.singular.uni-kl.de.

23. P. Demenocal, J. Ortiz, T. Guilderson, J. Adkins, M. Sarnthein, L. Baker, and M. Yarusinsky. Abrupt onset and termination of the african humid period:: rapid climate responses to gradual insolation forcing. *Quaternary science reviews*, 19(1):347–361, 2000.

24. A. Dhooge, W. Govaerts, and Y. A. Kuznetsov. Matcont: a matlab package for numerical bifurcation analysis of odes. *ACM Transactions on Mathematical Software (TOMS)*, 29(2):141–164, 2003.

25. I. Dobson. Computing a closest bifurcation instability in multidimensional parameter space. *Journal of nonlinear science*, 3(1):307–327, 1993.

26. I. Dobson. Distance to bifurcation in multidimensional parameter space: Margin sensitivity and closest bifurcations. In *Bifurcation control*, pages 49–66. Springer, 2003.

27. M. Dowd. A sequential monte carlo approach for marine ecological prediction. *Environmetrics*, 17(5):435–455, 2006.

28. M. Dowd. Estimating parameters for a stochastic dynamic marine ecological system. *Environmetrics*, 22(4):501–515, 2011.

29. K. L. Drury and D. M. Lodge. Using mean first passage times to quantify equilibrium resilience in perturbed intraguild predation systems. *Theoretical Ecology*, 2(1):41–51, 2009.

30. K. L. Drury and D. M. Lodge. Using mean first passage times to quantify equilibrium resilience in perturbed intraguild predation systems. *Theoretical Ecology*, 2(1):41–51, 2009.

31. T. W. Dubé. The structure of polynomial ideals and gröbner bases. *SIAM Journal on Computing*, 19(4):750–773, 1990.

32. H. El-Samad, S. Prajna, A. Papachristodoulou, J. Doyle, and M. Khammash. Advanced methods and algorithms for biological networks analysis. *Proceedings of the IEEE*, 94(4):832–853, 2006.

33. B. Ermentrout. *Simulating, analyzing, and animating dynamical systems: a guide to XPPAUT for researchers and students*, volume 14. Siam, 2002.

34. V. Fairén and B. Hernández-Bermejo. Mass action law conjugate representation for general chemical mechanisms. *The Journal of Physical Chemistry*, 100(49): 19023–19028, 1996.

35. M. Feinberg. Lectures on chemical reaction networks. *Notes of lectures given at the Mathematics Research Center, University of Wisconsin*, 1979.

36. C. Folke, S. Carpenter, B. Walker, M. Scheffer, T. Elmqvist, L. Gunderson, and C. Holling. Regime shifts, resilience, and biodiversity in ecosystem management. *Annual Review of Ecology, Evolution, and Systematics*, pages 557–581, 2004.

37. A. Friedman. *Stochastic differential equations and applications. Vol. 1.* Academic Press, New York, 1975.

38. G. F. Fussmann, S. P. Ellner, K. W. Shertzer, and N. G. Hairston Jr. Crossing the hopf bifurcation in a live predator-prey system. *Science*, 290(5495):1358–1360, 2000.

39. F. Gantmacher. *The theory of matrices*. Taylor & Francis, 1960.

40. C. W. Gardiner. *Handbook of Stochastic Methods: For Physics, Chemistry, and the Natural Sciences*. Springer, New York, 1985.

41. C. W. Gardiner and C. Gardiner. *Stochastic methods: a handbook for the natural and social sciences*, volume 4. Springer Berlin, 2009.

42. K. Gatermann. Counting stable solutions of sparse polynomial systems in chemistry. 286:53, 2001.

43. K. Gatermann and B. Huber. A family of sparse polynomial systems arising in chemical reaction systems. *Journal of Symbolic Computation*, 33(3):275–305, 2002.

44. K. Gatermann, M. Eiswirth, and A. Sensse. Toric ideals and graph theory to analyze hopf bifurcations in mass action systems. *Journal of Symbolic Computation*, 40(6):1361–1382, 2005.

45. S. Ghosh, A. K. Pal, and I. Bose. Noise-induced regime shifts: A quantitative characterization. *The European Physical Journal E*, 36(10):1–10, 2013.

46. D. R. Grayson and M. E. Stillman. Macaulay2, a software system for research in algebraic geometry. Available at http://www.math.uiuc.edu/Macaulay2/, 2013.

47. G.-M. Greuel, G. Pfister, and H. Schönemann. Singular—a computer algebra system for polynomial computations. In *Symbolic computation and automated reasoning*, pages 227–233. AK Peters, Ltd., 2001.

48. J. Guckenheimer and P. Holmes. Nonlinear oscillations, dynamical systems, and bifurcations of vector fields. 1983.

49. H. Haario, M. Laine, M. Lehtinen, E. Saksman, and J. Tamminen. Markov chain monte carlo methods for high dimensional inversion in remote sensing. *Journal of the Royal Statistical Society: Series B (Statistical Methodology)*, 66 (3):591–607, 2004.

50. H. Haario, M. Laine, A. Mira, and E. Saksman. Dram: efficient adaptive mcmc. *Statistics and Computing*, 16(4):339–354, 2006.

51. W. M. Haddad and V. Chellaboina. Stability and dissipativity theory for nonnegative dynamical systems: a unified analysis framework for biological and physiological systems. *Nonlinear Analysis: Real World Applications*, 6(1):35–65, 2005.

52. W. M. Haddad, V. Chellaboina, and Q. Hui. *Nonnegative and compartmental dynamical systems*. Princeton University Press, 2010.

53. V. Hárs and J. Tóth. On the inverse problem of reaction kinetics. In *Colloquia Mathematica Societatis János Bolyai,(Szeged, Hungary, 1979) Qualitative Theory of Differential Equations (M. Farkas ed.)*, volume 30, pages 363–379, 1981.

54. A. Hastings and T. Powell. Chaos in a three-species food chain. *Ecology*, pages 896–903, 1991.

55. D. Henrion and J.-B. Lasserre. Gloptipoly: Global optimization over polynomials with matlab and sedumi. *ACM Transactions on Mathematical Software (TOMS)*, 29(2):165–194, 2003.

56. D. Herbert, R. Elsworth, and R. Telling. The continuous culture of bacteria; a theoretical and experimental study. *Journal of General Microbiology*, 14(3): 601–622, 1956.

57. C. S. Holling. Resilience and stability of ecological systems. *Annual review of ecology and systematics*, pages 1–23, 1973.

58. C. S. Holling. Engineering versus ecological resilience. In P. Schulze, editor, *Engineering with ecological constraints*, pages 31–44. National Academy Press, Washington D.C., 1996.

59. W. Horsthemke. *Noise induced transitions*. Springer, 1984.

60. M. Iwen. Lecture notes: Introduction to semidefinite programming. *Michigan State University*, Fall 2007.

61. M. D. Johnston and D. Siegel. Linear conjugacy of chemical reaction networks. *Journal of mathematical chemistry*, 49(7):1263–1282, 2011.

62. M. D. Johnston, D. Siegel, and G. Szederkényi. Computing weakly reversible linearly conjugate chemical reaction networks with minimal deficiency. *Mathematical biosciences*, 2012.

63. M. D. Johnston, D. Siegel, and G. Szederkényi. A linear programming approach to weak reversibility and linear conjugacy of chemical reaction networks. *Journal of Mathematical Chemistry*, 50(1):274–288, 2012.

64. E. Jones, J. Parslow, and L. Murray. A bayesian approach to state and parameter estimation in a phytoplankton-zooplankton model. *Australian Meteorological and Oceanographic Journal*, 59:7–16, 2010.

65. F. P. Kelly. *Reversibility and stochastic networks*. Cambridge University Press, 2011.

66. R. Kindermann, J. L. Snell, et al. *Markov random fields and their applications*, volume 1.

67. S. Klamt, J. Saez-Rodriguez, and E. D. Gilles. Structural & functional analysis of cellular networks with cellnetanalyzer. *BMC systems biology*, 1(1):2, 2007.

68. M. Klein, G. Rogers, P. Kundur, et al. A fundamental study of inter-area oscillations in power systems. 1991.

69. G. Kremer and D. Thompson. A bifurcation-based procedure for designing and analysing robustly stable non-linear hydraulic servo systems. *Proceedings of the IMechE, Part I: Journal of Systems and Control Engineering*, 212(5):383–394, 1998.

70. D. P. Kroese, T. Taimre, and Z. I. Botev. *Handbook of Monte Carlo Methods*, volume 706. John Wiley & Sons, 2011.

71. H. Kushner. Finite time stochastic stability and the analysis of tracking systems. *Automatic Control, IEEE Transactions on*, 11(2):219–227, 1966.

72. H. Kushner. Stochastic stability and control, volume 33 of mathematics in science and engineering, 1967.

73. Y. A. Kuznetsov. *Elements of applied bifurcation theory*. Springer-Verlag New York, Inc., 1998.

74. R. C. Lewontin. The meaning of stability. In *Brookhaven symposia in biology*, volume 22, pages 13–24, 1968.

75. J. Löfberg. Yalmip : A toolbox for modeling and optimization in MATLAB. In *Proceedings of the CACSD Conference*, Taipei, Taiwan, 2004. URL `http://users.isy.liu.se/johanl/yalmip`.

76. D. J. Lunn, A. Thomas, N. Best, and D. Spiegelhalter. Winbugs-a bayesian modelling framework: concepts, structure, and extensibility. *Statistics and computing*, 10(4):325–337, 2000.

77. O. Malve, M. Laine, H. Haario, T. Kirkkala, and J. Sarvala. Bayesian modelling of algal mass occurrences using adaptive mcmc methods with a lake water quality model. *Environmental Modelling & Software*, 22(7):966–977, 2007.

78. K. Martin and R. Lorenzo. Computational commutative algebra 1, 2000.

79. R. M. May. Thresholds and breakpoints in ecosystems with a multiplicity of stable states. *Nature*, 269(5628):471–477, 1977.

80. A. P. Mazzoleni and I. Dobson. Closest bifurcation analysis and robust stability design of flexible satellites. *Journal of Guidance, Control, and Dynamics*, 18 (2):333–339, 1995.

81. N. Metropolis, A. W. Rosenbluth, M. N. Rosenbluth, A. H. Teller, and E. Teller. Equation of state calculations by fast computing machines. *The journal of chemical physics*, 21(6):1087–1092, 2004.

82. A. N. Michel. Stability analysis of stochastic composite systems. *Automatic Control, IEEE Transactions on*, 20(2):246–250, 1975.

83. A. N. Michel. Stability analysis of stochastic large-scale systems. *ZAMM-Journal of Applied Mathematics and Mechanics/Zeitschrift für Angewandte Mathematik und Mechanik*, 55(2):113–123, 1975.

84. M. Mönnigmann and W. Marquardt. Normal vectors on manifolds of critical points for parametric robustness of equilibrium solutions of ode systems. *Journal of nonlinear science*, 12(2):85–112, 2002.

85. B. K. Øksendal and A. Sulem. *Applied stochastic control of jump diffusions*, volume 498. Springer.

86. M. Pal, A. K. Pal, S. Ghosh, and I. Bose. Early signatures of regime shifts in gene expression dynamics. *Physical biology*, 10(3):036010, 2013.

87. P. A. Parrilo. *Structured semidefinite programs and semialgebraic geometry methods in robustness and optimization.* PhD thesis, California Institute of Technology, Pasadena, CA, 2000.

88. P. A. Parrilo. Semidefinite programming relaxations for semialgebraic problems. *Mathematical programming*, 96(2):293–320, 2003.

89. S. Prajna, A. Papachristodoulou, and P. Parrilo. Introducing sostools: A general purpose sum of squares programming solver. In *Decision and Control, 2002, Proceedings of the 41st IEEE Conference on*, volume 1, pages 741–746. IEEE, 2002.

90. S. Prajna, A. Papachristodoulou, P. Seiler, and P. A. Parrilo. *SOSTOOLS: Sum of squares optimization toolbox for MATLAB*, 2004.

91. S. Prajna, A. Jadbabaie, and G. J. Pappas. A framework for worst-case and stochastic safety verification using barrier certificates. *Automatic Control, IEEE Transactions on*, 52(8):1415–1428, 2007.

92. P. E. Protter. *Stochastic Integration and Differential Equations: Version 2.1*, volume 21. Springer, 2004.

93. S. Redner. *A guide to first-passage processes.* Cambridge University Press, 2001.

94. L. C. G. Rogers and D. Williams. *Diffusions, Markov processes and martingales: Volume 2, Itô calculus*, volume 2. Cambridge university press, 2000.

95. F. Ronquist and J. P. Huelsenbeck. Mrbayes 3: Bayesian phylogenetic inference under mixed models. *Bioinformatics*, 19(12):1572–1574, 2003.

96. M. Scheffer. *Ecology of shallow lakes.* Springer, 2004.

97. M. Scheffer and S. R. Carpenter. Catastrophic regime shifts in ecosystems: linking theory to observation. *Trends in ecology & evolution*, 18(12):648–656, 2003.

98. M. Scheffer, S. Hosper, M. Meijer, B. Moss, and E. Jeppesen. Alternative equilibria in shallow lakes. *Trends in ecology & evolution*, 8(8):275–279, 1993.

99. M. Scheffer, S. Carpenter, J. A. Foley, C. Folke, B. Walker, et al. Catastrophic shifts in ecosystems. *Nature*, 413(6856):591–596, 2001.

100. M. Scheffer, S. R. Carpenter, T. M. Lenton, J. Bascompte, W. Brock, V. Dakos, J. Van De Koppel, I. A. Van De Leemput, S. A. Levin, E. H. Van Nes, et al. Anticipating critical transitions. *Science*, 338(6105):344–348, 2012.

101. K. W. Shertzer, S. P. Ellner, G. F. Fussmann, and N. G. Hairston. Predator–prey cycles in an aquatic microcosm: testing hypotheses of mechanism. *Journal of Animal Ecology*, 71(5):802–815, 2002.

102. H. L. Smith. *The theory of the chemostat: dynamics of microbial competition*, volume 13. Cambridge university press, 1995.

103. G. Stengle. A nullstellensatz and a positivstellensatz in semialgebraic geometry. *Mathematische Annalen*, 207(2):87–97, 1974.

104. M. H. Stone. The generalized weierstrass approximation theorem. *Mathematics Magazine*, 21(5):237–254, 1948.

105. J. F. Sturm. Using sedumi 1.02, a matlab toolbox for optimization over symmetric cones. *Optimization methods and software*, 11(1-4):625–653, 1999.

106. B. Sturmfels. Grobner bases of toric varieties. *Tohoku Mathematical Journal, Second Series*, 43(2):249–261, 1991.

107. B. Sturmfels. *Gröbner bases and convex polytopes*, volume 8. AMS Bookstore, 1996.

108. B. Sturmfels. *Solving systems of polynomial equations*, volume 97. American Mathematical Soc., 2002.

109. G. Szederkényi. Computing sparse and dense realizations of reaction kinetic systems. *Journal of Mathematical Chemistry*, 47(2):551–568, 2010.

110. G. Szederkényi. Computing reaction kinetic realizations of positive nonlinear systems using mixed integer programming. In *8th IFAC Symposium on Nonlinear Control Systems-NOLCOS*, pages 1–6, 2010.

111. G. Szederkényi and K. M. Hangos. Finding complex balanced and detailed balanced realizations of chemical reaction networks. *Journal of Mathematical Chemistry*, 49(6):1163–1179, 2011.

112. P. Tankov. *Financial modelling with jump processes*. CRC Press, 2004.

113. K.-C. Toh, M. J. Todd, and R. H. Tütüncü. Sdpt3a matlab software package for semidefinite programming, version 1.3. *Optimization methods and software*, 11(1-4):545–581, 1999.

114. A. I. Vol'pert. Differential equations on graphs. *Mathematics of the USSR-Sbornik*, 17(4):571, 1972.

115. S. Waldherr and F. Allgöwer. Robust stability and instability of biochemical networks with parametric uncertainty. *Automatica*, 47(6):1139–1146, 2011.

116. T. Yoshida, L. E. Jones, S. P. Ellner, G. F. Fussmann, and N. G. Hairston. Rapid evolution drives ecological dynamics in a predator–prey system. *Nature*, 424(6946):303–306, 2003.

This document was prepared & typeset with pdfLaTeX*, and formatted with* NDdiss2$_\varepsilon$ *classfile (v3.2013[2013/04/16]) provided by Sameer Vijay and updated by Megan Patnott.*